INVESTIGATING THE EFFECT OF LOW HEATING-COOLING RATE AND THE THERMOMECHANICAL TREATMENTS ON THE SHAPE MEMORY BEHAVIOR OF NITIHF ALLOYS

YAVAŞ ISITMA-SOĞUTMA HIZININ VE TERMOMEKANIK IŞLEMLERIN NITIHF ALAŞIMLARININ ŞEKIL HAFIZA DAVRANIŞLARI ÜZERINE ETKISININ INCELENMESI

OĞULCAN AKGÜL

PROF. DR BENAT KOÇKAR

Supervisor

Submitted to
Graduate School of Science and Engineering of Hacettepe University
as a Partial Fulfillment to the Requirements
for the Award of the Degree of Master of Sciences
in Mechanical Engineering

2022

ABSTRACT

INVESTIGATING THE EFFECT OF LOW HEATING-COOLING RATE AND THE THERMOMECHANICAL TREATMENTS ON THE SHAPE MEMORY BEHAVIOR OF NITIHF ALLOYS

Oğulcan AKGÜL

Master of Sciences, Department of Mechanical Engineering

Supervisor: Prof. Dr. Benat KOÇKAR

January 2022, 103 pages

Shape memory alloys (SMAs) have an extraordinary ability to recover their shape via martensitic transformation. That ability provides SMAs to be used as actuators in many applications as a result of doing work against load. Superelasticity and shape memory are two key phenomena observed in SMAs as a result of the martensitic transformation. Superleasticity takes place when SMA is in parent phase. Under the applied load, parent phase transforms to martensite phase and elongates via martensite reorientation and detwinning and martensite transforms back to austenite and the alloy remembers its original shape via unloading. On the other hand, shape memory effect is triggered via heating the alloy above Austenite Finish (A_f) and cooling to Martensite Finish (M_f) temperatures.

Nickel Titanium-based shape memory alloys are the most popular SMAs due to their excellent shape memory characteristics however their transformation temperatures are limited to 100-120 ˚C if the alloy is Ni-Lean. As Nickel content increases above 50 at. %, transformation temperatures decrease. However, many applications require higher

transformation temperatures. Addition of Hf element effectively strengthens the alloy and increases transformation temperatures of NiTi-Based SMAs. However, as service temperature increases, cyclic stability of SMAs decreases due to the softening at elevated temperatures thus it is crucial to have knowledge about shape memory behavior at these temperatures.

In the first part of this thesis, $Ni_{50}Ti_{30}Hf_{20}$ at. % shape memory alloy was used to investigate the heating/cooling rate effect on the shape memory properties. Material was purchased from Sophisticated Alloys Inc. and produced with high purity Ni, Ti and Hf elements via vacuum induction melting. Melting process was conducted under high purity argon atmosphere. Material was sealed within mild steel can and extrusion process with an area reduction of 4:1 was conducted. DSC experiments were conducted via Perkin Elmer Differential Scanning Calorimetry 800 on extruded specimens to reveal heating/cooling rate effect on equiatomic $Ni_{50}Ti_{30}Hf_{20}$ at. % shape memory alloy. Isobaric heating/cooling experiments were run to investigate shape memory effect via following different heating/cooling rates which were the same rates used in DSC experiments. Thermal stability was investigated via DSC experiments while mechanical stability was investigated via isobaric experiments.

Stress-free DSC experiments showed that transformation temperatures were not affected by different heating/cooling rates while transformation enthalpy increased as scanning rate was increased. Isobaric experiments, which were done under 200 MPa demonstrated no variety in terms of shape memory properties such as the transforming volume and transformation temperatures with different heating/cooling rates.

In the second part of this thesis, cyclic stability and shape memory characteristics were investigated on equiatomic Ni50Ti25Hf25 at. % SMA. Material was produced with the same procedure as defined above and purchased from Sophisticated Alloys Inc. Addition to the extrusion process, material was subjected to homogenizing heat treatment at 1050 °C for 2 hours. High Hf content of NiTiHf alloy has been admitted as a great candidate for very high temperature (up to 600 °C) actuation applications. DSC studies were conducted to characterize transformation behavior of the alloy under no load. After determining transformation characteristics, functional fatigue experiments were conducted under pre-determined load on homogenized sample to investigate shape

memory behavior of Ni50Ti25Hf25 at. % shape memory alloy. It is known that plastic deformation methods are effective way to improve shape memory characteristics of SMAs. Cold rolling was applied to homogenized sample with thickness reduction of 5% then cold rolled sample was subjected to annealing heat treatment at 500 °C for 30 minutes to further improve SME behavior. Warm rolling study was also conducted at 500 °C with same thickness reduction as it was achieved with cold rolling operation.

Recoverable strain, transformation temperatures, hysteresis, irrecoverable strain values were gathered from the experiments. It was observed that cyclic stability of Ni50Ti25Hf25 at. % HTSMA was increased via both cold and warm rolling processes although the operating temperatures were very high.

Keywords: Shape Memory Alloys, Cold Rolling, Warm Rolling, Thermo-Mechanical treatments, Functional Fatigue

ÖZET

YAVAŞ ISITMA-SOĞUTMA HIZININ VE TERMOMEKANİK İŞLEMLERİN NİTİHF ALAŞIMLARININ ŞEKİL HAFIZA DAVRANIŞLARI ÜZERİNE ETKİSİNİN İNCELENMESİ

Oğulcan AKGÜL

Yüksek Lisans, Makina Mühendisliği Bölümü

Tez Danışmanı: Prof. Dr. Benat KOÇKAR

OCAK 2022, 103 sayfa

Şekil hafızalı alaşımlar (ŞHA'lar) martensitik dönüşüm sayesinde şekillerini geri kazanma gibi olağanüstü bir yeteneğe sahiptir. Bu yetenek ile yüke karşı iş yapabildikleri için, ŞHA'lar birçok uygulamada aktüatör olarak kullanılabilirler. Martensitik dönüşüm, süperelastisite ve şekil hafıza etkisi olarak adlandırılan iki ana etkinin gözlemlenmesine yol açar. Süperleastisite, ŞHA yüksek sıcaklık fazında iken gerçekleşir. Uygulanan yük ile yüksek sıcaklık fazı martensit faza dönüşür ve martensitin yeniden oryantasyonu ve ikizlenmenin bozulması yoluyla uzama gerçekleştirir. Yükün ortadan kaldırılması ile martensit yüksek sıcaklık fazına geri döner ve yüksek sıcaklık fazındaki şeklini geri hatırlar. Şekil hafıza etkisi ise alaşımın Af (östenit bitiş) sıcaklığının üzerine ısıtılması ve Mf (martenzit bitiş) sıcaklığının altına soğutulması ile vuku bulur.

Nikel-Titanyum bazlı şekil hafıza alaşımları mükemmel şekil hafıza özellikleri sebebiyle en popüler ŞHA'lardır, ancak dönüşüm sıcaklıkları 100-120 ˚C ile sınırlıdır. Nikel içeriği atomik olarak %50'nin üzerine çıktıkça dönüşüm sıcaklıkları düşüş gösterir, bu sebeple daha yüksek sıcaklıklardaki birçok uygulama için bu alaşımların dönüşüm sıcaklıklarının arttırılması gerekmektedir. Hf elementinin eklenmesi, alaşımı etkili bir şekilde

güçlendirdiği gibi bahsi geçen dönüşüm sıcaklıklarını da arttırır. Ancak yüksek sıcaklıklarda malzemenin gösterdiği yumuşama sebebiyle ŞHA'ların döngüsel kararlılığı azalır bu sebeple yüksek sıcaklıklarda şekil hafıza davranışı hakkında bilgi sahibi olmak önem arz etmektedir.

Tezin ilk bölümünde, ısıtma/soğutma hızının şekil hafıza özellikleri üzerindeki etkisini araştırmak için Ni50Ti30Hf20 (at. %) şekil hafızalı alaşım kullanılmıştır. Sophisticated Alloys Inc. şirketinden temin edilen malzeme, yüksek saflıkta Ni, Ti ve Hf elementleri kullanılarak vakum indüksiyon ergitme yoluyla üretilmiştir. Ergitme işlemi yüksek saflıkta Argon atmosferi altında gerçekleştirilmiştir. Malzeme, yumuşak çelik ile kaplandıktan sonra 4:1 oranında alan küçültecek şekilde ekstrüzyon işlemine tabii tutulmuştur. Diferansiyel Taramalı Kalorimetre (DSC) deneyleri eş atomlu Ni50Ti30Hf20 şekil hafızalı alaşım üzerinde ısıtma/soğutma hızının etkisini ortaya çıkarmak için ekstrüde edilmiş numuneler kullanılarak Perkin Elmer Diferansiyel Taramalı Kalorimetre 800 ile gerçekleştirilmiştir. DSC deneylerine ek olarak izobarik ısıtma/soğutma deneyleri, DSC deneylerinde kullanılan hız ile aynı olacak şekilde farklı ısıtma/soğutma hızları kullanılarak gerçekleştirilmiştir. Bu şekilde farklı ısıtma/soğutma hızlarının şekil hafıza etkisi (ŞHE) üzerindeki etkileri incelenmiştir. DSC deneyleri ile termal kararlılık incelenirken izobarik deneyler ile mekanik kararlılık incelenmiştir.

Gerilmesiz DSC deneyleri, tarama hızı arttıkça dönüşüm entalpisi artarken dönüşüm sıcaklıklarının farklı ısıtma/soğutma hızlarından etkilenmediğini göstermiştir. 200 MPa altında yapılan izobarik deneyler ise farklı ısıtma/soğutma hızlarında dönüşüm hacmi ve dönüşüm sıcaklıkları gibi şekil hafıza özellikleri açısından çeşitlilik göstermemiştir.

Tezin ikinci bölümünde, eş atomlu Ni50Ti25Hf25 at. % şekil hafızalı alaşımı kullanmış ve alaşım üzerinde çevrimsel kararlılık ve şekil hafıza özellikleri incelenmiştir. Malzeme yukarıdaki ile aynı prosedür ile üretilmiş ve temin edilmiştir. Ekstrüzyon işlemine ek olarak malzeme 1050 °C'de 2 saat homojenleştirme ısıl işlemine tabi tutulmuştur. NiTiHf alaşımları, yüksek Hf içeriği ile çok yüksek sıcaklıklardaki (600 °C'ye kadar) uygulamalar için harika bir aday olarak kabul edilmiştir. Alaşımın yüksüz dönüşüm davranışını karakterize etmek için DSC çalışmaları yapılmıştır. Dönüşüm özellikleri

belirlendikten sonra, Ni50Ti25Hf25 at. % alaşımının şekil hafıza davranışını araştırmak için homojenize edilmiş numune üzerinde önceden belirlenmiş yük altında fonksiyonel yorulma deneyleri yapılmıştır. Plastik deformasyon yöntemlerinin ŞHA'ların şekil hafıza özelliklerini iyileştirmede etkili bir yol olduğu bilinmektedir. Homojenize edilmiş numuneye %5 kalınlık azaltılacak şekilde soğuk haddeleme uygulanmıştır, ardından soğuk haddelenmiş numune, ŞHE davranışını iyileştirmek için 500 °C'de 30 dakika tavlama ısıl işlemine tabi tutulmuştur. Sıcak haddeleme çalışması da soğuk haddeleme işleminde olduğu gibi %5 kalınlık azalmasıyla 500 °C'de gerçekleştirilmiştir. Deneylerden geri kazanılabilir gerinim, dönüşüm sıcaklıkları, histerezis, geri döndürülemez gerinim değerleri elde edilmiştir. Ni50Ti25Hf25 at. % şekil hafızalı alaşımının çevrimsel kararlılığı araştırılmıştır. Çalışma sıcaklıkları çok yüksek olmasına rağmen hem soğuk hem de sıcak haddeleme işlemleri ile çevrimsel kararlılık arttırılmıştır.

Anahtar Kelimeler: Şekil Hafızalı Alaşım, Soğuk Haddeleme, Sıcak Haddeleme, Termo-Mekanik işlem, Fonksiyonel Yorulma

ACKNOWLEDGEMENTS

I would like to thank my advisor Prof. Dr. Benat Koçkar for providing guidance with her invaluable expertise in scientific research. In addition, her feedback during my master's degree brought my scientific inquiry to a higher level. I am grateful to Dr. Koçkar for her never-ending patience throughout my study. I also would like to express my gratitude to Assoc. Prof. Dr. Mustafa Kerem Koçkar for his support.

I am thankful to jury members Prof. Dr. Bora Maviş, Prof. Dr. Ziya Esen , Assoc. Prof. Bilsay Sümer and Assist. Prof. Okan Görtan for their valuable comments and feedback.

I am also thankful to my labmates in Hacettepe University Mechanics and Microstructural Engineering Laboratory, to Erhan Akın, Halil Onat Tuğrul, Meriç Ekiciler, Günce Dugan and Özlem Nur Açık for their valuable friendship, precious help and useful critiques.

Finally, I thank to my mother Semra Akgül, my father Şenol Akgül, my brother Serkut Akgül and my grandparents for their unconditional support.

Oğulcan AKGÜL

January 2022, Ankara

TABLE OF CONTENTS

LIST OF FIGURES

LIST OF TABLES

SYMBOLS AND ABBREVIATIONS

Symbols

Au	Gold
Cu	Copper
Fe	Iron
Hf	Hafnium
Nb	Niobium
Ni	Nickel
Pd	Palladium
Pt	Platinum
Ti	Titanium
Zr	Zirconium

Abbreviations

Af	Austenite Finish Temperature
As	Austenite Start Temperature
Mf	Martensite Finish Temperature
Ms	Martensite Start Temperature
TT	Transformation Temperature
SMA	Shape Memory Alloy
SME	Shape Memory Effect
SE	Superelasticity
HTSMA	High Temperature Shape Memory Alloy

DSC	Differential Scanning Calorimeter
ECAE	Equal Channel Angular Extrusion
SPD	Severe Plastic Deformation
HPT	High Pressure Torsion
UCT	Upper Cycle Temperature
CR	Cold Rolled
WR	Warm Rolled

1. INTRODUCTION

Shape memory alloys (SMAs) are able to maintain their shape of parent phase after deforming and then heating the alloy to achieve martensite to austenite phase transformation. When SMA is in martensite phase, it can be deformed and shape change is accommodated via twinning. If twinned martensite is heated to austenite phase, detwinning occurs and SMA remembers its original shape in austenite phase. Material exhibits work against an applied load via following the aforementioned route due to specific nature of SMAs. Shape change takes place thermo-elastically and the repetition of the shape change can be achieved with this thermo-elastic phase transformation. This extraordinary ability provides them to be used as actuators in many industries such as aerospace, biomedical and automotive [1–7].

NiTi binary alloys have great shape memory properties although their transformation temperatures are restricted to approximately 100°C. There is an emerging need for high-temperature SMAs to be utilized for high-temperature actuation applications in aerospace industry. Ternary element addition is necessary to increase transformation temperatures. Hf, Zr, Pd, Pt, Au are the most common ternary element candidates. Pd, Pt, and Au are more expensive than Hf and Zr. Zr element makes the alloy more brittle than that of Hf element. Also Hf increases the transformation temperatures more effectively than that of Pd and Zr. Addition to that, Hf added NiTi alloys show better ductility than Zr added ones thus Hf is one of the best ternary element addition due to aforementioned reasons [8].

Superelasticity occurs upon loading forward transformation (parent phase to martensite phase transformation) and reverse transformation (martensite phase to parent phase transformation) occurs upon unloading while shape memory effect (SME) takes place via heating and cooling. Material transforms to parent phase via heating and martensite phase via cooling. Superelastic response of NiTi-based SMAs are frequently utilized in medical applications while aerospace applications rely on SME. It is possible to do work against load via SME since material is able to recover its original shape upon reverse transformation against applied load.

One of the parameters that affect martensitic transformation behavior has been told as heating/cooling rate. There are only few studies that were conducted to investigate heating/cooling rate effect on martensitic transformation [9–12].

Additionally, to the author's best knowledge; there is no study in the literature that shows the heating cooling rate effect on the shape memory and actuation properties of equiatomic Ni50Ti30Hf20 at. % SMA under constant load. It is important to expand and verify the knowledge in the literature considering the thermodynamic via investigation of actuation properties and transformation temperatures with applying different heating/cooling rates.

The aim of the first section of the thesis is to investigate the cooling rate effect on martensitic transformation of Ni50Ti30Hf20 at. % SMA under no load and via applying constant load conditions. Controlled heating/cooling rate experiments were conducted to observe and investigate the rate effect since it is crucial for the actuation applications.

It is also important for SMAs to have thermal and mechanical stability due to the importance of stable behavior in actuation applications. Thermal stability can be explained by achieving stable transformation temperatures with thermal cycling and mechanical stability can be explained by achieving stable actuation strain behavior with thermal-mechanical cycling.

It is possible to improve thermal and mechanical stability via thermo-mechanical treatments. Dislocation induction with plastic deformation, grain refinement, precipitation hardening and alloying methods are the ones to improve cyclic stability. It is known that severe plastic deformation techniques lead to observe grain refinement and increase in dislocation density and also lead to increase in cyclic stability although many of the Severe Plastic Deformation (SPD) techniques are hard to perform on Hf-rich NiTiHf alloys [13,14].

Precipitation formation is also a way to improve cyclic stability nevertheless precipitation formation may not be favorable owing to chemical composition of the alloy. Alloy hardening is also a possible method to improve cyclic stability however, additional

elements may cause some disadvantages such as unexpected change in transformation temperatures and segregation of some intermetallics which lead to have undesirable SME behavior [15–18].

The aim of the second section of the thesis is to investigate the effects of cold and warm rolling on shape memory behavior of equiatomic Ni50Ti25Hf25 at. % SMA, which can be called as very High Temperature Shape Memory Alloy (HTSMA). Rolling is an effective deformation process to improve shape memory properties of SMAs and relatively easy to apply. Higher actuation temperatures are huge drawbacks for actuation applications due to the instable actuation properties at high temperatures. High Hf content NiTiHf HTSMAs soften at high temperatures and lose their stability with the formation of dislocations during phase transformations. Thus, investigation and enhancement of shape memory behavior of HTSMAs are of great importance for actuation applications.

2. THEORY AND LITERATURE

2.1. Martensitic Transformation

Martensitic transformation (MT) is a phase transformation that occurs without diffusion but through shear mechanism. Atoms move cooperatively with a military manner. Parent phase which is the stable phase at elevated temperatures is cubic. The martensite phase, which is the stable phase at lower temperature, has lower symmetry. At Martensite Start (M_s) temperature, forward transformation starts to occur by a shear like mechanism which can be seen in Figure 2.1-1. Martensite phase has lower symmetry as aforementioned above, therefore low symmetry leads to the formation of numerous martensite variants during transformation from parent phase to martensite phase. Above the Austenite Start (A_s) temperature, martensite phase becomes unstable which causes reverse transformation due to the instability of martensite at high temperatures. Although the atomic movements are small compared to inter-atomic distances, these movements cause macroscopic shape change which is the underlying mechanism of both shape memory effect (SME) and superelasticity (SE)

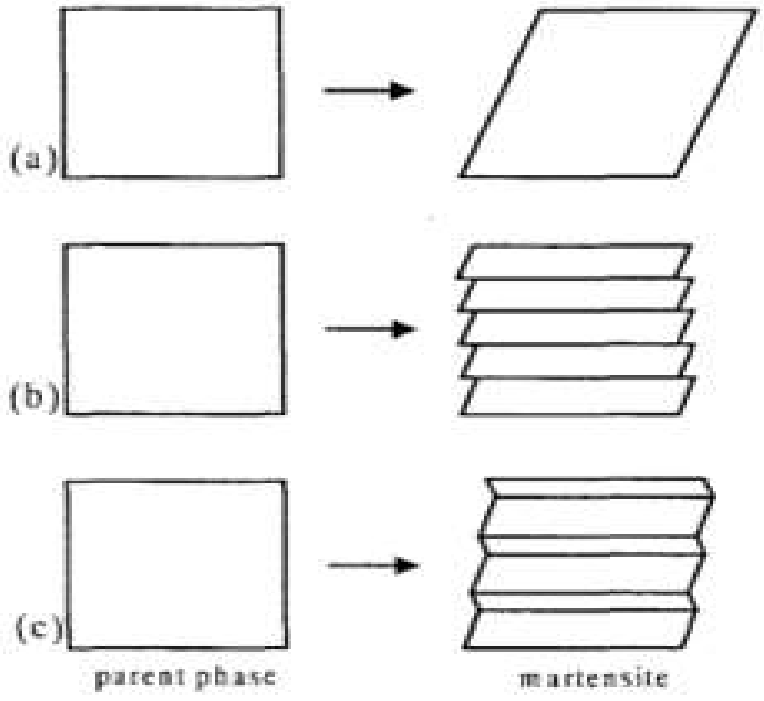

Figure 2.1-1 Schematic showing the importance of invariant shear upon martensitic transformation (a) shape change via martensitic transformation (b) strain accommodation via slip (c) strain accommodation via twinning [19].

Shape change that caused by martensitic transformation also causes a large strain. There are two main mechanisms to accommodate the shape change due to this large strain, which is called as lattice invariant shear (LIS). The shape change is accommodated by slip (Fig. 2.1-1 b) and twinning. (Fig. 2.1-1 c) These Slip leads to the formation of dislocations and is irreversible but accommodation of shape change via twinning is reversible. Twins and dislocations can be observed by electron microscopes. Twinning which is observed in shape memory alloys causes strain to relieve.

Figure 2.1-2 shows the Gibbs free energy evolution with the change in temperature of parent and martensite phases. T_0 is the equilibrium temperature at which martensite and parent phases exist together theoretically while Ms is the temperature where forward transformation begins and As is the temperature where reverse transformation begins. The difference between Gibbs free energy of martensite and the Gibbs free energy of parent phases at M_s and A_s temperatures represents driving force of martensite nucleation or martensite regression.

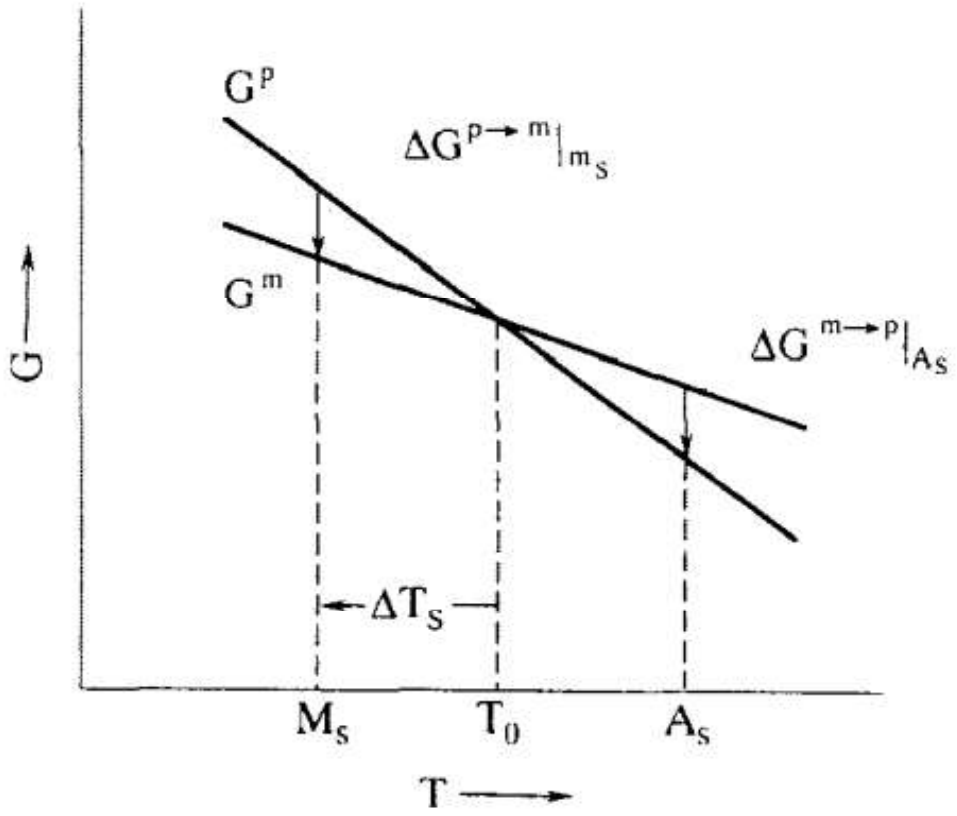

Figure 2.1-2 Gibbs free energy curves of martensite and austenite phases [19].

$\Delta Gp \rightarrow m|Ms = Gm - Gp$ [19] (Eqn 1)

The system's Gibbs Free energy change can be written as

$\Delta G = \Delta Gc + \Delta Gnc = \Delta Gc + \Delta Girr + \Delta Ge$ [19] (Eqn 2)

Where Gc denotes the chemical energy change from parent to martensite phase, and Gnc denotes non-chemical energy, which is the total of irreversible and elastic energy. ΔGirr represents irreversible energy which is related with friction energy which is required for the propagation of the interface between parent phase and martensite. Lastly ΔGe represents the elastic energy of martensite.

In many of martensitic transformations ΔGnc term cannot be ignored by reason of the term is as large as ΔGe which brings the necessity of supercooling with the magnitude of ΔTs to enable martensite nucleation as it is shown in Fig 2.1-2, also superheating is a necessity for the reverse transformation to occur. Martensite has elastic energy around itself which is the reason of difference in Ms and Mf hence undercooling is necessary for the continuity of the martensitic transformation.

One can categorize martensitic transformations in two main group which are thermo-elastic and non-thermoelastic. In thermo-elastic transformation, small temperature hysteresis indicates that driving force to transform austenite to martensite is small. The parent and martensite interface is mobile and the transformation is crystallographically reversible such that martensite withdraws and parent phase appears with the initial orientation.

If the non-chemical energy term is high, mobility of martensite austenite interface decreases due to especially the increase in friction energy thus driving force becomes very large and causes reverse transformation to occur by renucleation of parent phase which leads the transformation to occur non-thermoelastically [19,20].

Another factor that influences martensitic transformation is applied stress, which may be determined using the Clausius-Clapeyron relationship. Clausius-Clapeyron equation is shown below:

$$\frac{d\sigma}{dT} = -\frac{\Delta S}{\varepsilon} = \frac{\Delta H*}{\varepsilon T} \quad [19] \quad \text{(Eqn 3)}$$

σ: stress.

ε: transformation strain.

ΔS: transformation entropy per unit volume.

ΔH*: transformation enthalpy per unit volume.

2.2. Shape Memory Effect and Superelasticity

SMAs undergo thermo-elastic martensitic transformation with the help of twinning mechanism thus, they have an ability to 'return to' their parent phase shape when heated or unloaded. Twinning occurs with the application of certain stress level when martensite phase is deformed. Above a certain stress level, slip is induced to the system and leads to the formation of irreversible shape changes. In this context, martensite should be formed by twinning to observe shape memory effect in SMAs. Self-accommodation occurs while parent to martensite transformation under no load condition. Energy change is minimum with the twinning formation. Deformation under load condition causes twin boundary motion which leads to martensite reorientation. The reorientation occurs in a manner such that the most favorable martensite variant grows with the sacrifice of less favorable variants under load which was demonstrated in the literature [20].

There are two mechanisms to induce austenite to martensite phase transformation:

1. Shape Memory Effect
2. Superelasticity

Transformation via cooling and heating the SMA below Mf temperature and above Af temperature, is called shape memory effect.

Shape memory effect region in Figure 2.2-1 shows the region where SME behavior can be observable. The critical stress for slip (CSS) for two different cases is also shown in the same figure and above CSS threshold, irreversible deformation occurs since slip is induced to the system.

The shaded region in the figure shows superelastic region. Superelasticity occurs with the help of stress, when SMA is in the austenite phase. Austenite to martensite transformation takes place via stress which is called stress induced martensitic transformation (SIM). The stress should not be able to introduce slip to the system yet should be enough to transform austenite to martensite. Transformation from martensite to austenite occurs when the material is unloaded since martensite is not the favorable phase at the temperature at which the austenite is stable.

Another important parameter is Md temperature. It is the limit temperature that martensite can be induced via application of stress. When the stress is applied above Md temperature, however, superelasticity cannot be observed because slip occurs instead of twinning.

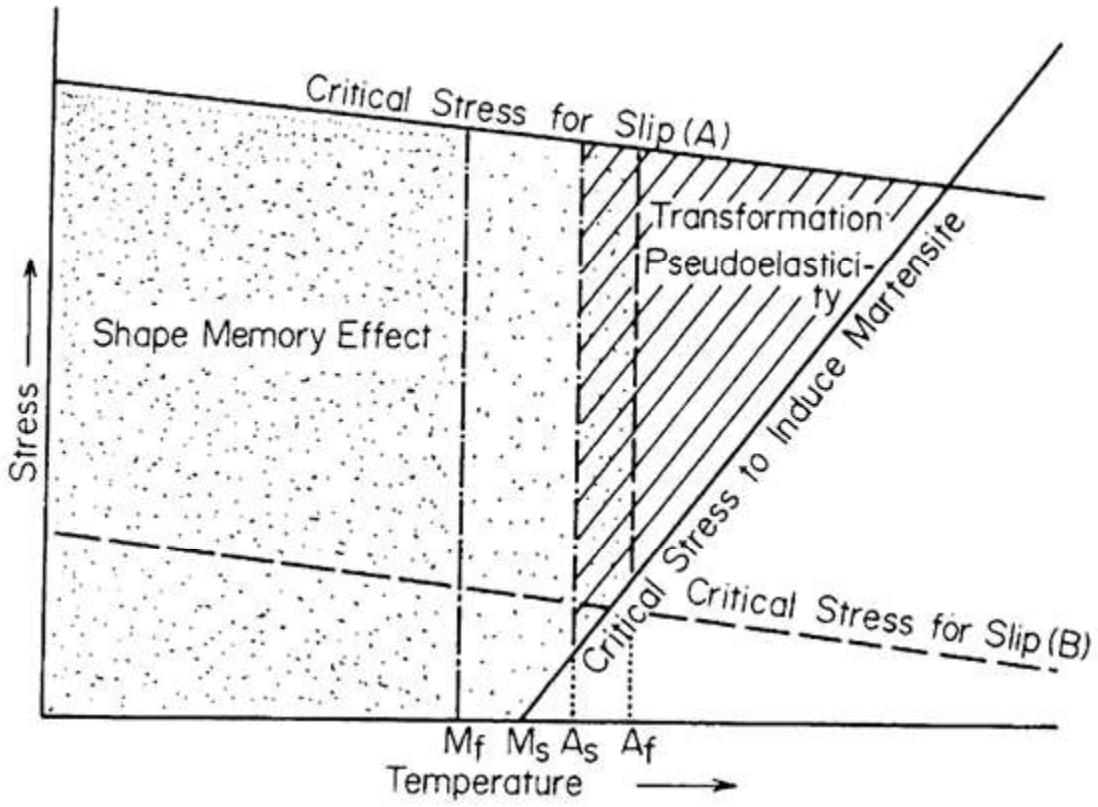

Figure 2.2-1 Illustrative figure of shape memory effect and superelasticity [19].

Fig 2.2-2 represents shape memory effect mechanism. Material is in austenite phase at point A and as the material is cooled, self-accommodation of martensite occurs and martensite forms with twinning. Then, SMA is loaded at point B and detwinning takes place at a certain stress level. Strain increases and the energy increase with the loading is spent for detwinning. Material in martensite phase starts to deform elastically when the detwinning region ends. Material is unloaded between point C and D. Material is in detwinned martensite state at point D until heating is performed. The material fully transformed to austenite via heating and martensite to austenite transformation occurs thus material fully remembers its original shape if it is not plastically deformed.

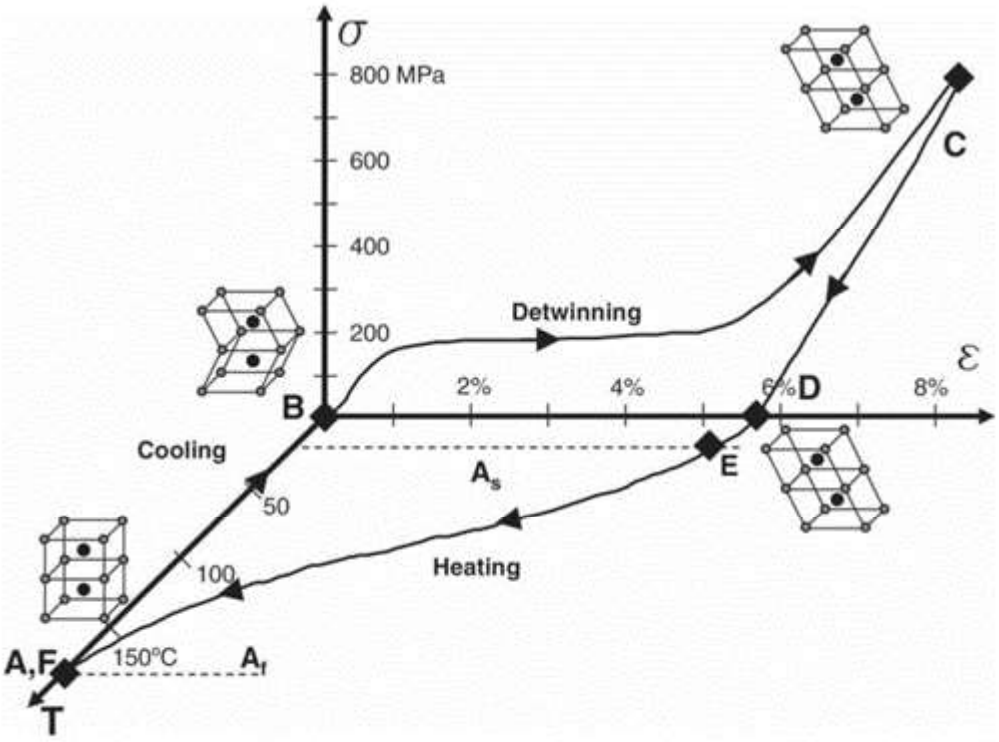

Figure 2.2-2 Illustrative figure of SME [19].

SMAs are able to ‘memorize’ their original parent phase shape as aforementioned earlier. There is another effect named as Two-Way Shape Memory Effect (TWSME), in which alloy is able to remember both phase shapes. This effect can be observed under certain conditions. Internal stress field is a necessity to observe TWSME. Internal stress fields can be obtained via applying following procedures:

- Plastic deformation [21,22]
- Constrained Aging [20]
- Thermal cycling [20]
- Martensite aging [23]

Dislocations and precipitations that are formed during above thermal and thermo-mechanical processes causes internal stress fields. Certain martensite variants are formed as a result of these stress fields and SMA is able to remember both shapes in austenite and martensite. After the discovery of TWSME, various studies have been conducted in the literature [24–28].

2.3. NiTi Based Shape Memory Alloys

Shape memory properties of NiTi alloy have been found in Naval Ordnance Laboratory in 1963. The discovery attracted great attention to shape memory alloys although the shape memory effects and diffusionless transformation were found earlier in Au-Cd and In-Tl alloys [29–31].

NiTi shape memory alloys are the most popular alloys among all SMAs because of its high work output, great superelastic and shape memory properties, biocompatibility and corrosion resistance [2,9,10,11].

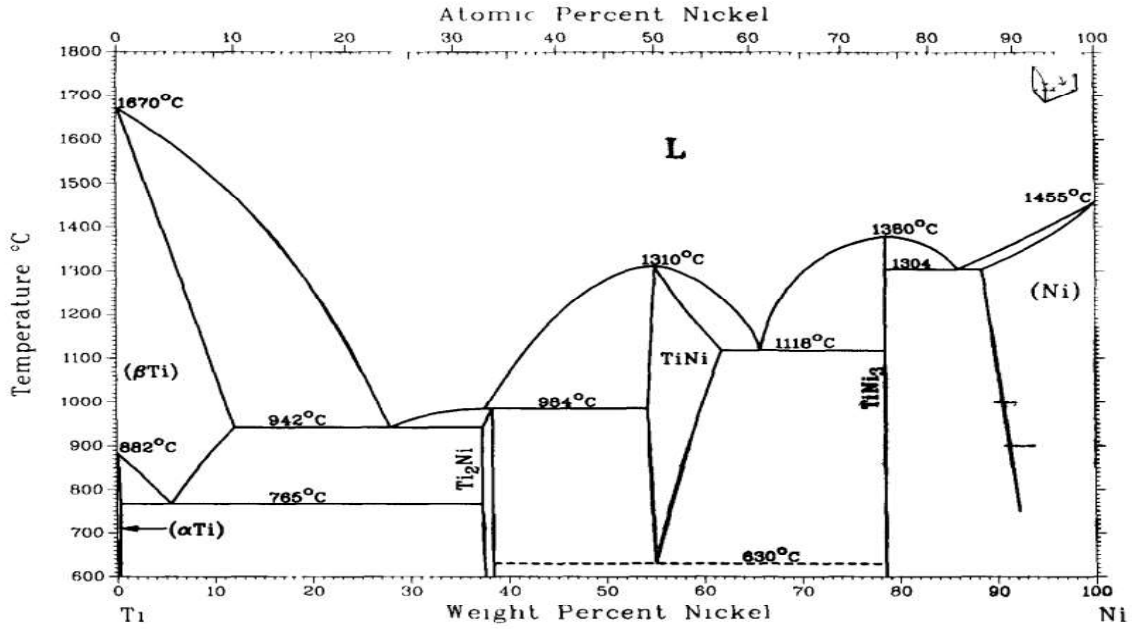

Figure 2.3-1 Ni-Ti phase diagram [31].

Ni-Ti alloys exhibits SME and SE via thermoelastic martensitic transformation. This transformation occurs from parent phase called austenite which has B2 crystalline structure to martensite which has B19' crystalline structure. This transformation may occur in multiple steps. B2 phase transforms to trigonal R-Phase then R-phase transforms to B19' although reverse transformation takes place through a single step which is B19' to B2. Two step martensitic transformation is shown in Figure 2.3-2 with a Differential Scanning Calorimetry experiment result. Ni content, microstructure, aging and thermo-mechanical treatments are important factors to control shape memory behavior of the alloy. For instance, R-phase formation is expected when high internal stress fields exist in the matrix. Alloy prefers to transform from austenite phase to R-phase before martensite due to the necessity of less energy during austenite to R-phase formation.

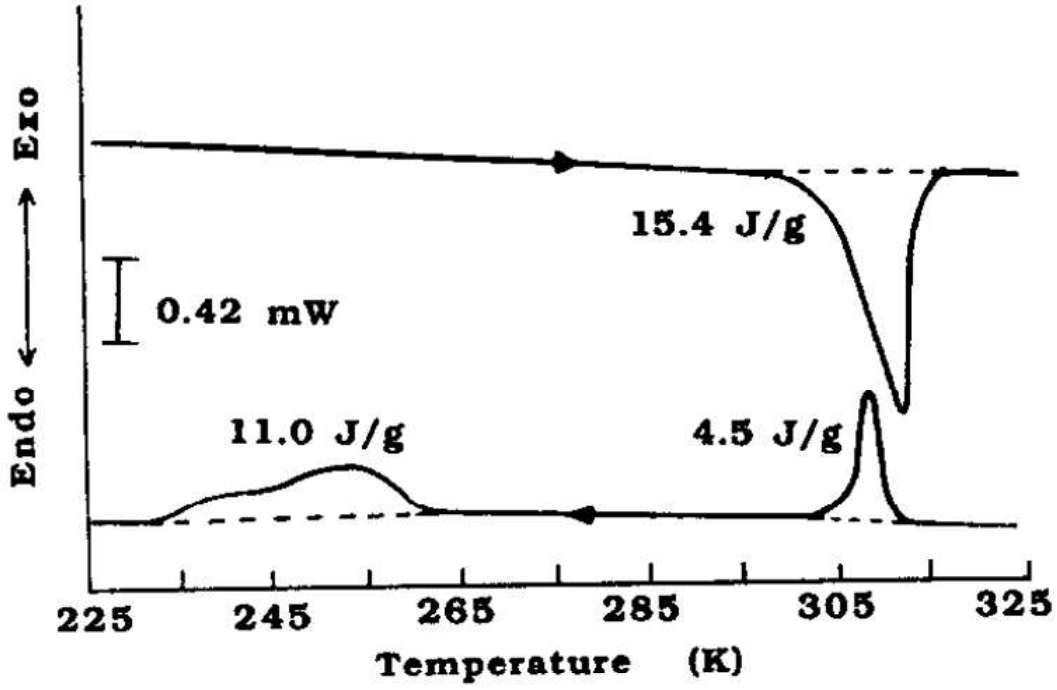

Figure 2.3-2 DSC thermogram of Ti49.8Ni50.2 at. % aged at 773K for 15 minutes[34]

The transformation between B2 to R phase is also martensitic transformation. Two-step transformation is observable in Ni-rich Ni-Ti alloys. It is also observable in ternary Ni-Ti-Fe and Ni-Ti-Al alloys.

In Ni-rich NiTi alloys, Gibbs Free Energy curve of B19' shifts upwards in the presence of Ti_3Ni_4 precipitations thus R-phase transition is triggered before martensitic transformation by precipitation formation due to the stress fields around micron-sized precipitates.

Nucleation and growth take place when B2 phase transforms to R phase in Ti-48Ni-2Al (at. %) alloy on cooling. R-phase diminishes and disappears and B2 austenite phase takes its place on heating. This behavior repeats itself as the heating and cooling cycle continues [19].

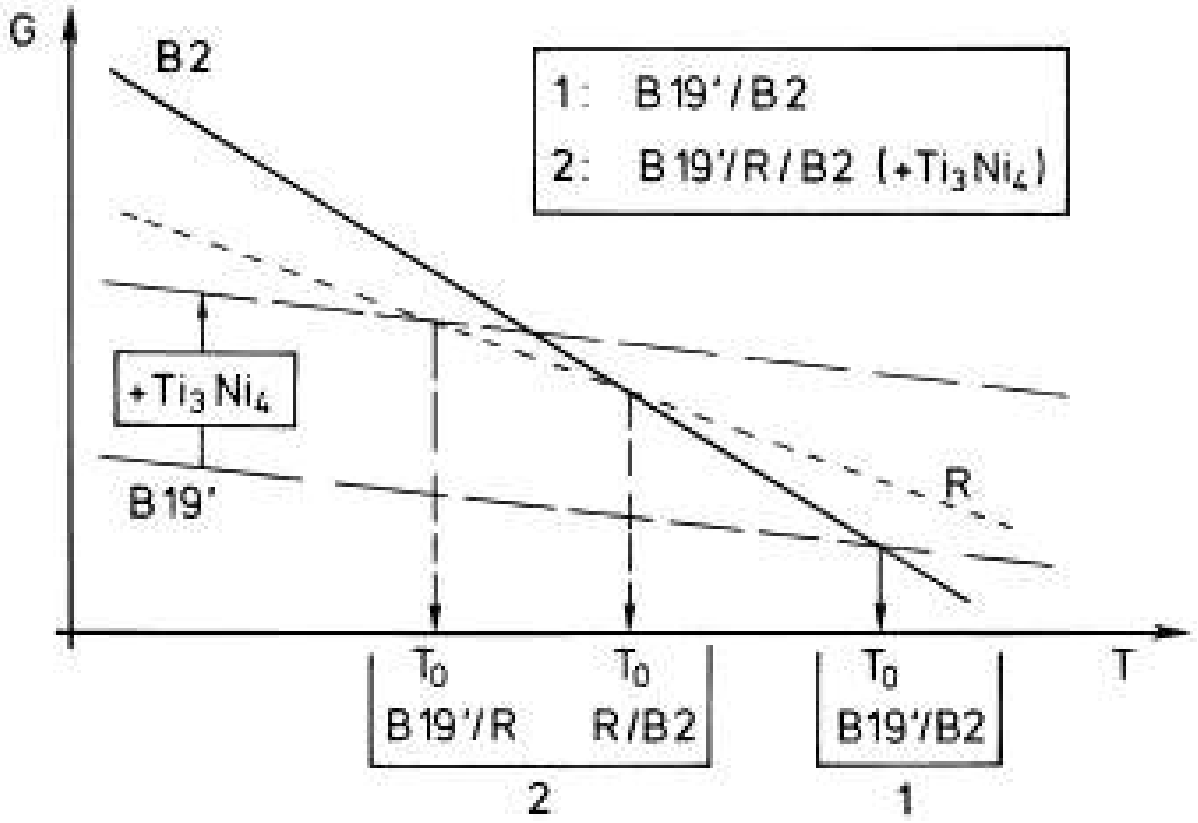

Figure 2.3-3 Thermodynamic explanation of R-Phase of Ni-Rich NiTi alloy [19].

Mechanical and SM properties of Shape memory alloys are highly reliant on the thermal and thermo-mechanical treatments. Thermoelastic alloys can undergo reversible transformation. On the other hand, plastic deformation causes slip which is irreversible. Therefore, increasing the resistance of these alloys to plastic deformation is critical. Increasing the critical stress for slip (CSS) value of these alloys is one way to improve their resistance to plastic deformation, and there are four methods to increase CSS and these are:

1) Work hardening.
2) Precipitation Hardening.
3) Grain refinement.
4) Alloy Hardening.

Alloy hardening will be discussed later in the HTSMA Section

1) Work Hardening

It is important to have good shape memory properties for shape memory alloys thus plastic deformation methods are used to enhance and increase shape memory properties and critical stress for slip (CSS) of SMAs.

High amount of plastic deformation is possible for Ni-Ti alloys since the alloy is highly ductile due to its low elastic anisotropy. It is relatively easy to introduce dislocation to Ni-Ti alloys owing to its high ductility [4]. Dislocation density can be increased by work hardening methods. These are rolling, extrusion or thermo-mechanical cycling.

As can be clearly seen from Figure 2.3-4, tensile experiments that were conducted on cold rolled equiatomic NiTi alloy showed that σ_y^M value was increased about 2.5 times with cold rolling. Besides, SME and PE characteristics were also improved by cold rolling due to the strengthening via plastic deformation [35].

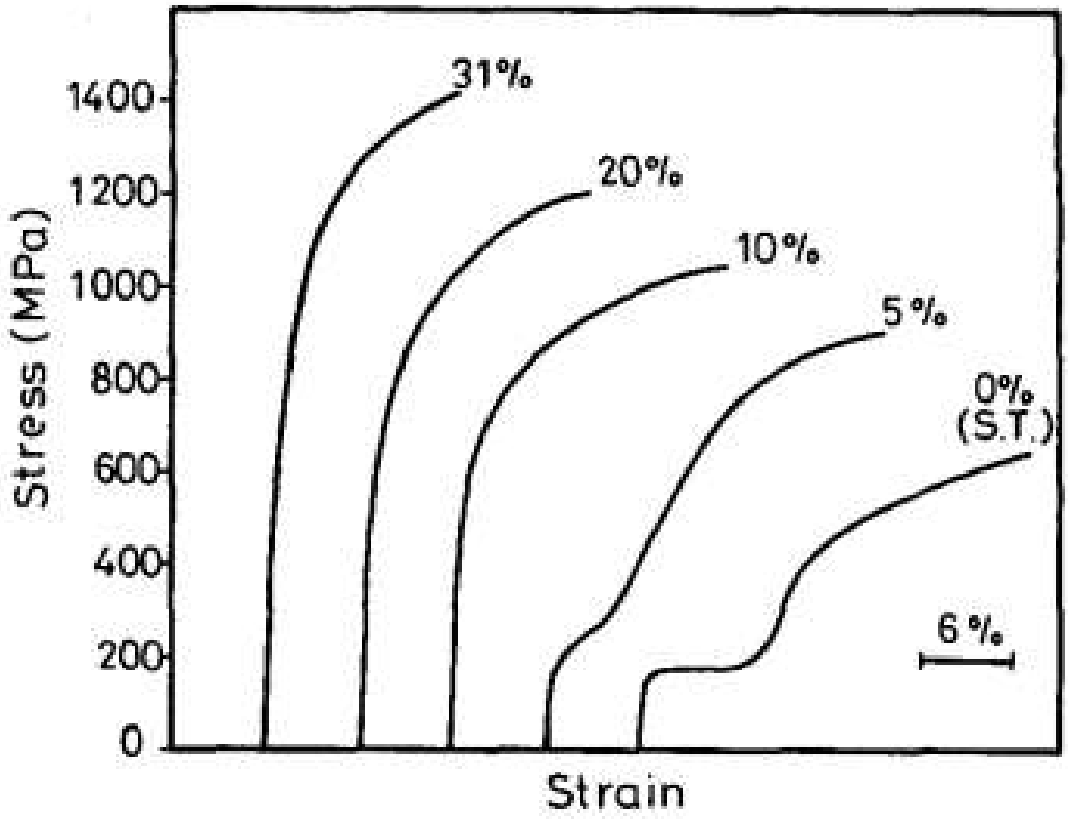

Figure 2.3-4 Effect of cold rolling on strength of the equiatomic TiNi alloy [35].

It is shown in the literature that plastic strain development due to thermal cycling under constant load also decreases with cold rolling and proper heat treatment [36].

Fig 2.3-5 shows the effects of thermomechanical treatments on superelastic behavior of NiTi SMA. Annealing at 400 °C for 1 hour was done after different cold rolling percentages. Experiment was conducted at 50 °C which was 40°C higher than Ms temperature. It can be seen from the Figure 2.3-5 that as cold rolling percentage was increased, recovered strain values increased as well. The alloy showed complete recovery when cold rolling percentage reached 25%.

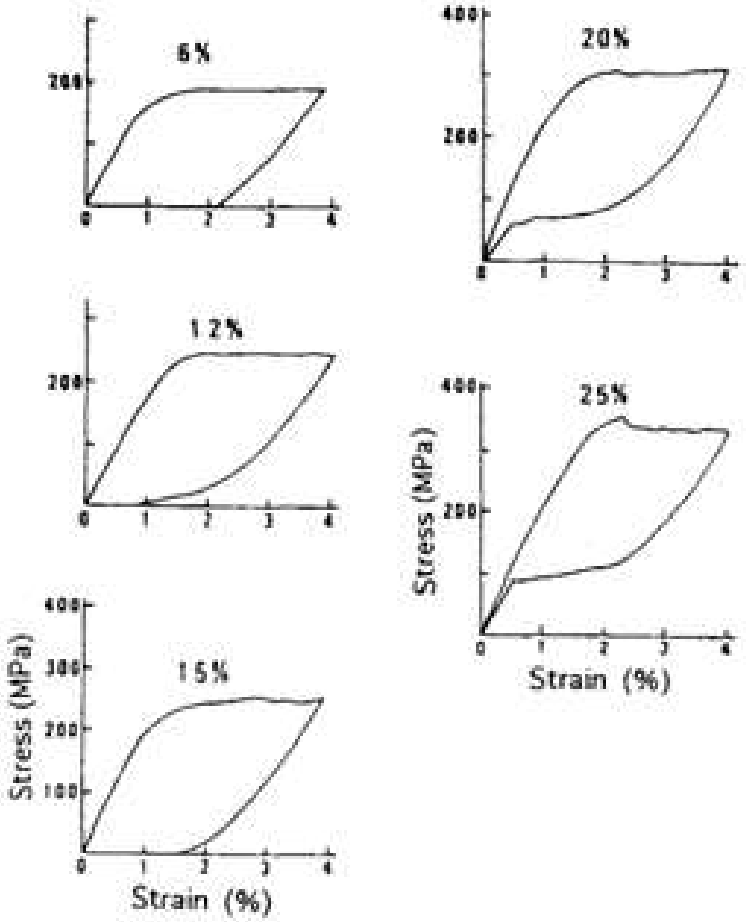

Figure 2.3-5 Cold rolling and annealing effect on superelasticity [19].

Thermal or thermo-mechanical cycling also leads to observe an increase in dislocation density with work hardening addition to the work hardening via applying deformation processes. Dislocation density increase with thermal and thermomechanical cycling leads to observe less irrecoverable strain values and cyclic stability.

As mentioned before, thermal and thermomechanical cycling change the shape memory properties such as the transformation temperatures, actuation, transformation or

irrecoverable strain values and thermal hysteresis together with the stability of these properties with the number of cycles due to the evolution of the microstructure.

For instance, Figure 2.3-6 shows the loading-unloading cycling effect on the superelastic behavior of Ni50.2Ti49.8 at. % alloy. The figure clearly demonstrated that the stress levels of upper and lower plateau decrease as number of cycle increases. As a result, the difference in stress levels between the upper and lower plateaus, known as mechanical hysteresis, reduces as the number of cycles increases. This might be due to the fact that the dislocation density increase leads to the formation of internal stresses and thus, lower stress magnitude is enough to induce martensite to the alloy. Additionally, the irrecoverable strain value, which is noticeable in first cycle after unloading, disappears with the cycling.

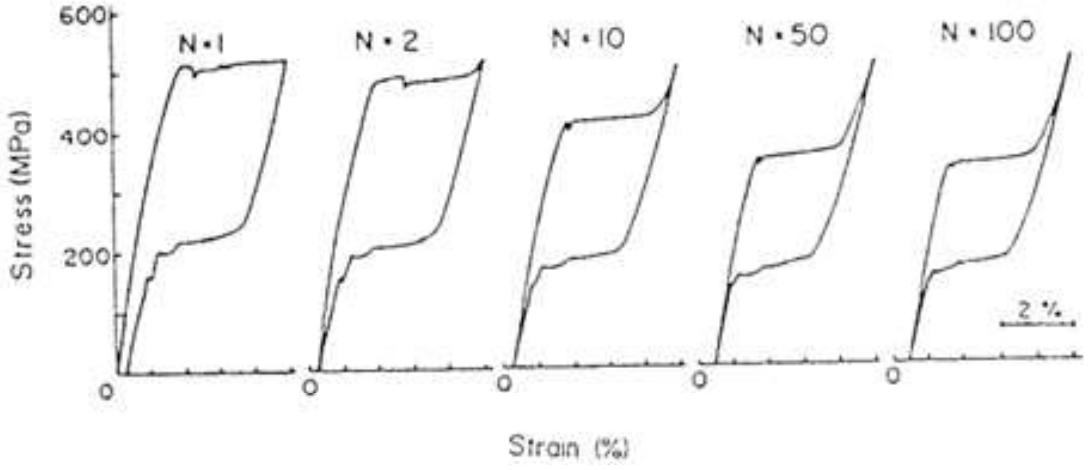

Figure 2.3-6 Mechanical cycling effect on superelasticity [19].

Fig 2.3-7 shows the results of thermal cycling under constant stress experiment on Ti-50.2at%Ni alloy. R-phase transformation diminishes after 20 cycles and as cycle number increases transformation and irrecoverable strain values together with hysteresis decrease. Additionally, transformation temperature change during the first 20 cycles is more than that of the change after 20th cycle. This means that the stability of the shape memory properties is attained with the thermal cycling under constant load. All these observations are due to the formation of dislocations and the increase in the strength of the alloy. As the CSS increases all metals and metal alloys show higher strength magnitudes [19].

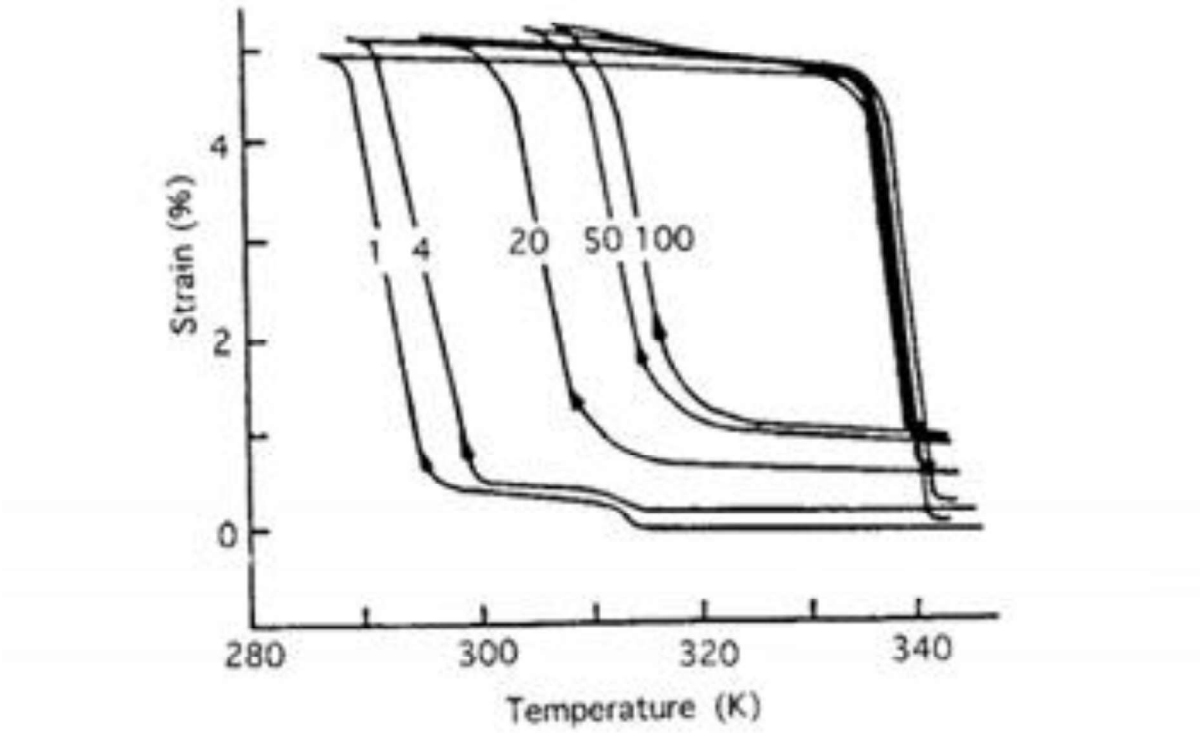

Figure 2.3-7 Thermal cycling effect on shape memory behavior [19].

2) Precipitation Hardening

TTs of NiTi and NiTi-based alloys can be tailored by the change in chemical composition, application of various aging procedures and plastic deformation. Nickel content plays an important role for transformation temperatures. For instance, if at% of Nickel is higher than 50% the transformation temperatures of the alloy decreases [37].

In Ni-rich NiTi alloy system, various precipitation formation is observed with certain aging heat treatments [4]. Ni-rich compositions tends to form precipitations due to their instability of B2 compositions at low temperatures. Precipitation formation affects diffusionless phase transformation because of the alteration in the local chemical composition and stress fields around the coherent precipitates [37].

Khalil-Allafi et.al. studied the influence of Ni4Ti3 precipitates on MT of 50.7 at. -% Ni-Ti shape memory alloy. Different aging procedures were compared. Solution annealed and aging at 773 K for 100h showed single step transformation such that transformation

follows the route B2 to B19' upon cooling and B19' to B2 upon heating. Nevertheless, aging at 773K for 1h and 10h specimens demonstrated multiple step transformation both upon heating and cooling that is caused by R-phase transformation which became prominent with the aging heat treatment. In literature it was told that the transformation route became B2 to R to B19' through cooling and B19' to R to B2 through heating however it was shown that R-Phase and B19' phases coexist after the first cooling peak in two step transformation [38].

It is energetically favorable to follow intermediate R-Phase stage with Ni4Ti3 precipitation formation which leads to multiple step transformation in the case of aging at 773K for 1h and 10h and it is also said in the same study that precipitation nucleation is influenced by external and internal stresses. It is said that precipitation formation behavior changed from heterogeneous to homogeneous under stress aging condition. Three-step transformation that occurred in 10h aged specimen is explained such that first peak demonstrates R-phase formation. Second peak demonstrates B19' formation in regions which contains precipitates. Third peak demonstrates B2 to B19' transformation in regions which are precipitate-free [39].

Martensitic transformation was not affected by precipitations when precipitates become larger as in the 100h aged condition. Large precipitates cause the interparticle space to be large as well thus, transformation becomes single step. Also, larger precipitates are not able to affect the nucleation process of martensite phase as a consequence of loose coherency[38].

As a summary of the subsection, various precipitation formation (Ti_3Ni_4, Ti_2Ni_3 and $TiNi_3$, is possible with proper thermal treatment. Ti_3Ni_4 and Ti_2Ni_3 precipitates significantly improves the strength of the alloy at the cost of embrittlement which causes low ductility. Aging is also practical application to modify transformation temperatures for desirable application [40].

3) Grain Refinement

The main problem that is needed to overcome in NiTi-based SMAs is the cyclic instability of the shape memory properties such as transformation temperatures, transformation and

irrecoverable strains and transformation hysteresis. Therefore, the instability of the properties with the number of actuation cycles limits their applications. To tackle with this problem, increasing the slip resistance and thus, minimizing the plastic accommodation during phase transformation is the main objectives in NiTi-based alloys. One method to increase the slip resistance is to obtain smaller grains and the grain refinement can be achieved via applying Severe Plastic Deformation (SPD) techniques. High pressure torsion (HPT) and equal channel angular extrusion (ECAE) methods are among severe plastic deformation methods. It is reported in the literature that HPT and ECAE methods improves the mechanical properties due to the microstructural enhancement [41].

Kockar et.al. investigated near equiatomic NiTi alloy's shape memory behavior after severe ausforming with ECAE and stated that decrease in thermal hysteresis compared to cold rolled+ low temperature annealed sample. Isobaric thermal cycling experiments were done to investigate mechanical stability and these experiments showed that ECAE processed sample demonstrated better stability than that of cold rolled+annealed sample. This stability difference became more pronounced under higher stress level. Hysteresis values of ECAE'd sample stayed constant under both 100 and 200 MPa stress levels. The enhancement of mechanical behavior of equiatomic NiTi alloy was attributed to refinement of microstructure which increased the CSS) due to fine deformation twin formation during ECAE [42]. Another ECAE study revealed that ECAE procedure at high temperatures such as 400 and above leads to nano ranged (100-300 nm) grain refinement. [43].

It can be seen from the Figure 2.3-8 that DSC cycles shift while the alloy was in homogenized condition. On the other hand, ECAEd samples' DSC graphs were stable throughout three DSC cycles which indicates the increase in thermal stability after ECAE processes.

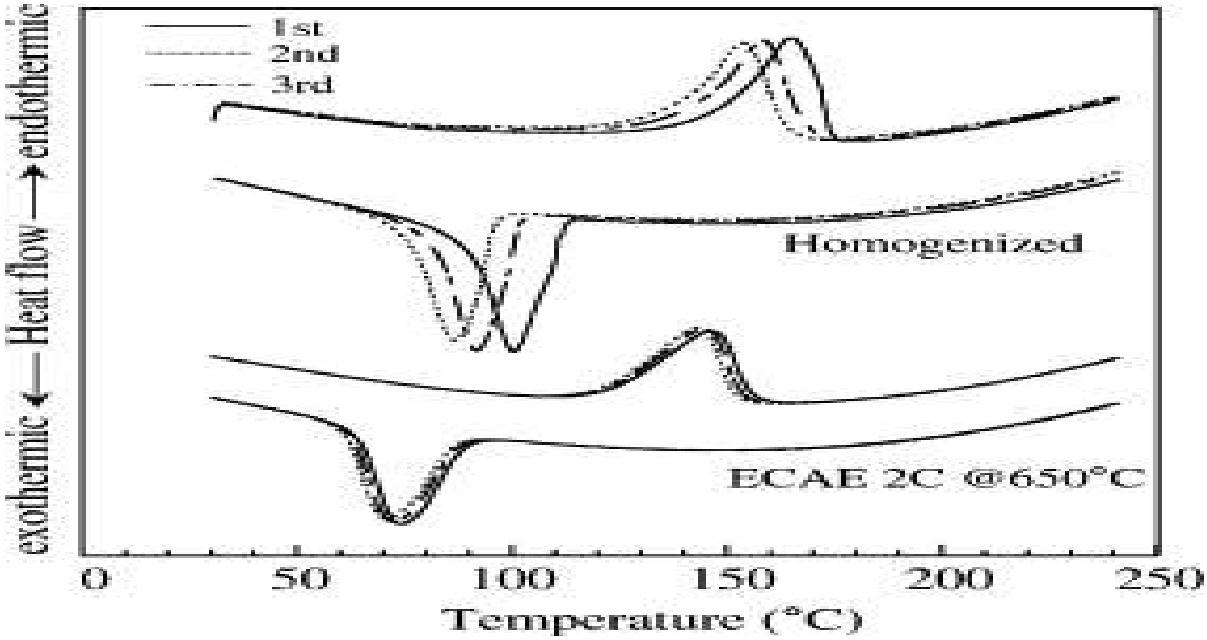

Figure 2.3-8 DSC results of 49.8Ni–42.2Ti–8Hf alloy after ECAE and homogenization process [43].

Recoverable transformation and total irrecoverable strain results, which were gathered from isobaric experiments conducted under 100 and 200MPa are shown in Figure 2.3-9. Comparison between cold drawn + annealed sample and ECAEd sample showed that ECAE process decreased the accumulated irrecoverable strain values. The dimensional stability was maintained with ECAE while the recoverable transformation strain magnitudes stayed constant [42].

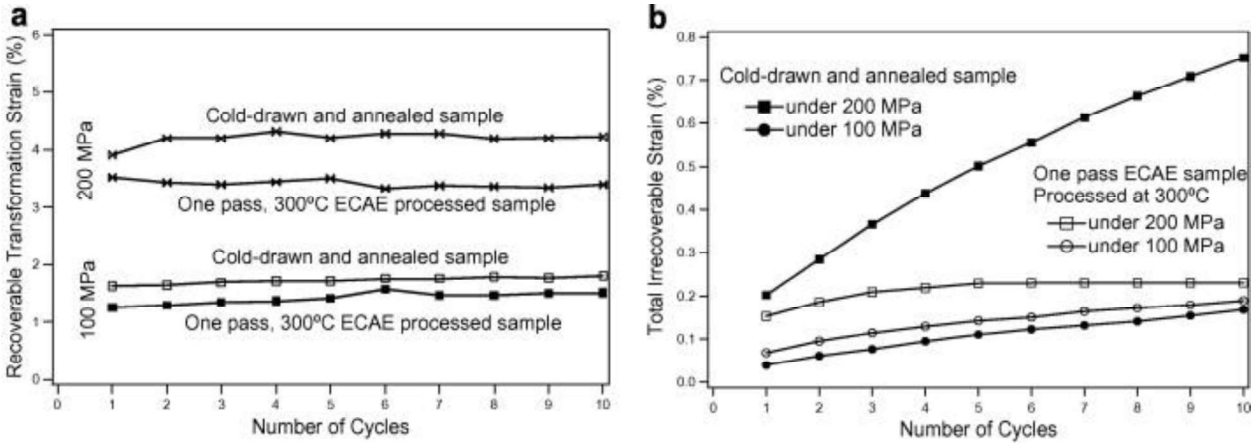

Figure 2.3-9 Comparison of (a) recoverable and (b) accumulated irrecoverable strains of ECAEd and cold drawn + annealed samples [42].

2.3.1. Ternary Additions to NiTi

Ni-Ti binary alloys' transformation temperatures are limited to 100-120 °C. These transformation temperatures strongly depend on chemical composition of the alloy. Increasing Ni content above equiatomic composition leads to decrease of transformation temperatures but changing Ti content barely affects transformation temperatures. Limitation of transformation temperatures leads researchers to choose a way investigating ternary element addition to NiTi system. It is reported that vanadium, chromium, manganese or aluminum substitution with titanium decreases transformation temperatures. Similarly, cobalt or iron replacement of Nickel also decreases transformation temperatures [19]. Most popular Ni-Ti-based ternary alloys, which are frequently emphasized in the literature, will be briefly discussed below.

2.3.1.1. NiTiCu

Cu addition to Ni-Ti alloy led to a decrease in thermal hysteresis since interface movement became easier as an effect of Cu addition [19].
Hysteresis decrease became more prominent as Cu content increases as shown in Figure 2.3.1.1-1, which is represented below.

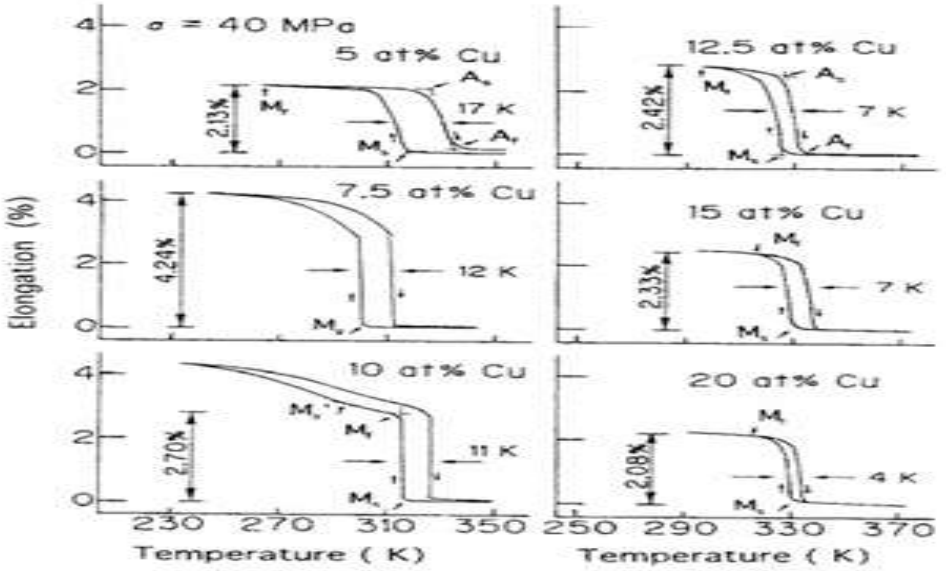

Figure 2.3.1.1-1 Thermal cycling of Ti-Ni-Cu alloy under constant load [19].

Figure 2.3.1.2-1 shows that mechanical hysteresis values also decreased with the addition of Cu under same stress level when compared to Ni-Ti and Ni-Ti-Nb alloys [19].

Another effect of Cu addition to binary Ni-Ti alloy is that Cu suppresses aging effects therefore prevents Ti3Ni4 formation. Thus, composition sensitivity of transformation temperatures to the composition of NiTi alloy was reduced with addition of Cu. However, Cu addition of more than 10 at. % detoriated formability and caused embrittlement [19].

2.3.1.2. Ni-Ti-Nb

Wide mechanical hysteresis is sometimes desirable for applications such as coupling devices [19]. Nb addition is effective to widen the mechanical hysteresis. During martensitic transformation Nb particles deforms plastically which is the reason of having wide thermal hysteresis.

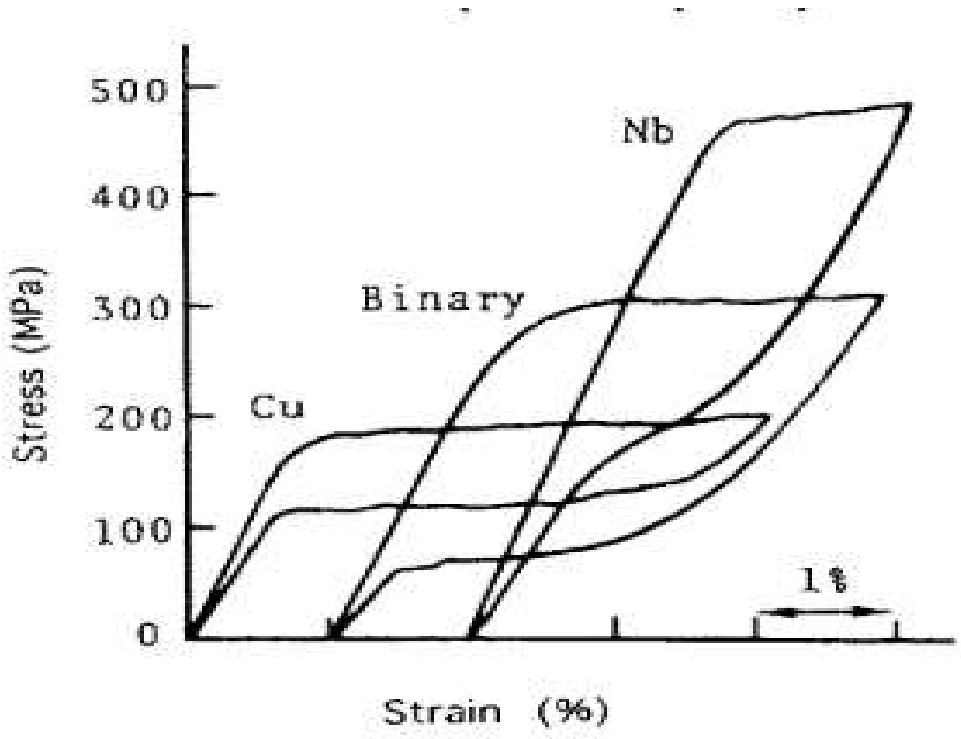

Figure 2.3.1.2-1 Ternary alloying effect on mechanical hysteresis of binary 30% cold rolled + annealed at 400 °C, Ni50.2Ti49.8 at.%, Ti20Ni40Cu10 at. % annealed at 800 °C and Ti48Ni50Nb2 at. % annealed at 850 °C [19].

Addition of Pd, Pt, Zr and Hf to NiTi alloy leads to an increase in TTs. Below, ternary alloys which show high transformation temperatures are summarized.

2.3.1.3. Ti-Ni-Pd

Pd addition to Ni-Ti binary alloy increases transformation temperatures. It is possible to control TTs with controlling the alloy composition. It is stated in the literature that austenite finish temperature can be even increased to around 800 K with the addition of 45 at. % Pd [44].

The same study also revealed that transformation strain decreased as Pd content was increased due to the alloy hardening. Thus, work output decreased under same stress level with increasing Pd content.

The drawback of Pd addition is poor SME at high temperatures due to the decrease in CSS thus plastic deformation takes place before martensite reorientation. It is possible to improve SME behavior of the thermo-mechanically treated alloy such as cold rolling and annealing at proper temperatures. Figure 2.3.1.3-1 shows the improvement of superelastic recovery via applying thermo mechanical treatments on Ti-Ni-Pd ternary alloy. Contrary to this observation, irrecoverable strain decreased with increasing Pd content.

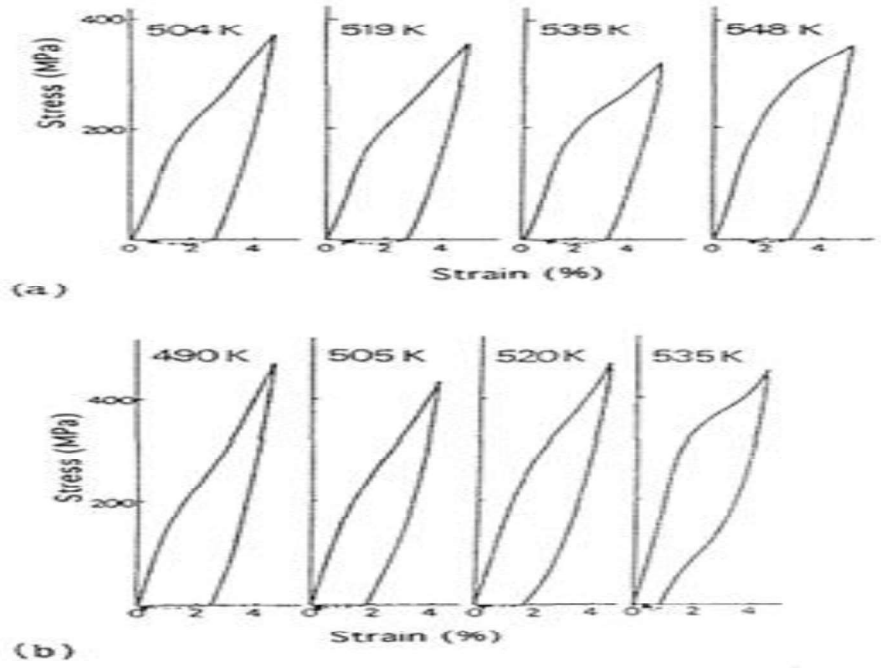

Figure 2.3.1.3-1 Improvement achieved by thermomechanical treatment (a) fully annealed (b)thermos-mechanically treated Ti50Pd30Ni20 SMA [19].

2.3.1.4. NiTiPt

Effect of Pt addition to NiTi alloy was investigated and Pt was found to be another element to increase transformation temperatures of binary NiTi alloy [2,3,4]. Pt addition is effective to increase transformation temperatures when the content of Pt is above 10 at% and below 10at%, transformation temperatures barely change [47]. There have been also studies on NiTiPt ternary alloy with low Pt content. Ti-42.5at. %Ni-7.5at. %Pt was investigated and compared with NiTi binary alloy. Failure strength of aforementioned NiTiPt SMA was found higher than that of NiTi alloy at elevated temperatures. Failure strain was also compared and NiTi and NiTiPt alloy revealed similar failure strain levels at the same testing temperatures. Additionally, NiTiPt alloy showed less residual elongation values than that of NiTi alloy under 7 MPa stress level and both alloys in this study were in the same heat treatment conditions. Besides, NiTiPt alloy showed smaller stress hysteresis when compared to NiTi alloy in addition to less temperature dependence against increasing stress level [47].

2.3.1.5. NiTiZr

Addition of Zr to Ni-Ti binary alloy increases transformation temperatures when Zr content is above 10 at.%. However, transformation strain decreases as Zr content increases [48].

Aging studies were done on Ni-Rich NiTiZr alloy at 500,550 and 600 °C. Aging durations were investigated from 1 hour up to 200 hours. It is found from the aging studies that precipitates which are smaller than 160 nm did not affect martensite growth. Martensite variants are able to grow through nano-sized precipitates. On the contrary, aging at 600 °C for long periods led to form larger precipitates which are several hundred nanometers long. These relatively larger precipitates interfered with martensite variants and made martensite variants difficult to grow thus the transformation was inhibited. It is reported that aged specimens with precipitates that are smaller than 160 nm exhibit great dimensional stability up to 300 MPa applied stress level although precipitates with the size of several hundred nanometers showed unrecovered strain under 200 MPa and above [49].

Different aging procedures were applied to Ni-Ti-Zr ternary alloy to investigate the stability of the alloy. It is found that thermal cycling has notable effects on transformation temperatures which are vigorously connected by starting microstructure. Prolonged aging duration (1-3) was investigated in order to observe long exposure to working temperatures and it is found that prolonged aging suppressed the martensitic transformation of the alloy which showed the inadequate nature of NiTiZr ternary alloy at relatively higher working temperature (250°C) [50].

2.3.1.6. NiTiHf

Nickel-rich NiTiHf alloys were investigated widely in the literature since they have shown very optimistic thermal and dimensional stability and great shape memory properties by aging [37]. Increasing Ni content above equiatomic composition, caused transformation temperatures to decrease. Precipitation formation becomes possible in Ni-rich NiTiHf HTSMAs. Transformation temperatures increases via precipitation formation which needs proper heat treatment. The nano-sized precipitates which are generated in NiTiHf alloys with a Ni content higher than 50 at.%, have been named as H-phase in the literature [51].

H-phase precipitates decrease the nickel content from the matrix therefore the transformation temperatures of NiTiHf alloys can be tailored Precipitation not only leads transformation temperatures to increase but also strengthens the alloy. Therefore, thermal and dimensional stability can be increased with precipitation formation as well [51].

Saghaian et.al. investigated Ni51.2Ti28.8Hf20 at% alloy in detail. Various aging procedures were applied, and materials were tested under compression. It is shown that as aging parameters changed, mechanical properties also changed. Alloy showed superelasticity up to stress magnitude of 2 GPa. It is stated that strength of the material strongly relies on the H-phase precipitates' sizes. Interparticular space between precipitates were small for low temperature (<500°C) aging conditions which leads precipitates to act as obstacles for dislocation motion thus, high level of strengthening was observed which cannot be observed when aging temperature was increased since interparticular space was widened and dislocation motion became easier [52].

There are also other studies regarding precipitation hardening. Karaca et.al. investigated Ni50.3Ti29.7Hf20 at% alloy via following numerous aging procedures. 300,400,500,600,700 and 800 °C were selected as aging temperatures and detailed aging studies were conducted at these temperatures for 5 mins,15 mins,30mins,1 hour, 3 hours and 24 hours. Transformation temperatures of aged specimens were shown and isobaric thermal cycling experiments were carried out on selected specimens. The shape memory properties of as-extruded, aged at 550 °C for 3 hours and 650°C for 3 hours specimens

were compared. It is shown that aging at 550 °C for 3 hours revealed the best mechanical behavior. Sample which was aged at 550 °C for 3 hours also showed the best superelastic response. Work output values of same specimens were compared and it is shown that, the sample which was aged at 550 °C for 3 hours demonstrated highest work output value. Even though the transformation temperatures increase with precipitation formation, Ni-rich NiTiHf alloys' transformation temperatures are still lower than that of the equiatomic NiTiHf alloys [51].

Umale et. al. studied effects of compositional changes on MT of NiTiHf SMAs. NiTiHf alloys were fabricated via vacuum arc melting with various chemical compositions and martensitic transformation characteristics were compared. It is stated that transformation temperatures of NiTiHf alloys could be tailored from -170 °C to 500 °C by changing nickel and hafnium contents. It is shown that Hf addition to Ni-Lean NiTiHf alloy did not increase transformation temperatures up to 10% of Hf addition [8].

Karakoc et.al. studied the effects of applied stress on functional fatigue behavior of Ni-rich NiTiHf alloy. Ni50.3Ti29.7Hf20 specimens were aged at 550 °C for 3 hours and were tested under 200,300,400 and 500 MPa stress levels. Martensite strain, accumulated austenite strain, and actuation strain values were compared. It is stated that as stress level increased, actuation strain values also increased due to the oriented martensite under higher stress levels. Actuation strain values decreased at all stress levels as the cycle number increased which was attributed to the dislocations generated during thermal cycling such that generated dislocations led to pin martensite thus actuation strain values decreased. Post-mortem DSC graphs also supported this argument since transformation enthalpy values were lowered after functional fatigue experiments [53].

Karakoc et. Al. also investigated role of Upper Cycle Temperature (UCT) on martensitic transformation on the same alloy.300°C and 350°C of UCTs were selected and 300 MPa constant load was applied in the study. It is stated that actuation strain values increased as applied stress level was increased and as UCT was increased functional fatigue life decreased in these conditions. 50 °C of UCT increase led to higher irrecoverable strain under same stress level. Also, as stress increased irrecoverable strain increased as well while UCT was kept constant. Lower UCT resulted in a drop in actuation strain as the number of cycles increased, whereas greater UCT resulted in a rise in actuation strain as

the number of cycles increased. It is also stated that higher stress values and UCT led to intergranular fracture. On the other hand, lower stress level and higher UCT led to observe transgranular fracture [54].

There are also other studies regarding NiTiHf alloys other than their actuation abilities for long cycles. Hite et.al. investigated NiTiHf SMA in terms of thermal storage properties and considered NiTiHf alloy as a promising high temperature Phase Change Material (PCM). NiTiHf SMA was compared with other solid PCMs and stated that 10 times better Figure of Merit (FOM) was displayed by NiTiHf compared to other PCMs. Additionally, NiTiHf and NiTi were compared and lower hysteresis and at least 2 times better FOM were obtained with NiTiHf [55].

2.4. Rolling Studies on NiTiHf Alloys

Solid solution hardening is a possible way to improve SME, however, as entropy increases, heterogeneities and possibility of segregation become a serious problem in high entropy alloys which has been mentioned in the literature [15,16,17,18].

Aging studies on the literature mentioned earlier in this section. Precipitates are not possible to form in equiatomic and Ni-lean NiTiHf SMAs. Aging is not an option to improve SME in equiatomic and Ni-lean NiTiHf SMAs. Thus, grain refinement and work hardening are the only reasonable options to improve SME of these SMAs.

Work hardening effects on NiTi binary alloys were discussed earlier in this section. It is important to study work hardening on SMAs since rolling seriously effects shape memory behavior thus work hardening studies of NiTiHf ternary alloys will be briefly mentioned below.

Hot rolling studies were conducted in the literature since NiTiHf alloys are hard to deform materials at lower temperatures [19,20,21,22]. Belbasi et.al. investigated hot rolling effects on microstructure of NiTiHf alloy yet effects on shape memory behavior is not mentioned in the study [59]. Belbasi et.al studied hot deformation behavior of

Ni49Ti36Hf15 alloy under various strain rates and temperatures and mentioned the formation of flow localization for each strain rates and temperatures [60].

Kockar et.al studied equal channel angular extrusion effects on Ni-lean Ni49.8Ti42.2Hf8 shape memory alloy. It is stated that CSS for slip was increased after ECAE process as a result of grain refinement, texture formation with ECAE and strain hardening. ECAE leads to obtain better thermal stability. It is also mentioned that residual strains were decreased and higher actuation strains were obtained under constant stress experiments. ECAE is such a great technique to improve shape memory effect of SMAs nevertheless it is a challenging process to apply. Grain refinement that is achieved via ECAE may not be effective if the actuation takes place at elevated temperatures since it is well known that finer grains lead to grain boundary sliding at high temperatures and causes more serious creep damage [13].

Babacan et.al investigated cold and warm rolling effects on shape memory effects of Ni50Ti30Hf20 shape memory alloy. In this study, as-cast Ni50Ti30Hf20 alloy was subjected to homogenization at 1050 °C for 72 hours then extrusion was applied at 900 °C with a 4:1 reduction of area then, rolling was applied. 10 and 15% of cold rolling was applied and cold rolled specimen showed no transformation before additional heat treatment. Cold rolled specimens were subjected to short time annealing at 450,500,525,550 and 600 °C. Warm rolling studies were conducted at 300,400,500,600 and 700 °C. 55% of thickness reduction was obtained via warm rolling at temperatures 500 °C,600°C and 700 °C respectively. Additionally, thickness reduction of 10%, 15% and 40% were achieved by warm rolling the samples at 300, 400 and 500°C, respectively. No additional heat treatments were applied to warm rolled samples in the study.

All the rolled specimens' transformation temperatures were lower than that of the as-extruded condition except the specimen which was rolled at 700 °C showed higher transformation temperatures. It is stated that better shape memory properties were obtained via isobaric experiments which were conducted on the specimen cold rolled for 15% and annealed at 500 °C for 30 minutes. It is also stated that both cold rolled and warm rolled specimens demonstrated enhanced dimensional stability with respect to as-extruded specimen in the study [61].

In the study that was discussed above, functional fatigue experiments were done for only 100th cycle and all the conclusions were done by investigating the first 100 cycles. It is important to reveal life-time behavior of SMAs since SMAs can be utilized as actuators in numerous industries. Upper cycle temperature that was used in the study was 450 °C. Studies conducted on NiTiHf SMAs that have higher transformation temperatures are limited in the literature to the author's best knowledge and there is no rolling study on equiatomic Ni50Ti25Hf25 alloy thus it is important to reveal rolling effects on shape memory behavior on an alloy that has higher transformation temperatures since operating temperature severely affects shape memory behavior [54].

2.5. Heating/Cooling Rate Effect

Most of the studies in literature, DSC experiments have been conducted with heating/cooling rate of 10 °C/min. However, in some studies, different heating/cooling rates were investigated. Wang et.al. studied cooling/heating rate effect on the TiNiCu ternary shape memory alloy by DSC and stated that transformation temperatures of the SMA depends on heating cooling rate. It is also stated that austenite finish and martensite finish temperatures affected by heating cooling rate such that Af was increased while Mf was decreased as heating cooling rate was increased. Martensite start and austenite start temperatures were said to be not affected by heating cooling rate [9]. Nurveren et al. also investigated heating cooling rate effect on NiTi binary alloy and observed that As and Ms temperatures did not change while Af and Mf temperatures were affected by the heating cooling rate [10].

Shape memory alloys can be used as actuators thus it is important to determine cooling/heating effect on MT behavior. Monteiro et.al. investigated actuation behavior of Ni-rich NiTi binary alloy. Different heating rates were applied via joule heating while cooling was not controlled in this study and provided via natural convection. Different behaviors were observed with different rates although the difference was not clearly noticeable. Stress values were changed by around 20 MPa and strain values were obtained to be different by about 0.2%. Also, the experiment results did not show a meaningful trend [12].

There were other studies regarding cooling rate via applying furnace cooling, water quenching, and ice-water quenching after heat treatment process. It was reported that TTs of Ni-rich NiTi binary alloys were changed since Ni-rich NiTi alloys have the tendency to form precipitates during cooling as well [62,63].

These studies were not investigating the heating cooling rate while thermal cycling and studies above did not investigate mechanical behavior of an SMA with following controlled heating-cooling rates. Thus, it is important to investigate heating cooling rate effect under load and no-load conditions to observe the effect of rate change on the thermo-mechanical behavior of SMA. The studies, which were discussed above, did not take thermodynamical rules into consideration.

3. EXPERIMENTAL METHODS

3.1. Materials

Equiatomic Ni50Ti30Hf20 (at. %) alloy was used to investigate the effect of cooling rate on martensitic transformation and shape memory behavior of the alloy and equiatomic Ni50Ti25Hf25 (at. %) was used to investigate thermo-mechanical treatments on shape memory behavior of very high Hf content HTSMA. It is worth to mention that all compositions of the alloys in this study were given in atomic percentage.

Both materials were produced with the same method. Commercially pure Ni, Ti, Hf were melted via vacuum induction melting under the atmosphere of high purity argon. After the casting process, materials were sealed in mild steel can and subjected to hot-extrusion process at 900°C with 4:1 area reduction. Homogenization was conducted for Ni50Ti25Hf25 (at. %) at 1050°C for 2 hours Extruded materials will be referred as 'As-Extruded' and homogenized samples will be referred as ‘Homogenized’ throughout the thesis.

Figure 3.1-1 As-Extruded Billets

3.2. Heating/Cooling Rate

The importance of heating/cooling rates was summarized in the light of literature, in earlier section of the thesis. The heating/cooling experiments were carried out to investigate the rate effect on MT and SM properties of Ni50Ti30Hf20 (at. %) alloy.

Heating/Cooling rates were taken as 5 °C/min, 10 °C/min, 15 °C/min with a focus on maintaining the same heating/cooling rates in stress-free DSC experiments and isobaric experiments as well.

Heating/cooling rates were provided by custom built heating/cooling unit on UTEST universal material testing machine and heating was achieved via conduction with resistance heaters that are attached to the grips and cooling was sustained via conduction as well, with cycling water through copper tube that wrapped to the grips. Thermal blanket was used to insulate grips for minimizing heat transfer to the surroundings.

3.3. Sample Preparation

Differential Scanning Calorimeter (DSC) experiments were done with the aim of determining the transformation temperatures and enthalpy values of samples under no load condition.

All DSC samples were prepared as follows,

Samples were cut by diamond precision cutter via low speed and without load in order to avoid any remnant stress that might be induced during cutting process since transformation characteristics change in the presence of stress.

DSC samples were mechanically ground with 400 grid sandpaper to eliminate any stress induced regions close to the surfaces of the samples. Additionally, oxide layer that forms during thermo-mechanical process was also removed via grinding.

Dog bone tensile specimen was used in mechanical experiments. Dimensions of the sample were derived from ASTM E8. Sample dimensions were proportionally reduced according to standard. Fig 3.3-1 shows the dimensions of the dog-bone tensile test specimen that were used in this study.

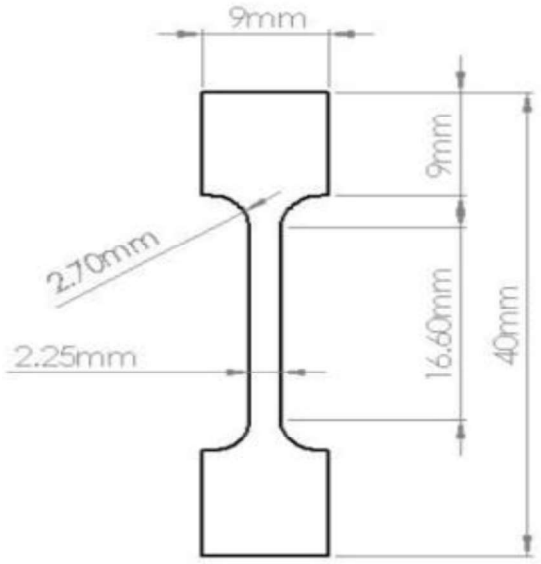

Figure 3.3-1 Dimensions of dog bone specimen [64].

Tensile test specimens were cut from the billet via Wire Electrical Discharge Machine (W-EDM). W-EDM is chosen for cutting process since W-EDM causes minimal residual stress on the surface.

Figure 3.3-2 Cylindrical Furnace that was used for homogenization

Ni50Ti30Hf20 specimens were used in 'as-extruded' condition while Ni50Ti25Hf25 alloys were solutionized in cylindrical furnace at 1050 C for 2 hours under high purity argon atmosphere to relieve extrusion induced stresses and achieving homogeneous microstructure and hence shape memory properties.

Rectangular rolling specimens were cut using W-EDM. Rolling specimens were mechanically ground using 400 Grid sandpaper to remove W-EDM residues from the surface. Edges and sides of the specimens were also mechanically ground to avoid any stress concentration factors on the samples.

3.4. Differential Scanning Calorimeter

DSC experiments were conducted by Perkin Elmer 8000 Differential Scanning Calorimeter. TTs and transformation enthalpy values were determined from DSC thermograms.

Heating rate was kept constant as 10°C/min while cooling rates were changed as 5°C/min,10°C/min,15°C/min in DSC experiments for the first study of the thesis. This was done to observe cooling rate effect on the martensitic transformation and shape memory properties of the Ni50Ti30Hf20 shape memory alloy.

Thermo-mechanical treatment effects on the shape memory behavior of Ni50Ti25Hf25 SMA were investigated in the second section of this thesis. DSC experiments were done on each thermo-mechanical treated samples. The summary of thermo-mechanical treatments is given in Table 3.4-1. Rolling percentages were calculated considering reduction in thickness.

Table 3.4-1: The summary of thermo-mechanical treatments that were conducted on Ni50Ti25Hf25 shape memory alloy

Sample Number	Homogenization	Cold Rolling	Warm Rolling at 500°C	Annealing
1	1050 °C for 2 hours	-	-	-
2	1050 °C for 2 hours	-	5%	-
3	1050 °C for 2 hours	5%	-	At 500°C for 30 minutes

Four DSC cycles were conducted for all samples. First cycle of DSC experiments was not taken into considerations due to what is named as “first cycle effect” in the literature [65,66]. Although DSC samples were cut via using low speed and without applying load, transformation temperatures and enthalpies may still deviate from the real values during the first cycle due to the induced stresses during DSC sample preparation. However, these stresses can be relieved especially during the first heating cycles of DSC experiments. DSC cycles were done between 100°C and 400°C on Ni50Ti30Hf20 alloy via using aluminum pans and were done between 200-550 on Ni50Ti25Hf25 via using copper pans since Ni50Ti25Hf25 alloy might have showed higher transformation temperatures because of having higher Hf content. The upper cycle temperatures for Ni50Ti25Hf25 in DSC experiments were kept as 550°C, that is relatively higher than that of the ones for Ni50Ti30Hf20 alloy. Therefore, copper pans were preferred since they have higher melting point than that of aluminum pans such that heating the samples to 550°C did not create a problem such as melting of the pans.

3.5. Isobaric Experiments

Experiments, which were conducted by cooling-heating the samples under constant stress, are called as Isobaric Experiments in the literature [67]. Isobaric experiments were done under 200 MPa constant stress magnitude. 200 MPa stress magnitude was chosen to investigate the effect of cooling rate on the shape memory properties of Ni50Ti30Hf20 since higher stress magnitudes led to observe irrecoverable strain, in other terms, plastic deformation during cycling. Tensile test specimens which are in the form dog-bone were first attached to the grips. Epsilon high temperature extensometer with ceramic rods was used to measure displacement values. Three J type thermocouple were used to control and monitor the temperature. Two of them were attached to the grips and one of them was attached to the middle part of the gauge length of the dog bone specimens. All strain vs temperature graphs were drawn using the temperature values that were measured directly from the middle of the specimen.

Samples were heated before loading in order to begin the experiment in austenitic state. After reaching above austenite finish temperature sample was loaded and cooling/heating cycles were started. The temperature, which the samples are heated to is called as Upper Cycle Temperature (UCT) [54]. UCT levels were determined according to the observation of full austenitic transformation. Three cooling/heating cycles were conducted to investigate thermal and mechanical stability under 200 MPa with the change of cooling rate.

Figure 3.5-1 Utest universal material testing machine equipped with heating/cooling unit that was used for isobaric heating/cooling experiments.

3.6. Rolling

Rolling studies were conducted using laboratory sized rolling mills which is driven by electrical motors. 5% thickness reduction was achieved in both cold and warm rolling procedures.

Before warm rolling process the sample was heated non-isothermally to 500°C via using Protherm PLF 100/3 cubic furnace. Sample was held in the furnace for 10 minutes at 500°C then the fed to roller. These steps were repeated around 5 times to achieve 5% deformation since the alloy is a hard to deform material due to high Hf content.

It is known from the literature that short time annealing after cold rolling improves the shape memory behavior of the alloy, thus annealing treatment at 500° C for 30 minutes was conducted for cold rolled sample to observe stable shape memory behavior in functional fatigue experiments [61].

Figure 3.6-1 Cubic Furnace and Rolling Machine

3.7. Functional Fatigue

In second study of the thesis, functional fatigue experiments were conducted on thermo-mechanically treated Hf rich Ni50Ti25Hf25. The samples were heated to UCT by joule heating which utilizes electricity that is provided by programmable DC power supply and heating/cooling rate control was obtained via using PI controller. LabView program was used to control the functional fatigue setup. Detailed information about the setup could be found in a previous study [68].

Natural convection was enough to cool the specimen to the lower cycle temperature. Addition to natural convection, forced air cooling was applied to achieve desired cooling rate during the thermal cycles.

Temperature was measured with Optris Ctlasr LTF-CF1 infrared thermometer. Laser was focused to the middle of the gauge section of the samples. Emissivity of the specimen is important to measure the correct temperature from the surface. Therefore, all samples were painted with a paint, which is resistant to high temperature applications (MOTIP Heat Resistant Paint) to gather consistent temperature measurements throughout thermal cycles. High temperature paint was applied at the end of every 50 cycles to avoid any paint peeling due to high temperature and high elongation of the sample.

Displacement values were measured using Linear potentiometric displacement sensor (LPDS) and dead weight was used to apply 200 MPa stress magnitude. Heating/Cooling rate was chosen as 15° C/sec, which is the common rate in the functional fatigue experiments that is used by our research group. Samples were heated up to UCT and loading was done in austenitic phase.

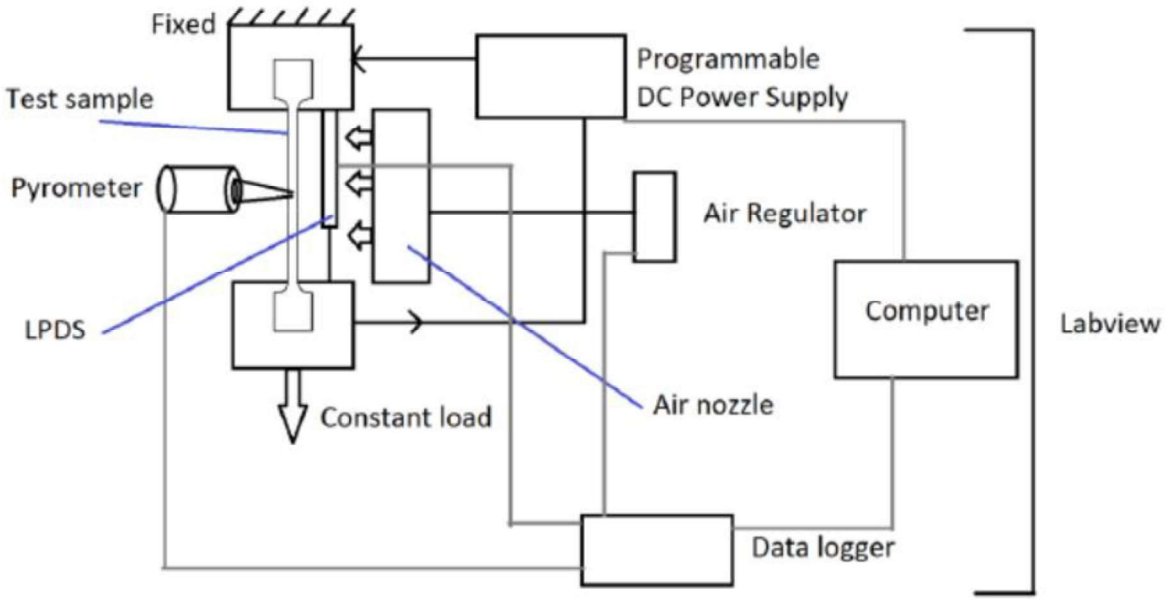

Figure 3.7-1 Functional fatigue diagram [68].

4. RESULTS AND DISCUSSION

4.1. Cooling Rate Effect on Shape Memory Properties of Equiatomic Ni50Ti30Hf20 (at. %) alloy

To investigate the effect of cooling rate on SM properties such as TTs and enthalpies under no load cooling-heating experiments together with actuation strain, thermal hysteresis and transformation temperatures under constant stress cooling-heating experiments, DSC and Isobaric Experiments were conducted. DSC experiments were run by constant heating rate at 10 °C/min while cooling rates were changed from 5 °C/min to 10 °C/min and to 15 °C/min. 10 °C/min was selected for constant heating rate since 10 °C/min is commonly used scanning rate in the literature. Three DSC samples which were around 6 mg of weight, were thermally cycled using DSC. Temperature interval for DSC experiments were selected as 100-400 °C to clearly see the transformation characteristics of the alloy. Four thermal cycles were conducted for each case and the first cycles were avoided due to the first cycle effect [65,66].

For simplifying the DSC results, only the second thermal cycles are presented in Figure 4.1-1. Heat flow values were normalized by dividing the data to the weight of the samples. Figure 4.1-2 presents the schematic of a thermal cycle which shows how the transformation temperatures and enthalpies and thermal hysteresis were determined from DSC curves. Transformation temperatures, enthalpies and thermal hysteresis that were determined from DSC curves are presented in Table 4.1-1.

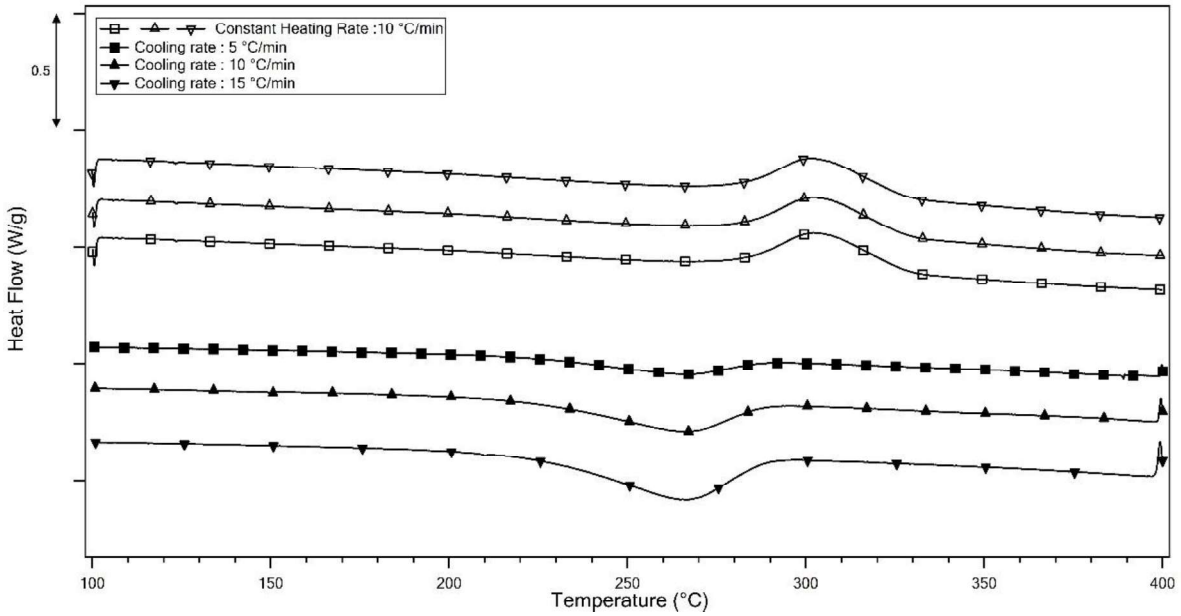

Figure 4.1-1 Second thermal cycles of DSC experiments which were run on Ni50Ti30Hf20 (at. %) alloy with cooling rates of 5,10, and 15 °C/min

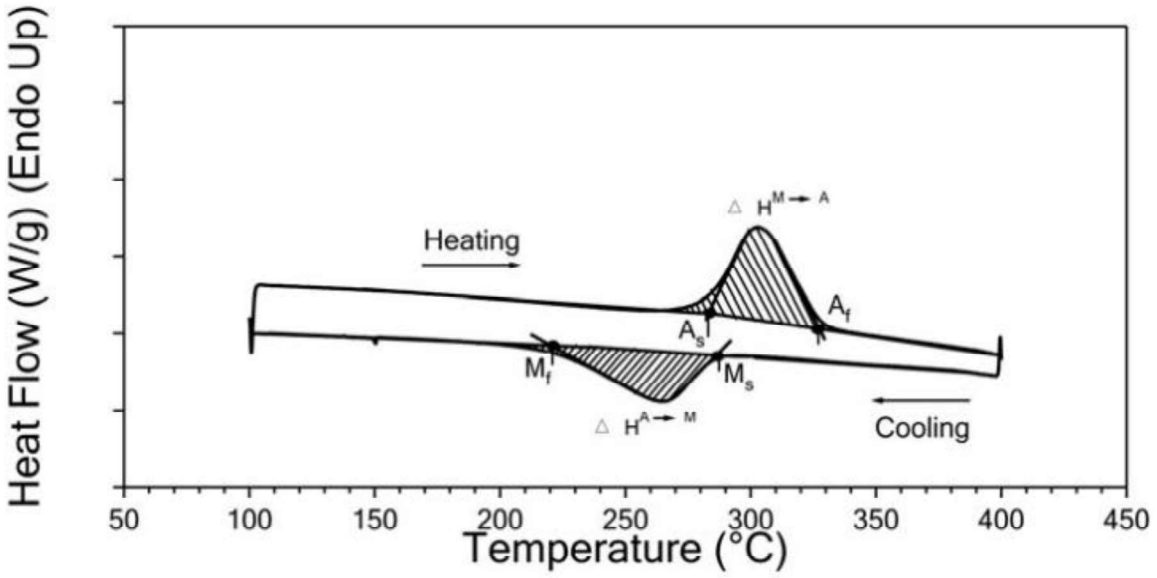

Figure 4.1-2 Schematic of a thermal cycle which shows the evaluation of TTs and transformation enthalpy [69].

Table 4.1-1: TTs, thermal hysteresis and transformation enthalpy values which were evaluated from DSC thermograms.

Cooling Rate (°C/min)	5	10	15
Af (°C)	331	330	331
As (°C)	278	278	277
Ms (°C)	286	287	287
Mf (°C)	226	226	225
Hysteresis (°C)	45	43	44
Enthalpy $\Delta H_{A\rightarrow M}$ (J/g)	23.6	24.1	27.1
Enthalpy $\Delta H_{M\rightarrow A}$ (J/g)	24.7	24.5	24.3

It is clearly seen from Figure 4.1-1 and Table 4.1-1 that the transformation temperature values do not differ with the change in cooling rate which is the reason of attaining almost constant hysteresis values. Transformation enthalpy values of martensite to austenite transformation stay constant, despite the fact that transformation enthalpy increases as cooling rate increases on austenite to martensite transformation. 0.5 J/g and 3 J/g of increase were observed respectively, when cooling rate was changed from 5 to 10 °C/min and 10 to 15 °C/min.

After investigating the cooling rate effect on the transformation characteristics of Ni50Ti30Hf20 (at. %) alloy with DSC experiments, isobaric cooling-heating experiments were conducted to determine the cooling rate effect with the application of constant stress. Figure 4.1-4 shows strain vs temperature curves, which were obtained from isobaric experiments with varying cooling rates of 5, 10 and 15 °C/min while heating rate was again kept constant as 10 °C/min under 200 MPa. Three cycles were done to investigate mechanical stability with the change of the cooling rate as well. Transformation temperatures, hysteresis, actuation strain and irrecoverable strain values were determined for each cycles. Table 4.1-2 shows the transformation temperatures, actuation strain values and thermal hysteresis gathered from second cycles of each isobaric thermal cycles

via The schematic, which presents the procedure to determine the aforementioned shape memory properties is shown in Figure 4.1-3.

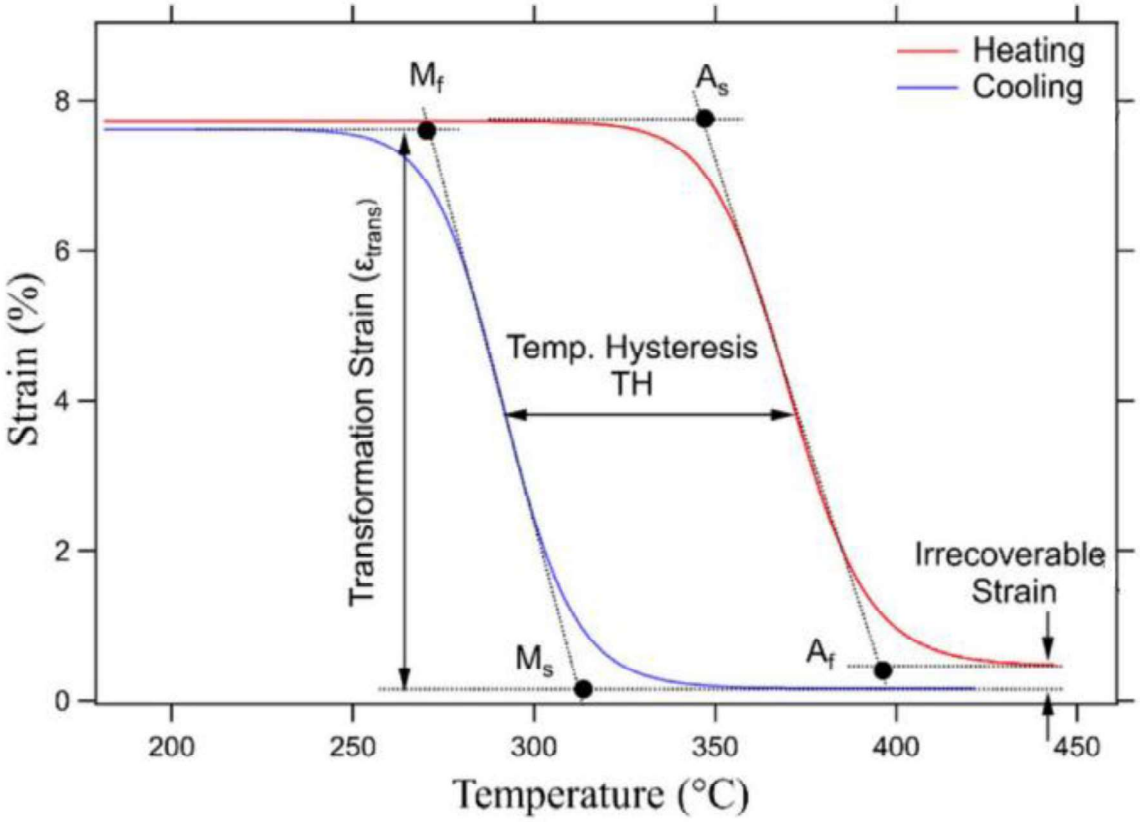

Figure 4.1-3 Schematic of isobaric experiment showing transformation strain, thermal hysteresis , irrecoverable strain and TTs [70].

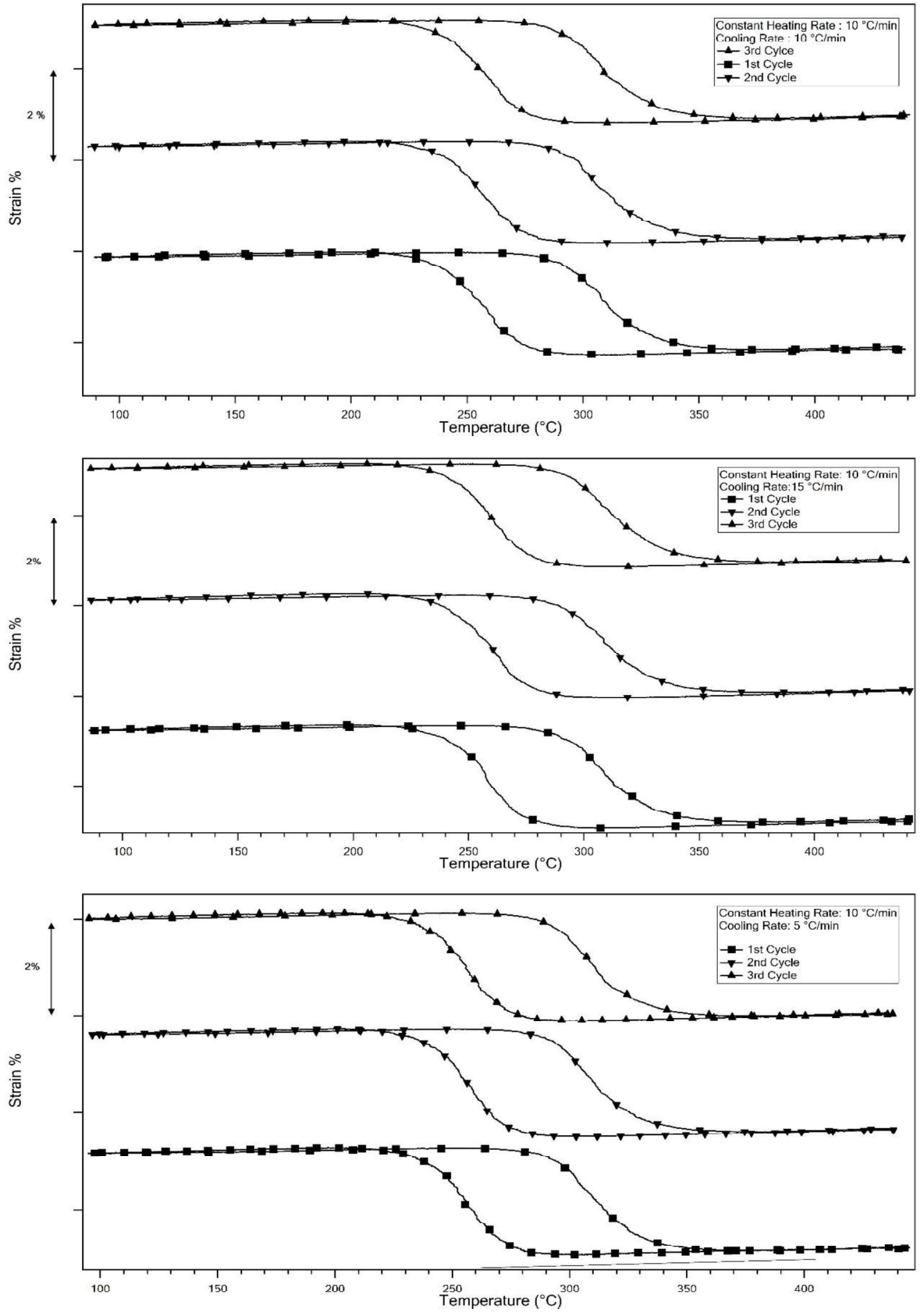

Figure 4.1-4 Strain vs Temperature Curves, which were obtained from Isobaric Experiments conducted on Ni50Ti30Hf20 (at. %) alloy with 5,10, and 15 °C/min cooling rates.

Table 4.1-2: Transformation temperatures, actuation strain and hysteresis evolution with the change in the cooling rate.

Cooling Rate (°C/min)	5	10	15
Af (°C)	330	333	334
As (°C)	290	287	287
Ms (°C)	274	275	278
Mf (°C)	239	238	240
Actuation Strain	2.1	2.1	2.1
Hysteresis (°C)	55	55	54

As it can be deduced from Table 4.1-2 that the transformation temperatures did not differ in Isobaric experiments with the change in the cooling rates likewise it was observed in DSC experiments thus, hysteresis stayed constant as well. Actuation strain values also did not differ although the cooling rates were changed.

Irrecoverable strain values could not be determined from the experiments since there was almost no irrecoverable strain through all the thermal cycles. 200 MPa stress magnitude is not sufficient to observe irrecoverable strain which was also observed in a previous study [71].

Controlled DSC experiments showed that there was no dependency of cooling rate since there was almost no change in transformation temperatures as cooling rate changes. Transformation hysteresis stayed almost constant due to the stable transformation temperatures. Controlled DSC experiments showed that transformation enthalpy on heating stayed constant since heating rate was kept constant as 10 °C/min.
Transformation enthalpy on the other hand, was increased as cooling rate was increased as aforementioned. Net transformation enthalpy change is given as [72]:

$$\Delta H^{M\rightarrow A} = -\Delta H_{ch}^{M\rightarrow A} - E_e^{M\rightarrow A} + E_{fr}^{M\rightarrow A} \quad \text{(Eqn 4)}$$

And

$$-\Delta H^{A\rightarrow M} = -\Delta H_{ch}^{A\rightarrow M} - E_e^{A\rightarrow M} + E_{fr}^{A\rightarrow M} \quad \text{(Eqn 5)}$$

$\Delta H^{M\rightarrow A}$: Enthalpy change of martensite to austenite transformation
$\Delta H^{A\rightarrow M}$: Enthalpy change of austenite to martensite transformation
ΔH_{ch}: Chemical energy change
E_e: Elastic strain energy
E_{fr}: Frictional (irreversible) energy

Difference between forward and reverse transformation in terms of transformation enthalpy was observed. $\Delta H^{M\rightarrow A}$ value was higher in the 15 °C/min condition as mentioned. Chemical composition of the alloy was the same since DSC samples were cut from the same batch thus there should be no difference in chemical energy. Elastic strain energy is the energy that is stored between starting and ending point of martensitic transformation since transformation temperatures were not changed there should be also no change in elastic strain energy. Lastly, E_{fr} term is related frictional energy, which is dissipated during transformation. Hysteresis term is directly related with this irreversible energy. As it is stated, there were also no change in hysteresis. These statements all together concludes that there should be no difference in transformation enthalpy between forward and reverse transformation thus, the increase in enthalpy values of Ni50Ti30Ti20 at% SMA with different cooling rates cannot be attributed to rate sensitivity contrary to literature. Enthalpy values increased due to the increased measurement sensitivity of differential scanning calorimeter equipment as cooling rate increases [73].

Transformation temperatures, especially martensite start temperature, increased under load due to Clausius-Clapeyron relation as it was mentioned in literature section nevertheless transformation temperatures that were measured from DSC experiments and isobaric experiments did not follow the above statement. Lower Ms temperature values under load condition was explained previously on NiTi binary alloys in the literature. The difference in transformation temperatures can be attributed to measurement methods.

DSC measures the exothermic or endothermic heat change while strain measurements on isobaric experiments were done according to macroscopic shape change. It was also shown by neutron diffraction studies that transformation takes place before macroscopic shape change [74] thus different transformation temperatures were observed under load and under no load conditions.

Thermal hysteresis values gathered from Isobaric Experiments were higher than that of obtained from DSC experiments and this can be attributed to dislocation formation with the application of load since defects and dislocations lead to have higher friction during the movement of martensite-austenite phase boundary.

4.2. Functional Fatigue Behavior of Ni50Ti25Hf25 (at. %)

DSC experiments were conducted on thermo-mechanically treated Ni50Ti25Hf25 (at. %) alloy before Functional Fatigue experiments since the TTs of SMAs are highly dependent on the deformation and heat treatment operations. The heating and cooling rates in DSC experiments were 10 /min. Figure 4.2-2 shows the comparison of DSC curves of homogenized, cold rolled, cold rolled and annealed and warm rolled samples. Transformation characteristics under no load condition were seriously affected from thermo-mechanical treatments which can be clearly seen from the Figure 4.2-1

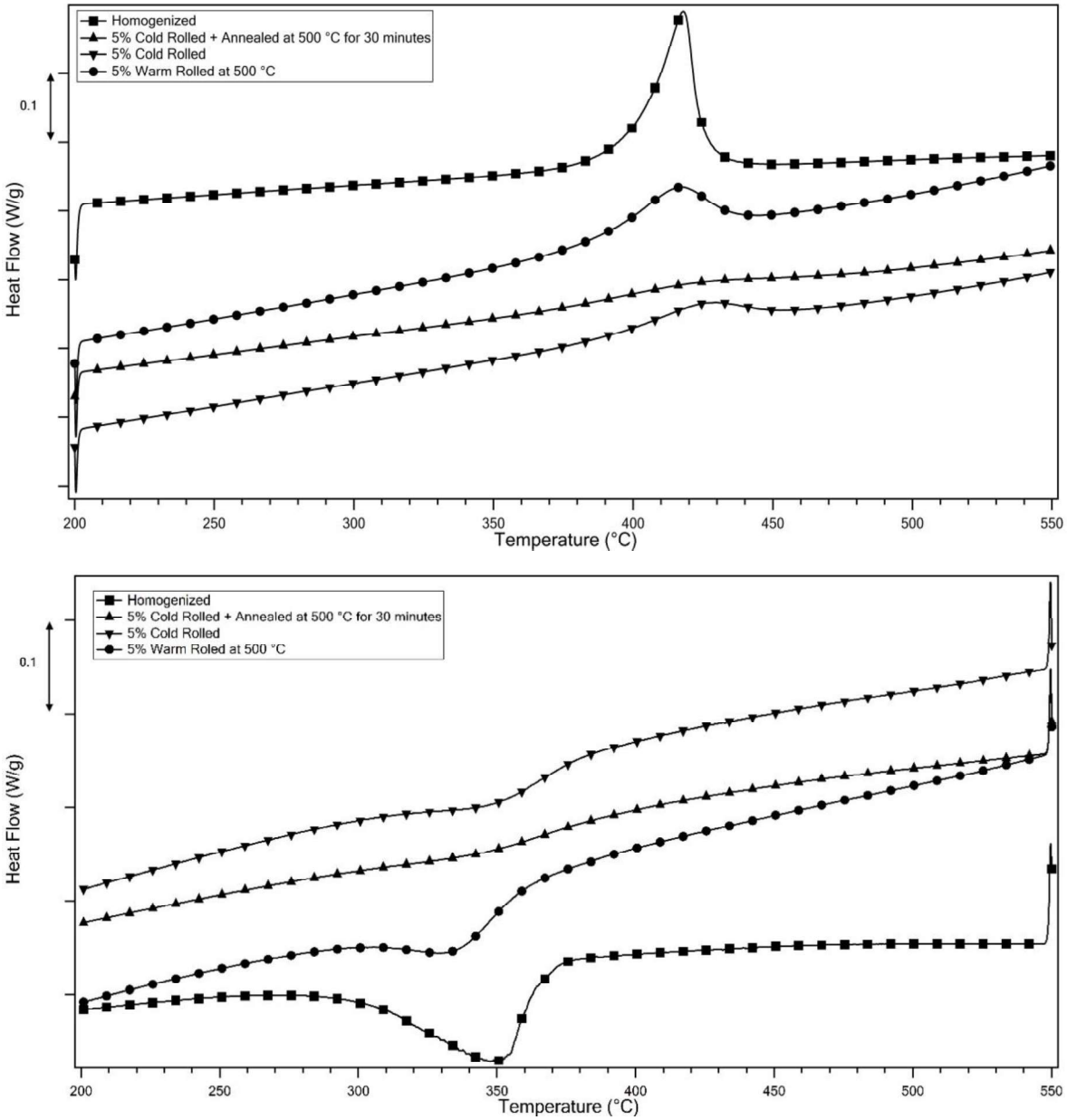

Figure 4.2-1 Comparison of DSC curves of homogenized, cold rolled, cold rolled + annealed and warm rolled Ni50Ti25Hf25 (at. %) samples

Table 4.2-1 shows the TTs, thermal hysteresis and transformation enthalpy values that were measured by DSC.

It has been already known that transformation temperatures decrease with the increase in dislocation density. Rolling led DSC curves to broaden thus transformation temperatures, especially Af and Ms were affected from this broadening. Transformation temperatures were determined according to ASTM F2004, which defines tangent method. Higher transformation temperatures were observed due to lower slope of broadened curves.

Table 4.2-1: TTs, thermal hysteresis and transformation enthalpy values that were evaluated from DSC thermograms of thermo-mechanical treated Ni50Ti25Hf25 (at. %) samples.

	As (°C)	Af (°C)	Ms (°C)	Mf (°C)	Hysteresis (Af-Ms) (°C)	ΔH (M→A) (J/g)
Homogenized	399	426	368	294	58	24.72
Cold Rolled	383	459	381	294	78	5.19
Cold Rolled + Annealed	372	482	404	287	78	6.05
Warm Rolled	383	440	365	293	75	10.26

Hysteresis values were increased from 58 °C to 75 and 78 °C by warm rolling and cold rolling operations, respectively. Annealing did not cause to a change in hysteresis values due to short time annealing since time was not enough to annihilate the dislocations caused by cold rolling and 78 °C of hysteresis value was observed in the cold rolled + annealed sample as well. Warm rolling caused hysteresis to increase to 75 °C, which is similar to the measured hysteresis value for the cold rolled sample since 500 °C is relatively lower deformation temperature for high Hf NiTiHf alloys.

Cold and warm rolling led to observe lower transformation enthalpy values due to dislocations induced during rolling processes. Homogenized specimen has an enthalpy value of 24.72 J/g while cold rolled, cold rolled and annealed, warm rolled have 5.19, 6.05, 10.26 J/g, respectively. Annealing effect is much clear when transformation enthalpies are considered since annealing led to an increase in transformation enthalpy yet not enough to decrease transformation hysteresis since short term annealing actually helps to relieve stress and rearrange dislocation forests, which were induced during cold rolling operation.

Functional Fatigue experiments of Ni50Ti25Hf25 (at. %) were conducted between 200°C of Lower Cycle Temperature (LCT) and 600°C of Upper Cycle Temperature (UCT) under 200MPa stress magnitude. Figure 4.2-2 shows the Strain Vs Temperature graph for the homogenized sample including all the cycles up to failure. Transformation temperatures, martensite and austenite strain, actuation strain and hysteresis values were gathered from the graphs. Total of 550 cycle was shown in the figure since the sample deformed plastically through cycles and cross-sectional area was reduced as a result of plastic deformation. Joule heating was utilized in the experiments as aforementioned in the experimental procedure section. Reduced cross sectional area of the gauge section due to plastic deformation was not enough to apply heating procedure and PI controller could not control the temperature. Therefore, thermal cycling and experiment were stopped if the control was not possible. Optical examination of the sample surface will be given in appendix section.

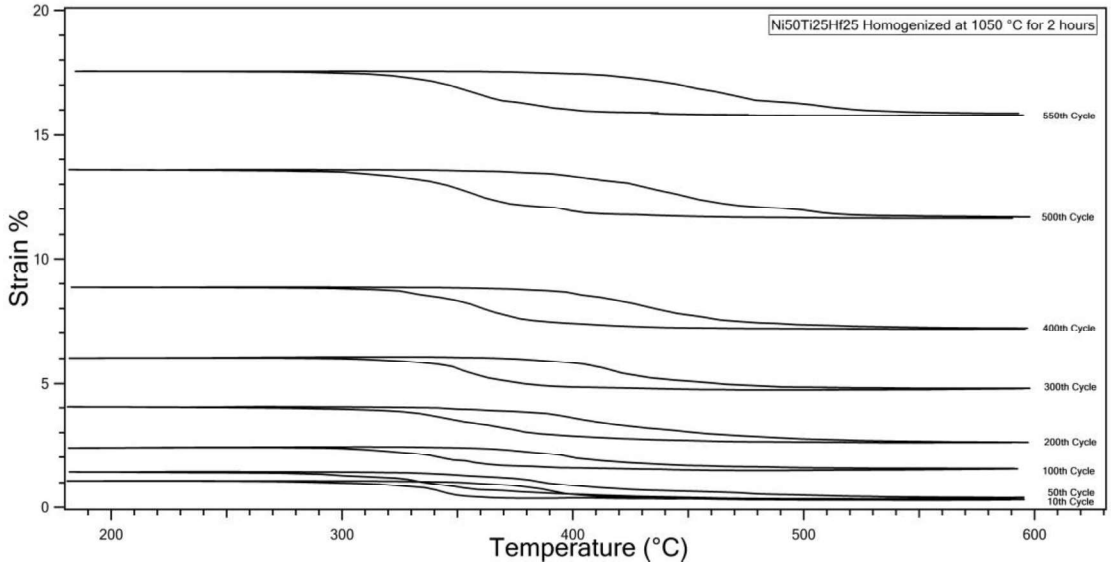

Figure 4.2-2 Strain vs Temperature curves obtained from the functional fatigue experiment of Homogenized Ni50Ti25Hf25 (at. %) sample.

It can be seen from the Figure 4.2-2 that, transformation induced plasticity (TRIP) and martensite pinning occurred with the dislocation formation via cycling under stress and caused strain vs temperature curves to shift upwards since the irrecoverable strain values accumulated throughout the cycles. As cycle number increased, TRIP+ martensite pinning effects were increased as well, which can be seen from the figure that initial cycles were close to each other such that it denotes TRIP+martensite pinning were small compared to later cycles which were clearly apart from each other. Irrecoverable strain is defined as the strain value which is not recovered upon the end of the heating, thus these values at each cycles were measured to be very small. However, austenite strain is the accumulation of each irrecoverable strain values, thus the total plastic deformation which is expressed with austenite strain is extremely very high. Additionally, actuation strain is calculated by the difference of martensite and austenite strain. The procedure, which is followed to find out, austenite, martensite and actuation strain together with transformation temperatures and thermal hysteresis is given in Figure 4.2-3.

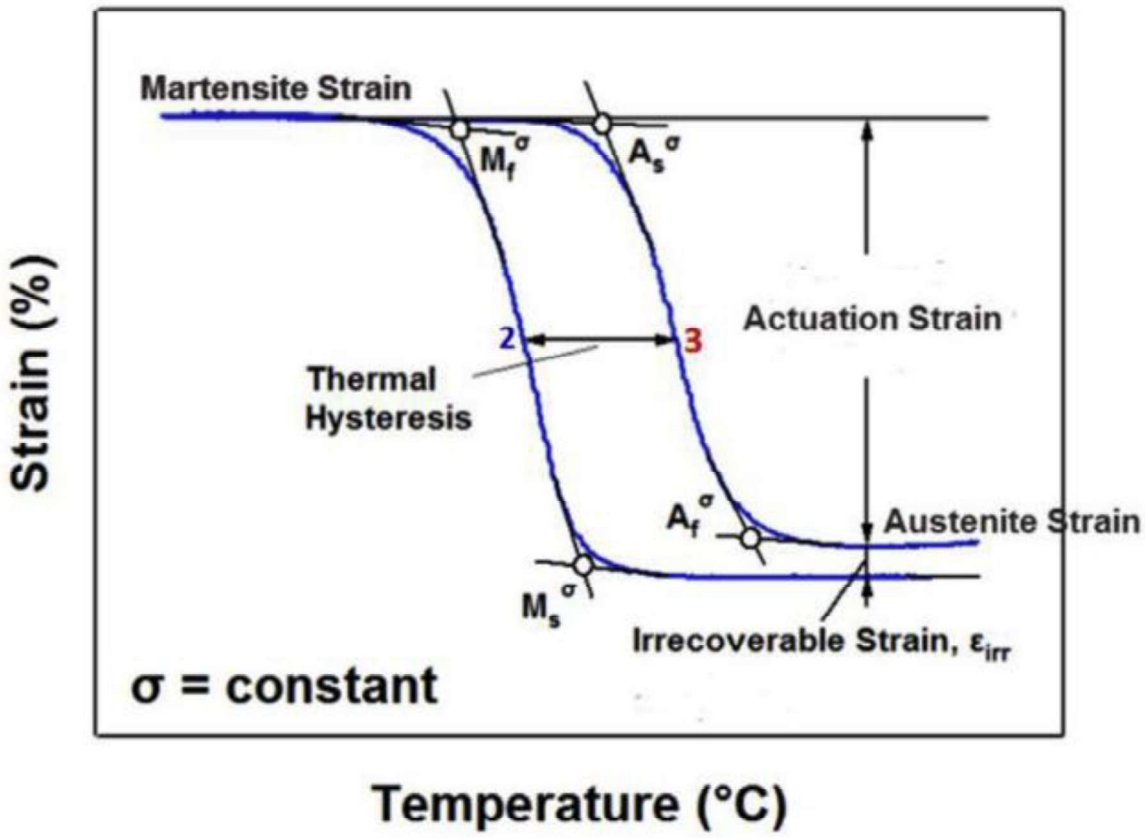

Figure 4.2-3 Schematic of constant load heating/cooling curve showing transformation temperatures, martensite, austenite, actuation, irrecoverable strains and thermal hysteresis [54].

Fig 4.2-4 shows the Strain vs Temperature curves, which were obtained from functional fatigue experiment of homogenized +cold rolled and annealed sample. Total of 542 cycles were conducted and experiment was stopped at 543rd cycle by the same reason as described above. Transformation temperatures, hysteresis, actuation strain, accumulated martensite and austenite strains were also determined from the graphs and will be given later in this section. Curves also shifted upwards as it was observed in the results of homogenized sample which is the indication of TRIP + martensite pinning due to dislocations which were induced during fatigue cycles.

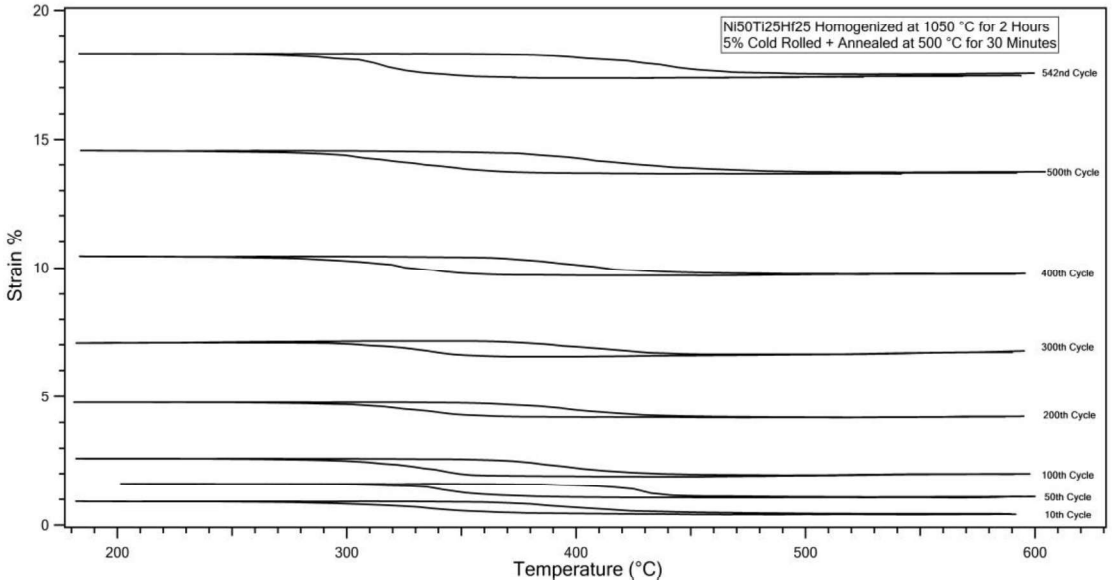

Figure 4.2-4 Strain vs Temperature curves obtained from the functional fatigue experiment of Homogenized and then cold rolled and annealed Ni50Ti25Hf25 (at. %) sample

Strain vs Temperature curves from the functional fatigue experiment of the sample, which was warm rolled for 5% at 500 °C were given in Figure 4.2-5. Total of 490 cycles were conducted and experiment was stopped thereafter as was done in earlier experiments with the same reasons. Similar to the previous results, curves shifted upwards in this experiment as well.

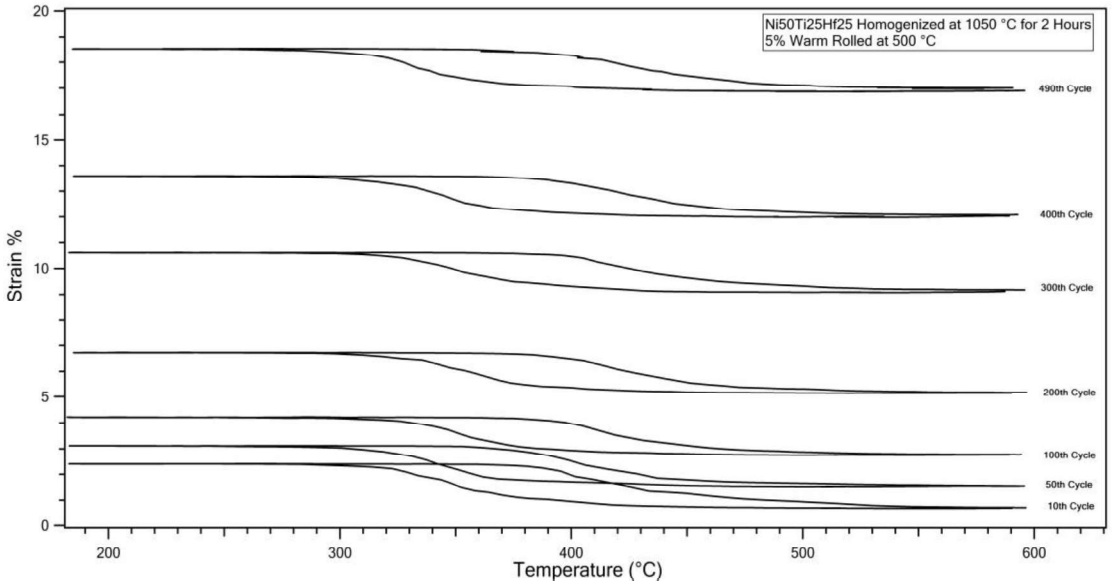

Figure 4.2-5 Strain vs Temperature curves obtained from the functional fatigue experiment of warm rolled Ni50Ti25Hf25 (at. %) sample.

TTs, which were evaluated from Strain vs Temperature curves of the Functional Fatigue experiment which was conducted on homogenized Ni50Ti25Hf25 (at. %) sample, were shown in the Figure 4.2-6. A slight increase was observed for Austenite Finish (A_f) temperature with the number of cycles. However, Austenite Start (A_s), Martensite Start (M_s) and Martensite Finish (M_f) temperatures were around 370 °C, 380 °C, 310 °C, respectively throughout the cycles and transformation temperatures apart from A_f temperature were quite stable since the slope of these temperatures were lower than the slope of austenite finish temperature. Increasing trend of A_f was due to the dislocation accumulation during thermal cycles.

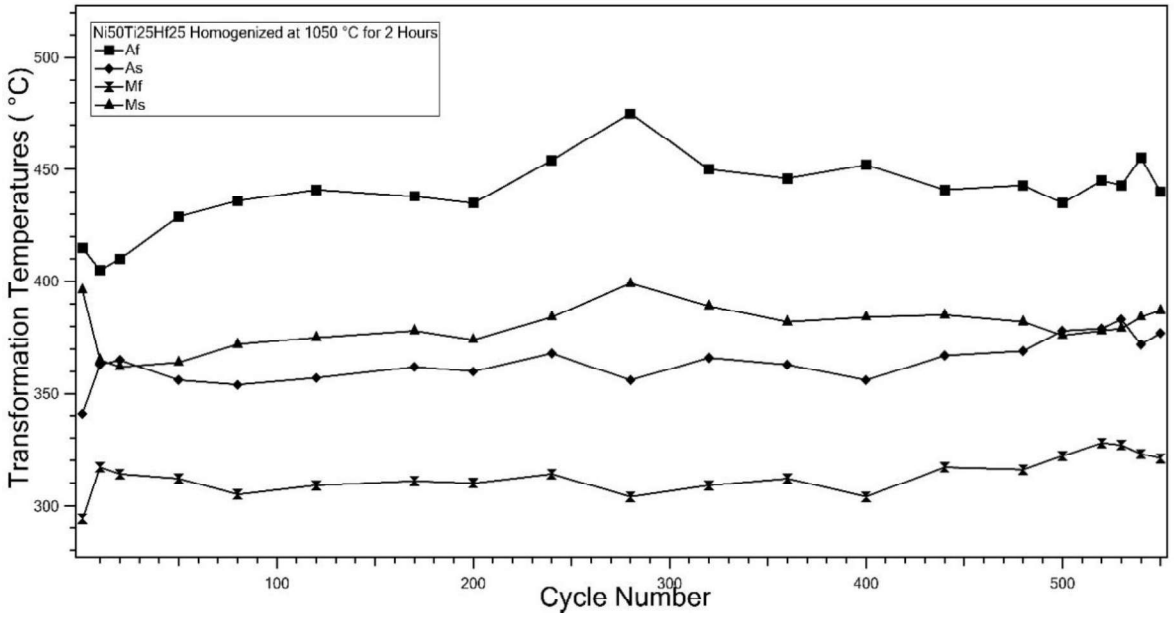

Figure 4.2-6 Evolution of transformation temperatures, which were determined from Functional Fatigue experiment conducted on homogenized Ni50Ti25Hf25 (at. %) sample.

Transformation temperatures of Homogenized+ cold rolled, and annealed sample were more stable than that of the homogenized sample as expected. During functional fatigue experiment, Af was around 440 °C while As, Ms and Mf were around 360°C,350 °C and 290 °C respectively. It is well known that the dislocation formation during cold rolling causes transformation temperatures to decrease which was the reason of observing lower TTs for homogenized + cold rolled + annealed sample than that of only homogenized sample. Strain hardening that was achieved during cold rolling, led the dislocation

formation more difficult during phase transformation in fatigue experiment, thus change in transformation temperatures was not realized as was attained in homogenized sample.

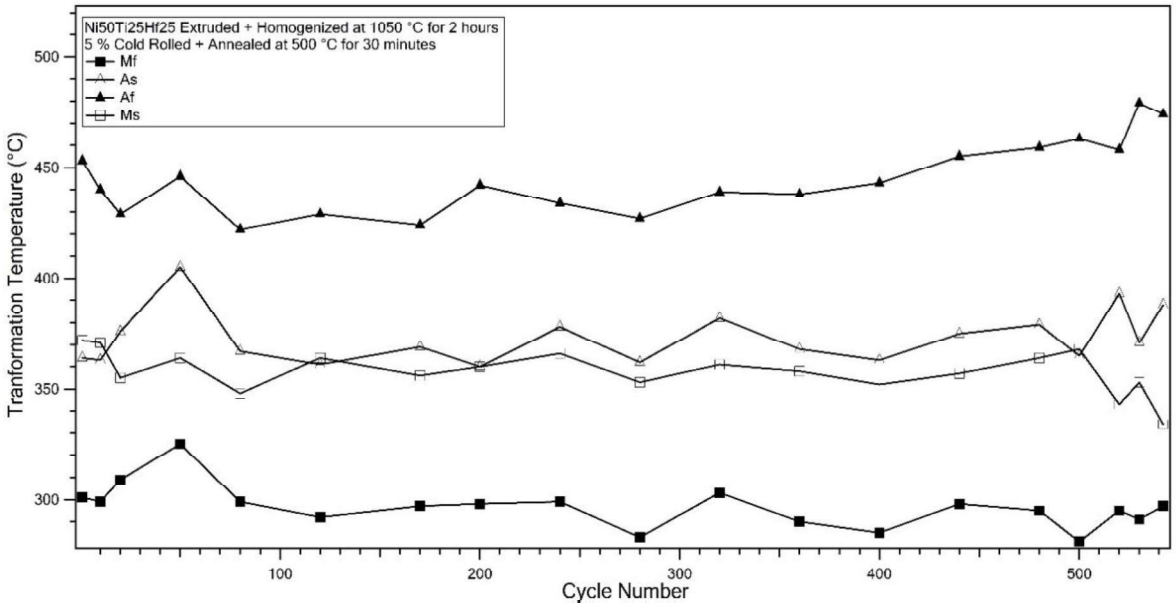

Figure 4.2-7 Evolution of transformation temperatures, which were determined from Functional Fatigue experiment conducted on homogenized and then cold rolled and annealed Ni50Ti25Hf25 (at. %) sample.

Evolution of the transformation temperatures of 5% warm rolled sample is shown in Fig 4.2-8. Trend of the change in the TTs of cold rolled specimen was also observed in the warm rolled specimen. Transformation temperatures were determined to be nearly stable throughout cycles. A_f, A_s, M_s and M_f temperatures were around 460 °C, 380 °C, 380°C and 320 °C, respectively and the temperatures were relatively higher than that of cold rolled specimen due to the higher deformation temperature. Rolling which was conducted at 500 °C induced less dislocations compared to the induction of dislocation amount at room temperature rolling operation. Nevertheless, induced dislocations in warm rolling process were enough to stabilize transformation temperatures throughout the cycles. Therefore, TTs of warm rolled specimen were more stable than homogenized one.

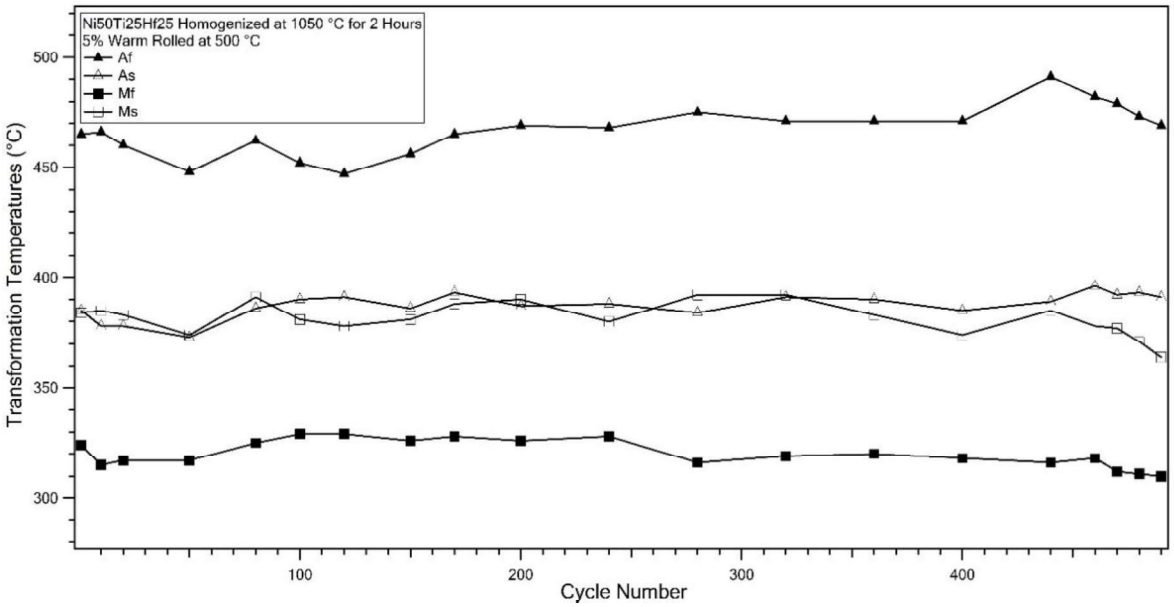

Figure 4.2-8 Evolution of transformation temperatures, which were determined from Functional Fatigue experiment conducted on warm rolled Ni50Ti25Hf25 (at. %) sample.

Martensite, austenite and actuation strain together with thermal hysteresis values which were determined from Strain vs Temperature curves were first drawn for each samples separately and then the comparison of the aforementioned values of all samples was shown.

Figure 4.2-9 demonstrates martensite and austenite strains, which were gathered from the functional fatigue experiment of homogenized Ni50Ti25Hf25 (at%) sample, exhibited increasing trend with the number of cycles. It is important to mention that austenite strain is the accumulated irrecoverable strain values throughout the fatigue cycles. Increasing trend of martensite strain and austenite strain were observed which was similar with the literature. Additionally, incremental increase in the strain values was determined. On the other hand, the rate of the increase in the accumulated irrecoverable strain (austenite strain) values decreases for most of the other NiTiHf alloys since strain hardening takes place via cycling under stress. In this experiment thermal cycles were conducted between 200 °C and 600 °C. Since the Upper Cycle Temperature (UCT) is relatively higher than that of the UCT values which are used for NiTiHf alloys containing less Hf strain hardening might not take place [54].

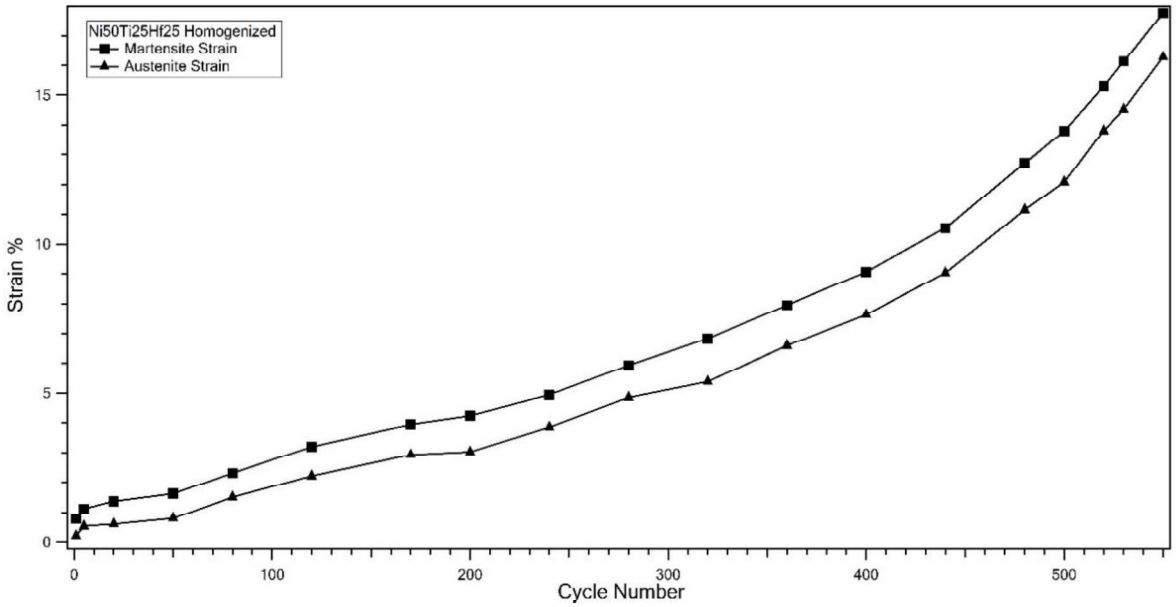

Figure 4.2-9 Martensite and Austenite Strain values, which were determined from Strain vs Temperature Curves obtained from Functional Fatigue experiment of Homogenized Ni50Ti25Hf25 (at%) sample

Actuation strain evolution with the number of cycles of homogenized sample was shown in Figure 4.2-10. Increasing trend of actuation strain values throughout cycles was observed. Actuation strain values of homogenized sample was started from 0.55% and increased to 1.7%.

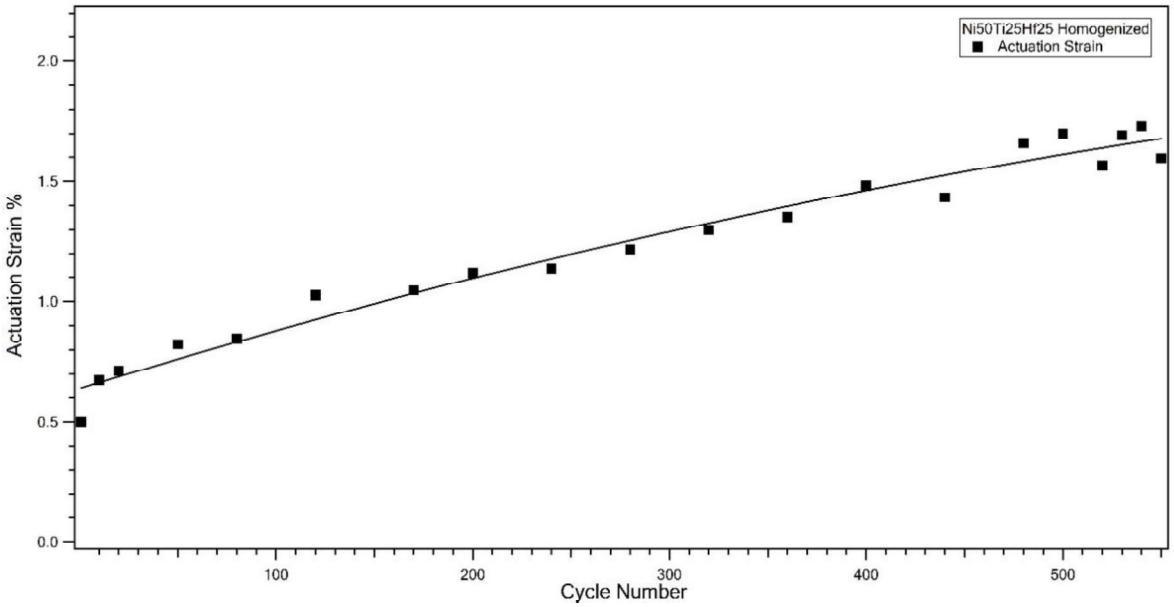

Figure 4.2-10 Actuation Strain values, which were determined from Strain vs Temperature Curves obtained from Functional Fatigue experiment of Homogenized Ni50Ti25Hf25 (at%) sample.

Hysteresis values of the homogenized sample are shown in Figure 4.2-11. It can be deduced from the figure that the thermal hysteresis value at the beginning was 45 °C and increased to 60 °C at 300th cycle. Until 300th cycle, the values almost stayed constant and then started to increase and reached around 110 °C at the end of the experiment. Hysteresis is directly related with dislocations and pinned martensite due to these dislocations such that higher energy should be supplied for the phase transformation. It can be said that dislocation formation was increased after 300th cycle

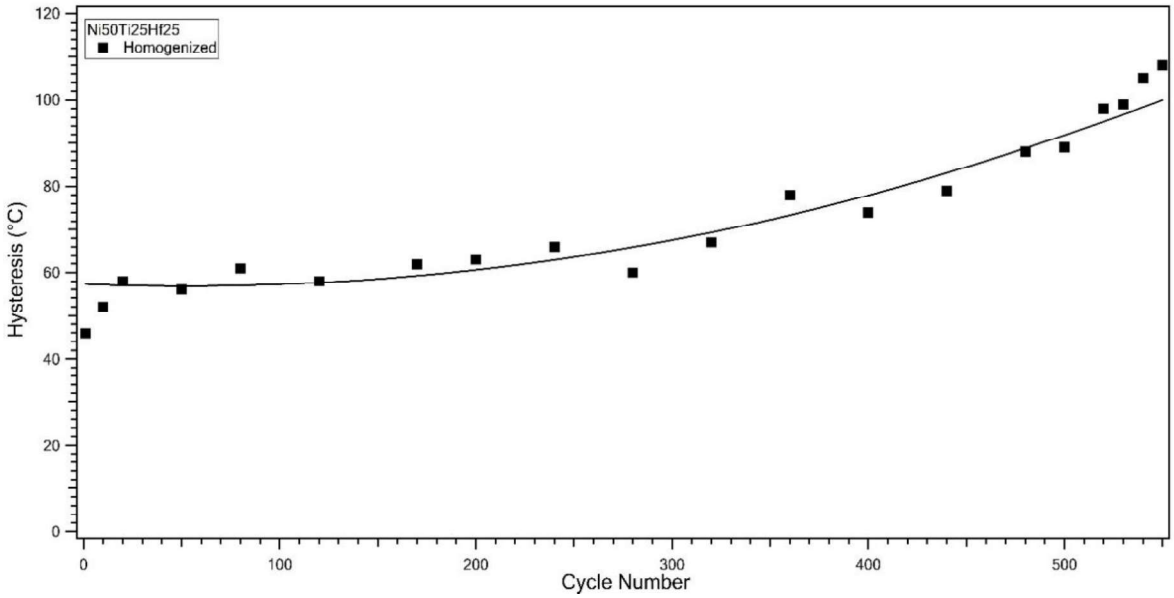

Figure 4.2-11 Thermal Hysteresis values, which were determined from Strain vs Temperature Curves obtained from Functional Fatigue experiment of Homogenized Ni50Ti25Hf25 (at%) sample.

Martensite and Austenite Strain evolutions of Homogenized + Cold Rolled and Annealed sample were similar to homogenized sample which can be seen in Figure 4.2-12. Strain hardening effect was not observed in cold rolled and annealed sample as well since UCT was also kept at 600°C as it was kept during the fatigue cycles of the homogenized sample. High UCT prevented dislocation formation [54].

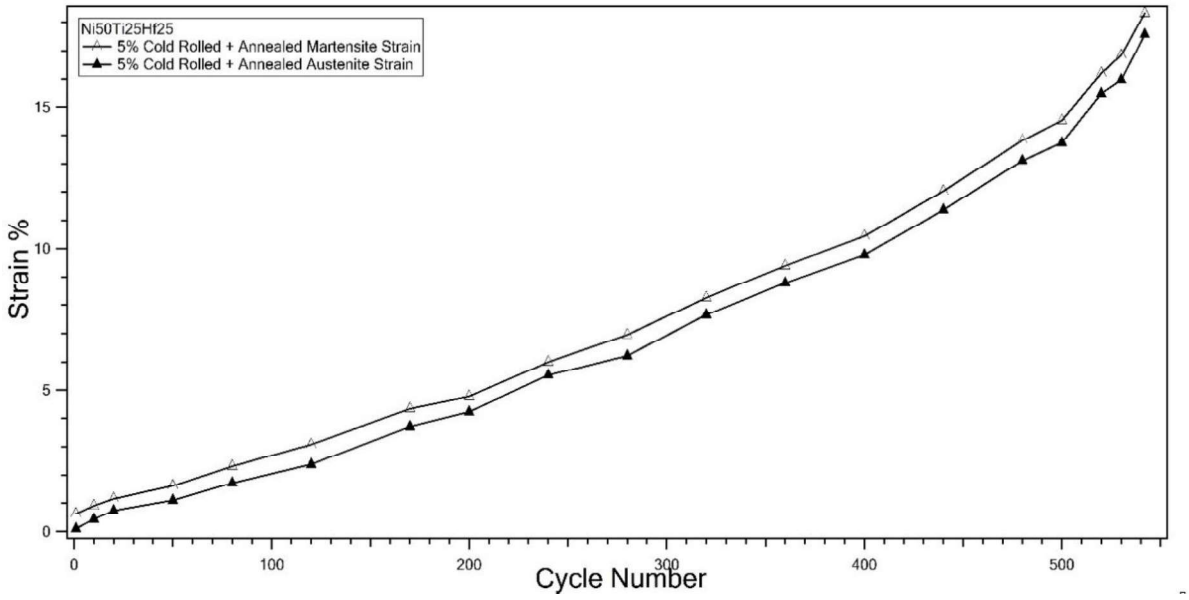

Figure 4.2-12 Martensite and Austenite Strain values, which were determined from Strain vs Temperature Curves obtained from Functional Fatigue experiment of cold rolled and annealed Ni50Ti25Hf25 (at%) sample

Homogenized + Cold Rolled and Annealed sample demonstrated increasing actuation strain values as it is shown in Figure 4.2-13, although the increase in the values with the number of cycles was much lower than cold rolled sample. Additionally, the magnitudes of the actuation strain of cold rolled samples were also lower than homogenized sample due to the high dislocation density. Actuation strain value at the beginning was around 0.5% and increased to 0.8%.

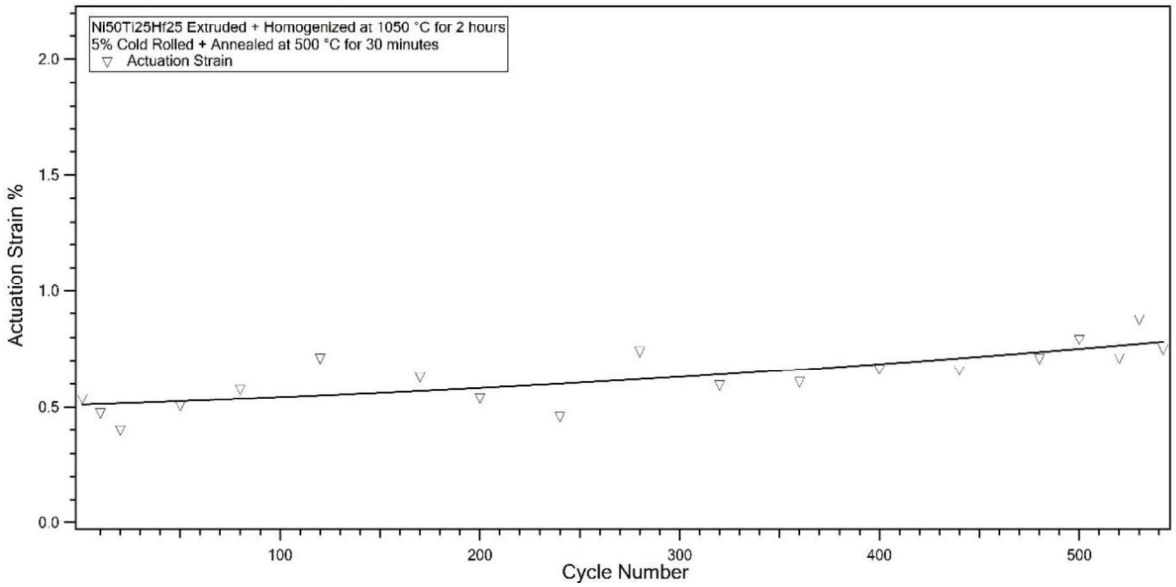

Figure 4.2-13 Actuation Strain values, which were determined from Strain vs Temperature Curves obtained from functional fatigue experiment of cold rolled and annealed Ni50Ti25Hf25 (at%) sample.

Fig 4.2-14 shows the hysteresis values of homogenized + cold rolled and annealed sample. Hysteresis values were higher compared to homogenized sample due to the dislocation formation during cold rolling, also values were slightly more stable than homogenized sample for the same reason as above. Hysteresis stayed constant around 80 °C until 400th cycle and increased to 120 °C at the 540th cycle.

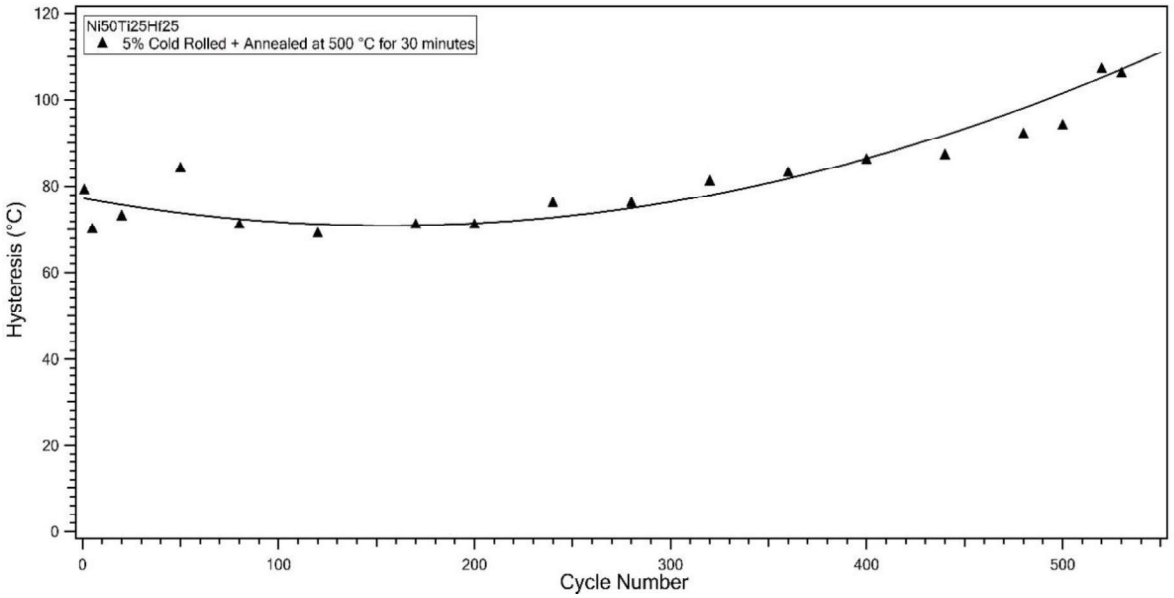

Figure 4.2-14 Thermal Hysteresis values, which were determined from Strain vs Temperature Curves obtained from Functional Fatigue experiment of Homogenized Ni50Ti25Hf25 (at%) sample.

Fig 4.2-15 shows martensite and austenite strains of 5% warm rolled at 500 °C specimen. Almost a linear increase was observed in warm rolled specimen as well.

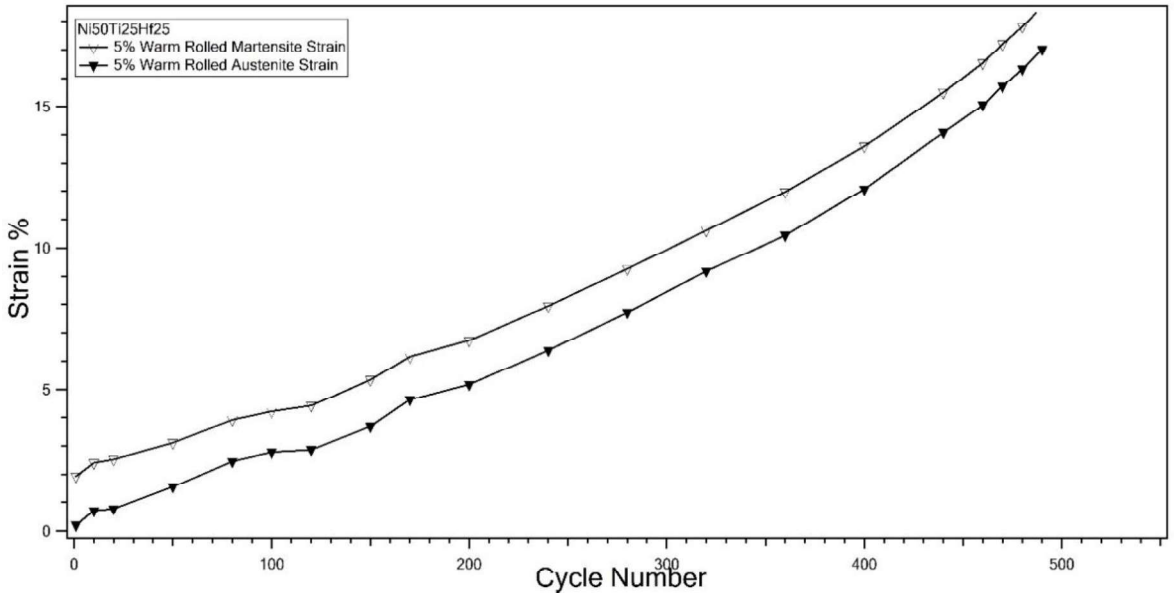

Figure 4.2-15 Martensite and Austenite Strain values, which were determined from Strain vs Temperature Curves obtained from functional fatigue experiment of Warm Rolled Ni50Ti25Hf25 (at%) sample.

Actuation strain evolution through the functional fatigue experiment of warm rolled sample is shown in Figure 4.2-16. The stability in the actuation strain values were attained in this sample like was achieved in the cold rolled sample. However, actuation strain values were slightly decreasing as number of cycles increased which might be due to martensite pinning as a result of dislocation formation.

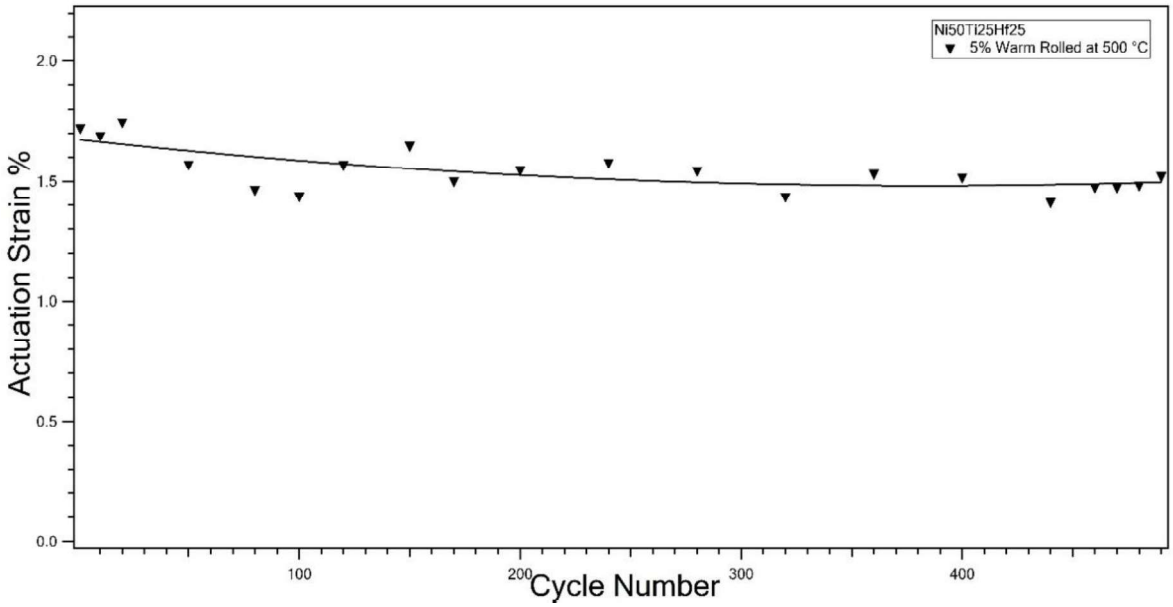

Figure 4.2-16 Actuation Strain values, which were determined from Strain vs Temperature Curves obtained from functional fatigue experiment of warm rolled Ni50Ti25Hf25 (at%) sample.

Fig 4.2-17 represents the hysteresis values of 5% warm rolled at 500 °C sample. Hysteresis was determined as 70 °C at the beginning and stayed almost constant until 350th cycle, then increased to 90 °C at the end of 490th cycle. The increment in the hysteresis was lower in the warm rolled case than homogenized and cold rolled +annealed specimen.

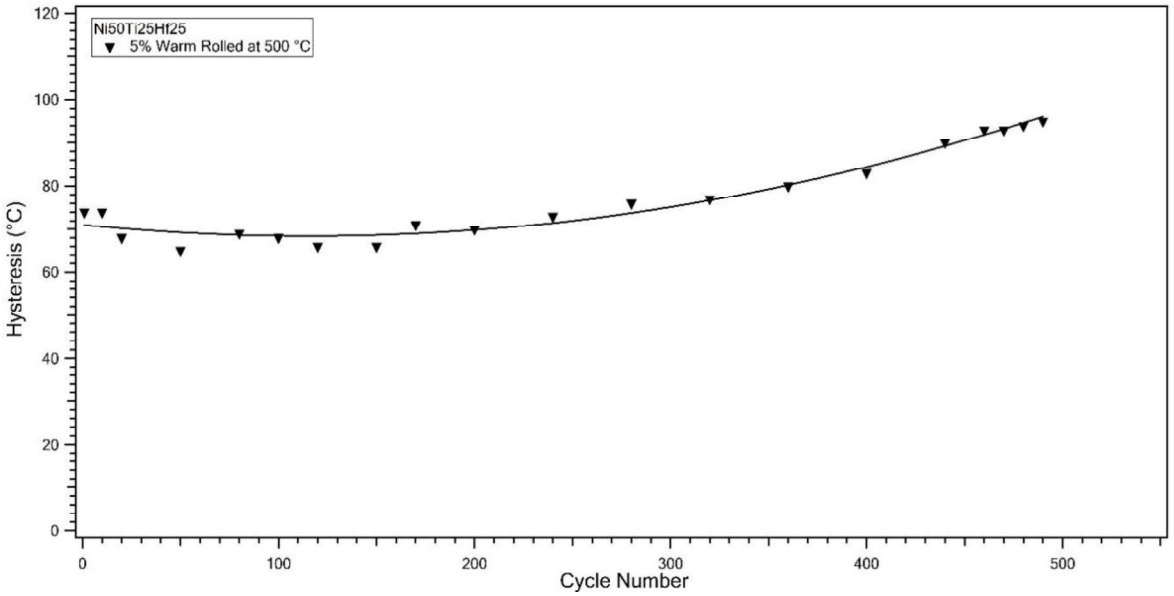

Figure 4.2-17 Thermal Hysteresis values, which were determined from Strain vs Temperature Curves obtained from functional fatigue experiment of warm rolled Ni50Ti25Hf25 (at%) sample.

Fig 4.2-18 demonstrates the comparison of martensite and austenite strain values of homogenized, cold rolled + annealed and warm rolled samples. It can be clearly seen from the figure that, warm rolled specimen showed the highest martensite and austenite strain values and failed earlier than others as expected from this behavior. Homogenized sample and cold rolled sample demonstrated similar behaviors in terms of martensite and austenite strains and they failed 550th and 540th cycle, respectively. Warm rolling at 500°C with 5% of thickness reduction did not improve the strength of the HTSMA effectively. The rolling temperature was relatively high but the percent of the deformation was low. The influence of the deformation might be cancelled with the rolling temperature.

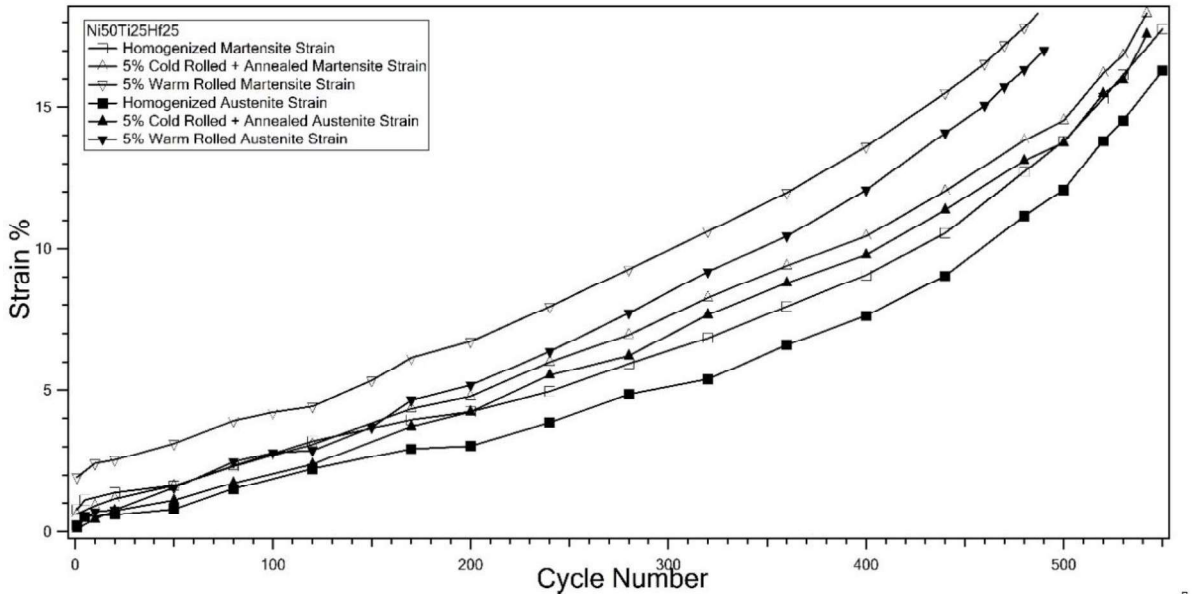

Figure 4.2-18 Comparison of Martensite and Austenite Strain values of homogenized, cold rolled and annealed and Warm Rolled Ni50Ti25Hf25 (at%) samples

The comparison of actuation strain values of all samples can be seen in Figure 4.2-19. Homogenized specimen showed an increasing trend of actuation strain while cold rolled and warm rolled specimens demonstrated more stable actuation strain behavior during functional fatigue experiments. It is worth to mention that the actuation strain values were calculated by taking the difference between martensite strain and austenite strain.

Actuation strain values were not stable for homogenized sample since most of the dislocations were annihilated during homogenization process. Actuation strain values of warm rolled specimen were higher than that of cold rolled specimen since rolling was done at elevated temperature which causes no or less dislocation formation than that of obtained in cold rolled specimen. Additionally, actuation strain values of warm rolled specimen were higher than the cold rolled + annealed specimens. This might be attributed to texture formation during the application of warm rolling. Furthermore, the actuation strain of warm rolled sample decreased with the cycles due to gradual vanishing of the texture during thermal cycling since the upper cycle temperature was 600 °C. Such behavior was not observed in cold rolled specimen since annealing at 500 °C for 30 minutes might lead to the diminish of the texture, which might be formed at the surface of the thin cold rolled sample. However, annealing time was enough to partly annihilate

dislocations that were induced during cold rolling thus, lower actuation strain values were observed during functional fatigue.

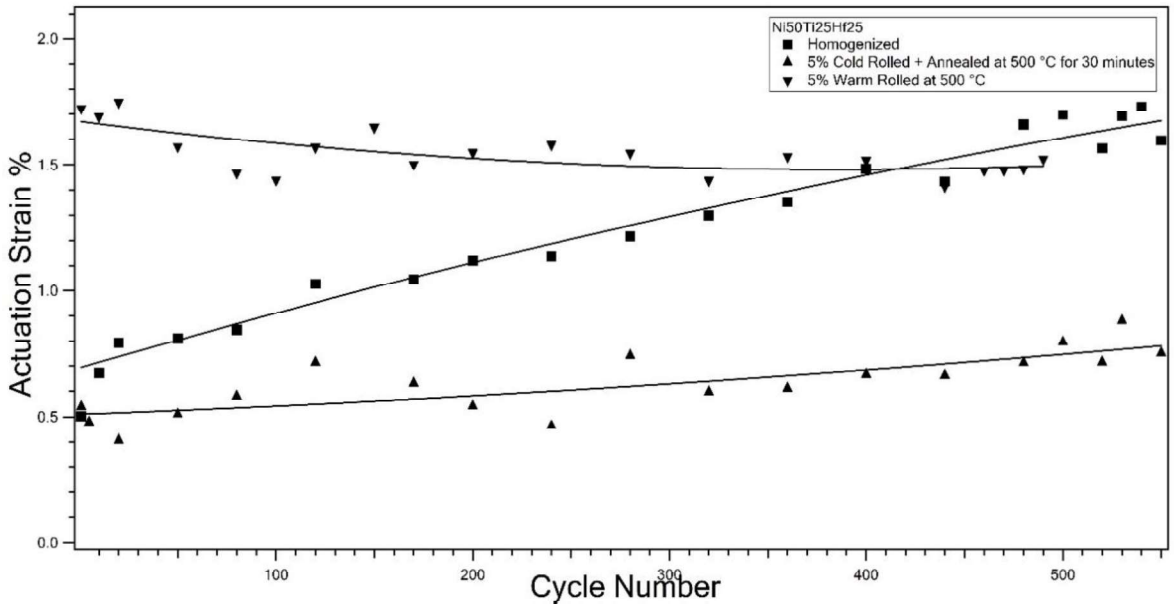

Figure 4.2-19 Comparison of Actuation Strain values of homogenized, cold rolled + annealed and Warm Rolled Ni50Ti25Hf25 (at%) samples.

Hysteresis comparison was shown in Figure 4.2-20. Homogenized sample demonstrated the lowest hysteresis values throughout the experiments since the martensite-austenite boundary should be mobile due to the lack of dislocations. On the other hand, the hysteresis values of warm rolled and cold rolled + annealed samples were very similar to each other. Higher hysteresis values of CR5 and 500WR5 specimens were attributed to plastic deformation procedure which led to induce dislocations during rolling and these dislocations contributed to obtain higher hysteresis values with respect to the values of homogenized sample as aforementioned earlier.

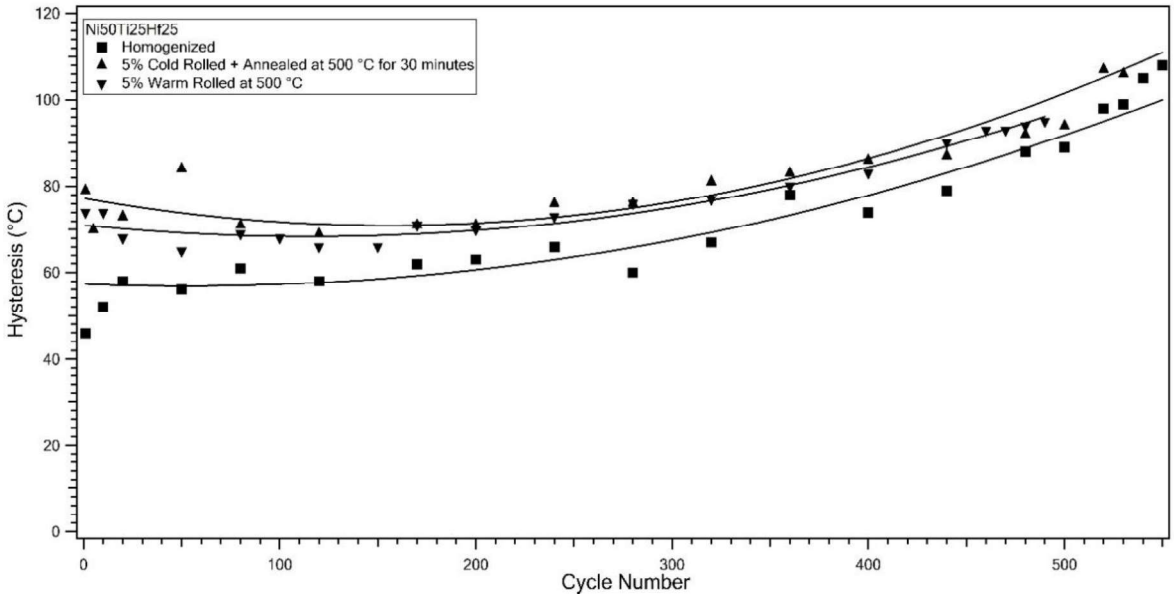

Figure 4.2-20 Comparison of Hysteresis values of homogenized, cold rolled + annealed and Warm Rolled Ni50Ti25Hf25 (at%) samples.

Last comparison was done on A_f and M_s temperatures of all samples and shown in Figure 4.2-21. It can be seen from the figure that CR5 specimen demonstrated lowest transformation temperatures due to the increase in dislocation density. Higher overcooling is necessary to fully transform the alloy to martensite. On the other hand, homogenized and 500WR5 specimen demonstrated almost the same transformation temperature behavior which is the indication of rolling at relatively higher temperature. The influence of deformation via rolling might not be effective to noticeable change the dislocation density.

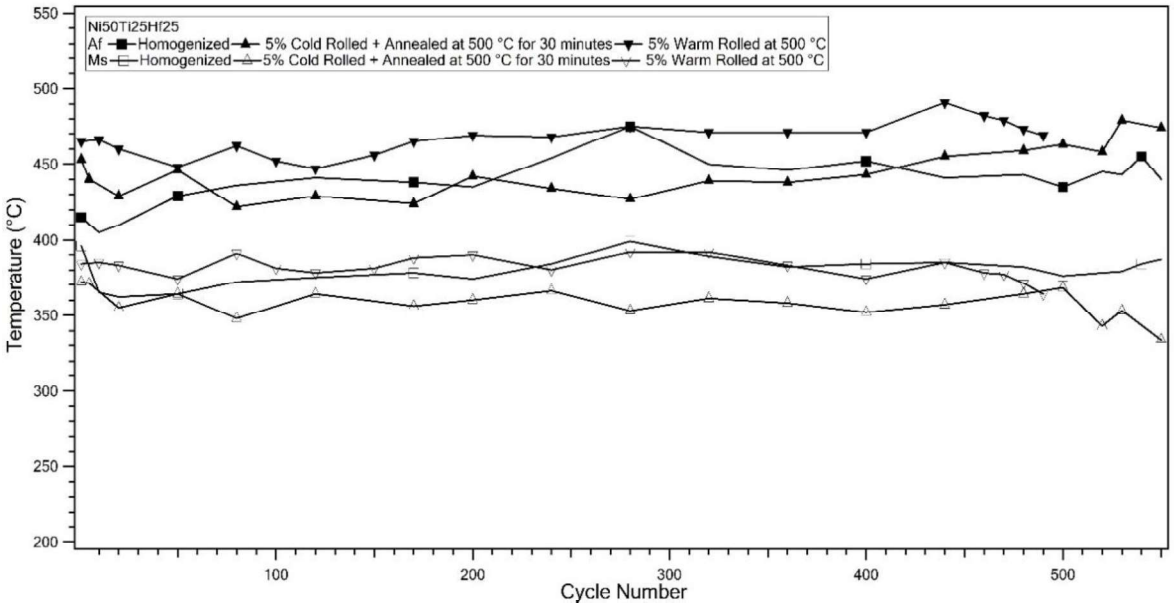

Figure 4.2-21 Comparison of Af and Ms values of homogenized, cold rolled +annealed and warm rolled Ni50Ti25Hf25 (at%) specimens

5. CONCLUSION

First section of the study was the investigation of the cooling rate effect on martensitic transformation of equiatomic Ni50Ti30Hf20 at% shape memory alloy.

DSC experiments demonstrated that transformation temperatures and transformation hysteresis values were not heating/cooling rate dependent since almost no difference was observed in both parameters.

Increase in transformation enthalpy with the increase in cooling rate cannot be attributed to transformation volume instead the increase in transformation enthalpy was due to increased measurement sensitivity of the DSC equipment thus scanning rates should be taken into consideration while comparing enthalpy values on different scanning rates. Additionally, the transformation enthalpy change is not possible from thermodynamical point of view since there is no change in energy parameters which were discussed previously in Results and Discussion section.

Isobaric experiments demonstrated the same transformation strain values under 200MPa via following different cooling rates since transformation strain mainly depends on the applied external stress magnitude which basically leads to a change in transforming volume.
As a summary, it is concluded that transformation enthalpy and strain do not depend on heating/cooling rate.

Second part of the study was the investigation of the effects of thermo-mechanical treatments on Ni50Ti25Hf25 at% SMA. Extruded specimens were homogenized and homogenized sample were subjected to cold and warm rolling processes. Thickness reduction for both cold and warm rolled specimen was 5%. Cold rolled specimen was subjected to annealing at 500 °C for 30 minutes and warm rolling was applied at 500 °C.

Shape memory alloys can be used as actuators as stated. Mechanical and thermal stabilities are important factors for actuation applications. Therefore, improving the thermo-mechanical stabilities of shape memory alloys is the main focus in this part of the

study. Cold and warm rolling processes were conducted to increase the strength of the alloy via dislocation induction with work hardening.
Functional fatigue experiments were conducted on homogenized, cold rolled + annealed and warm rolled samples and the results were shared. Transformation temperatures were quite stable for all samples through the functional fatigue experiment which revealed that thermal stability of the Ni50Ti25Hf25 shape memory alloy was promising with or without any thermo-mechanical treatment. Decrease in transformation temperatures about 20 °C was observed in cold rolled specimen as stated in the result section although almost no change was observed in warm rolled case.

Functional fatigue experiments revealed that homogenized specimen showed unstable actuation strain. On the other hand, cold rolled + annealed and warm rolled samples exhibited noticeable stability in terms of actuation strain values throughout the number of cycles. Thus, it is possible to improve mechanical stability of very high temperature Ni50Ti25Hf25 SMA by applying thermo-mechanical treatments.

Cold rolling led to a decrease in actuation strain. Dislocations that were induced during cold rolling were partly annihilated during annealing procedure and cold rolled + annealed specimen demonstrated quite stable actuation strain behavior although the upper cycle temperature was 600 °C. In addition to this, 5% warm rolled at 500 °C specimen also demonstrated stable actuation strain behavior with higher actuation strain values compared to cold rolled and annealed specimen. Achieving higher actuation strain values may be attributed to the possible texture formation during warm rolling operation.

Low percentage of rolling can be applicable to high Hf content NiTiHf alloys to improve thermo-mechanical stability. Both cold rolling and warm rolling procedures are effective way to improve shape memory behavior. However, further studies should be done on the microstructural evolution with the rolling processes to better understand the reason of achieving high stability.

6. REFERENCES

[1] D.J. Hartl, D.C. Lagoudas, Aerospace applications of shape memory alloys, Proceedings of the Institution of Mechanical Engineers, Part G: Journal of Aerospace Engineering. 221 (**2007**) 535–552. https://doi.org/10.1243/09544100JAERO211.

[2] J.M. Jani, M. Leary, A. Subic, Shape memory alloys in automotive applications, Applied Mechanics and Materials. 663 (**2014**) 248–253. https://doi.org/10.4028/www.scientific.net/AMM.663.248.

[3] K. Otsuka, X. Ren, Recent developments in the research of shape memory alloys, Intermetallics. 7 (**1999**) 511–528. https://doi.org/10.1016/S0966-9795(98)00070-3.

[4] K. Otsuka, X. Ren, Physical metallurgy of Ti-Ni-based shape memory alloys, Progress in Materials Science. 50 (**2005**) 511–678. https://doi.org/10.1016/j.pmatsci.2004.10.001.

[5] J. Ma, I. Karaman, R.D. Noebe, High temperature shape memory alloys, International Materials Reviews. 55 (**2010**) 257–315. https://doi.org/10.1179/095066010X12646898728363.

[6] A. Evirgen, F. Basner, I. Karaman, R.D. Noebe, J. Pons, R. Santamarta, Effect of aging on the martensitic transformation characteristics of a Ni-Rich NiTiHf high temperature shape memory alloy, Functional Materials Letters. 5 (**2012**). https://doi.org/10.1142/S1793604712500385.

[7] T.W. Duerig, K. N. Melton, D. Stöckel, C. M. Wayman, Engineering aspects of shape memory alloys, Butterworth-Heinemann, **1990**.

[8] T. Umale, D. Salas, B. Tomes, R. Arroyave, I. Karaman, The effects of wide range

of compositional changes on the martensitic transformation characteristics of NiTiHf shape memory alloys, Scripta Materialia. 161 (**2019**) 78–83. https://doi.org/10.1016/j.scriptamat.2018.10.008.

[9] Z.G. Wang, X.T. Zu, Y. Huo, Effect of heating/cooling rate on the transformation temperatures in TiNiCu shape memory alloys, Thermochimica Acta. 436 (**2005**) 153–155. https://doi.org/10.1016/j.tca.2005.06.028.

[10] K. Nurveren, A. Akdoğan, W.M. Huang, Evolution of transformation characteristics with heating/cooling rate in NiTi shape memory alloys, Journal of Materials Processing Technology. 196 (**2008**) 129–134. https://doi.org/10.1016/j.jmatprotec.2007.05.015.

[11] Q. Meng, H. Yang, Y. Liu, T.H. Nam, Transformation intervals and elastic strain energies of B2-B19′ martensitic transformation of NiTi, Intermetallics. 18 (**2010**) 2431–2434. https://doi.org/10.1016/j.intermet.2010.08.038.

[12] P.C.C. Monteiro, L.L. Silva, T.A. Netto, M.A. Savi, Experimental investigation of the influence of the heating rate in an SMA actuator performance, Sensors and Actuators, A: Physical. 199 (**2013**) 254–259. https://doi.org/10.1016/j.sna.2013.05.016.

[13] B. Kockar, I. Karaman, J.I. Kim, Y. Chumlyakov, A method to enhance cyclic reversibility of NiTiHf high temperature shape memory alloys, Scripta Materialia. 54 (**2006**) 2203–2208. https://doi.org/10.1016/j.scriptamat.2006.02.029.

[14] A. Shuitcev, D. V. Gunderov, B. Sun, L. Li, R.Z. Valiev, Y.X. Tong, Nanostructured Ti29.7Ni50.3Hf20 high temperature shape memory alloy processed by high-pressure torsion, Journal of Materials Science and Technology. 52 (**2020**) 218–225. https://doi.org/10.1016/j.jmst.2020.01.065.

[15] Y.F. Ye, Q. Wang, Y.L. Zhao, Q.F. He, J. Lu, Y. Yang, Elemental segregation in solid-solution high-entropy alloys: Experiments and modeling, Journal of Alloys

and Compounds. 681 (**2016**) 167–174. https://doi.org/10.1016/j.jallcom.2016.04.239.

[16] C. Hinte, K. Barienti, J. Steinbrücker, G. Gerstein, M.A. Swider, S. Herbst, G. Eggeler, H.J. Maier, Pattern-forming nanoprecipitates in NiTi-related high entropy shape memory alloys, Scripta Materialia. 186 (**2020**) 132–135. https://doi.org/10.1016/j.scriptamat.2020.05.007.

[17] S.W. McAlpine, J. V. Logan, M.P. Short, Predicting single phase stability and segregation in the NbMoTaTi–(W,V) high entropy alloy system with the vacancy exchange potential, Scripta Materialia. 191 (**2021**) 29–33. https://doi.org/10.1016/j.scriptamat.2020.08.043.

[18] T.M. Butler, J.P. Alfano, R.L. Martens, M.L. Weaver, High-Temperature Oxidation Behavior of Al-Co-Cr-Ni-(Fe or Si) Multicomponent High-Entropy Alloys, Jom. 67 (**2015**) 246–259. https://doi.org/10.1007/s11837-014-1185-7.

[19] K. Otsuka, C. M. Wayman Shape Memory Materials, Cambridge University Press. (**1998**) 284.

[20] B. Kockar, SHAPE MEMORY BEHAVIOR OF ULTRAFINE GRAINED NiTi AND TiNiPd SHAPE MEMORY ALLOYS, PhD Dissertation: Texas A&M University. (**2007**) 181 pp.

[21] A. Nagasawa, K. Enami, Y. Ishino, Y. Abe, S. Nenno, Reversible shape memory effect, Scripta Metallurgica. 8 (**1974**) 1055–1060. https://doi.org/10.1016/S0036-9748(74)80003-7.

[22] T. Saburi, S. Nenno, Reversible Shape Memory in Cu-Zn-Ga, Scripta Metallurgica. 8 (**1974**) 1363–1367.

[23] X. Ren, K. Otsuka, Universal symmetry property of point defects in crystals,

Physical Review Letters. 85 (**2000**) 1016–1019. https://doi.org/10.1103/PhysRevLett.85.1016.

[24] C. Hayrettin, O. Karakoc, I. Karaman, J.H. Mabe, R. Santamarta, J. Pons, Two way shape memory effect in NiTiHf high temperature shape memory alloy tubes, Acta Materialia. 163 (**2019**) 1–13. https://doi.org/10.1016/j.actamat.2018.09.058.

[25] Z. Bo, D.C. Lagoudas, Thermomechanical modeling of polycrystalline SMAs under cyclic loading, Part III: Evolution of plastic strains and two-way shape memory effect, International Journal of Engineering Science. 37 (**1999**) 1175–1203. https://doi.org/10.1016/S0020-7225(98)00115-3.

[26] X.L. Meng, Y.F. Zheng, W. Cai, L.C. Zhao, Two-way shape memory effect of a TiNiHf high temperature shape memory alloy, Journal of Alloys and Compounds. 372 (**2004**) 180–186. https://doi.org/10.1016/j.jallcom.2003.10.020.

[27] H. Scherngell, A.C. Kneissl, Training and stability of the intrinsic two-way shape memory effect in Ni-Ti alloys, Scripta Materialia. 39 (**1998**) 205–212. https://doi.org/10.1016/S1359-6462(98)00155-9.

[28] Y. Liu, Y. Liu, J. Van Humbeeck, TWO-WAY SHAPE MEMORY EFFECT DEVELOPED BY MARTENSITE DEFORMATION IN NiTi, n.d.

[29] M.W. Burkart, Diffusionless Phase Change in the Indiumthallium System, American Institute of Mining and Metallurgical Engineers, **1953**. https://books.google.com.tr/books?id=MLmYnQEACAAJ.

[30] L.C. Chang, T.A. Read, Plastic Deformation and Diffusionless Phase Changes in Metals — the Gold-Cadmium Beta Phase, Jom. 3 (**1951**) 47–52. https://doi.org/10.1007/bf03398954.

[31] Z. S. Basinski, J.W. Christian, Crystallography of deformation by twin boundary

movements in indium-thallium alloys, Acta Metallurgica. 2 (**1954**). https://doi.org/10.1016/0001-6160(54)90100-5.

[32] D. T., P. A., S. D., An overview of nitinol medical of applications, Materials Science and Engineering A. 273–275 (**1999**) 149–160.

[33] T.B. Massalski, Massalski T.B.-Binary alloy phase diagrams. V2, (**1986**) 1129.

[34] G.B. Stachowiak, P.G. McCormick, Shape memory behaviour associated with the R and martensitic transformations in a NiTi alloy, Acta Metallurgica. 36 (**1988**) 291–297. https://doi.org/10.1016/0001-6160(88)90006-5.

[35] H.C. Lin, S.K. Wu, The tensile behavior of a cold-rolled and reverse-transformed equiatomic TiNi alloy, Acta Metallurgica Et Materialia. 42 (**1994**) 1623–1630. https://doi.org/10.1016/0956-7151(94)90371-9.

[36] D.A. Miller, D.C. Lagoudas, Influence of cold work and heat treatment on the shape memory effect and plastic development of NiTi, Materials Science and Engineering A. 308 (**2001**) 161–175. https://doi.org/10.1016/S0921-5093(00)01982-1.

[37] J. Frenzel, E.P. George, A. Dlouhy, C. Somsen, M.F.X. Wagner, G. Eggeler, Influence of Ni on martensitic phase transformations in NiTi shape memory alloys, Acta Materialia. 58 (**2010**) 3444–3458. https://doi.org/10.1016/j.actamat.2010.02.019.

[38] J. Khalil-Allafi, A. Dlouhy, G. Eggeler, Ni4Ti3-precipitation during aging of NiTi shape memory alloys and its influence on martensitic phase transformations, Acta Materialia. 50 (**2002**) 4255–4274. https://doi.org/10.1016/S1359-6454(02)00257-4.

[39] D. Stroz, J. Kwarciak, H. Morawiec, Effect of ageing on martensitic transformation

in NiTi shape memory alloy, Journal of Materials Science. 23 (**1988**) 4127–4131. https://doi.org/10.1007/BF01106847.

[40] R.R. Adharapurapu, F. Jiang, K.S. Vecchio, Aging effects on hardness and dynamic compressive behavior of Ti-55Ni (at.%) alloy, Materials Science and Engineering A. 527 (**2010**) 1665–1676. https://doi.org/10.1016/j.msea.2009.10.069.

[41] A. V. Sergueeva, C. Song, R.Z. Valiev, A.K. Mukherjee, Structure and properties of amorphous and nanocrystalline NiTi prepared by severe plastic deformation and annealing, Materials Science and Engineering A. 339 (**2003**) 159–165. https://doi.org/10.1016/S0921-5093(02)00122-3.

[42] B. Kockar, I. Karaman, A. Kulkarni, Y. Chumlyakov, I. V. Kireeva, Effect of severe ausforming via equal channel angular extrusion on the shape memory response of a NiTi alloy, Journal of Nuclear Materials. 361 (**2007**) 298–305. https://doi.org/10.1016/j.jnucmat.2006.12.007.

[43] B. Kockar, I. Karaman, J.I. Kim, Y.I. Chumlyakov, J. Sharp, C.J. (Mike. Yu, Thermomechanical cyclic response of an ultrafine-grained NiTi shape memory alloy, Acta Materialia. 56 (**2008**) 3630–3646. https://doi.org/10.1016/j.actamat.2008.04.001.

[44] G.S. Bigelow, S.A. Padula, A. Garg, D. Gaydosh, R.D. Noebe, Characterization of ternary NiTiPd high-temperature shape-memory alloys under load-biased thermal cycling, Metallurgical and Materials Transactions A: Physical Metallurgy and Materials Science. 41 (**2010**) 3065–3079. https://doi.org/10.1007/s11661-010-0365-5.

[45] J.H.N. Donkersloot, H.C., Van Vucht, Martensitic Transformations, Microstructure, and Mechanical Workability of TiPt, Journal of the Less-Common Metals. 20 (**1970**) 83–91.

[46] T. Biggs, M.B. Cortie, M.J. Witcomb, L.A. Cornish, Martensitic transformations, microstructure, and mechanical workability of TiPt, Metallurgical and Materials Transactions A: Physical Metallurgy and Materials Science. 32 (**2001**) 1881–1886. https://doi.org/10.1007/s11661-001-0001-5.

[47] O. Rios, R. Noebe, T. Biles, A. Garg, A. Palczer, D. Scheiman, H.J. Seifert, M. Kaufman, Characterization of ternary NiTiPt high-temperature shape memory alloys, Smart Structures and Materials 2005: Active Materials: Behavior and Mechanics. 5761 (**2005**) 376. https://doi.org/10.1117/12.599608.

[48] Z. Pu, H. Tseng, K. Wu, MARTENSITE TRANSFORMATION AND SHAPE MEMORY EFFECT OF NiTi-Zr HIGH TEMPERATURE SHAPE MEMORY ALLOYS, 2441 (**1995**) 171–178.

[49] A. Evirgen, I. Karaman, J. Pons, R. Santamarta, R.D. Noebe, Role of nano-precipitation on the microstructure and shape memory characteristics of a new Ni50.3Ti34.7Zr15 shape memory alloy, Materials Science and Engineering A. 655 (**2016**) 193–203. https://doi.org/10.1016/j.msea.2015.12.076.

[50] A.M. Pérez-Sierra, J. Pons, R. Santamarta, I. Karaman, R.D. Noebe, Stability of a Ni-rich Ni-Ti-Zr high temperature shape memory alloy upon low temperature aging and thermal cycling, Scripta Materialia. 124 (**2016**) 47–50. https://doi.org/10.1016/j.scriptamat.2016.06.029.

[51] H.E. Karaca, S.M. Saghaian, G. Ded, H. Tobe, B. Basaran, H.J. Maier, R.D. Noebe, Y.I. Chumlyakov, Effects of nanoprecipitation on the shape memory and material properties of an Ni-rich NiTiHf high temperature shape memory alloy, Acta Materialia. 61 (**2013**) 7422–7431. https://doi.org/10.1016/j.actamat.2013.08.048.

[52] S.M. Saghaian, H.E. Karaca, H. Tobe, A.S. Turabi, S. Saedi, S.E. Saghaian, Y.I. Chumlyakov, R.D. Noebe, High strength NiTiHf shape memory alloys with tailorable properties, Acta Materialia. 134 (**2017**) 211–220.

https://doi.org/10.1016/j.actamat.2017.05.065.

[53] O. Karakoc, C. Hayrettin, D. Canadinc, I. Karaman, Role of applied stress level on the actuation fatigue behavior of NiTiHf high temperature shape memory alloys, Acta Materialia. 153 (**2018**) 156–168. https://doi.org/10.1016/j.actamat.2018.04.021.

[54] O. Karakoc, C. Hayrettin, M. Bass, S.J. Wang, D. Canadinc, J.H. Mabe, D.C. Lagoudas, I. Karaman, Effects of upper cycle temperature on the actuation fatigue response of NiTiHf high temperature shape memory alloys, Acta Materialia. 138 (**2017**) 185–197. https://doi.org/10.1016/j.actamat.2017.07.035.

[55] N. Hite, D.J. Sharar, W. Trehern, T. Umale, K.C. Atli, A.A. Wilson, A.C. Leff, I. Karaman, NiTiHf shape memory alloys as phase change thermal storage materials, Acta Materialia. 218 (**2021**) 117175. https://doi.org/10.1016/j.actamat.2021.117175.

[56] C.C. Wojcik, Properties and heat treatment of high transition temperature Ni-Ti-Hf alloys, Journal of Materials Engineering and Performance. 18 (**2009**) 511–516. https://doi.org/10.1007/s11665-009-9357-2.

[57] M.M. Javadi, M. Belbasi, M.T. Salehi, M.R. Afshar, Effect of aging on the microstructure and shape memory effect of a hot-rolled NiTiHf alloy, Journal of Materials Engineering and Performance. 20 (**2011**) 618–622. https://doi.org/10.1007/s11665-011-9885-4.

[58] K.S. Suresh, D.I. Kim, S.K. Bhaumik, S. Suwas, Evolution of microstructure and texture in Ni49.4Ti 38.6Hf12 shape memory alloy during hot rolling, Intermetallics. 42 (**2013**) 1–8. https://doi.org/10.1016/j.intermet.2013.04.009.

[59] M. Belbasi, M.T. Salehi, Influence of chemical composition and melting process on hot rolling of nitihf shape memory alloy, Journal of Materials Engineering and Performance. 23 (**2014**) 2368–2372. https://doi.org/10.1007/s11665-014-1006-8.

[60] M. Belbasi, M.T. Salehi, S.A.A.A. Mousavi, S.M. Ebrahimi, A study on the mechanical behavior and microstructure of NiTiHf shape memory alloy under hot deformation, Materials Science and Engineering A. 560 (**2013**) 96–102. https://doi.org/10.1016/j.msea.2012.09.039.

[61] N. Babacan, M. Bilal, C. Hayrettin, J. Liu, O. Benafan, I. Karaman, Effects of cold and warm rolling on the shape memory response of Ni50Ti30Hf20 high-temperature shape memory alloy, Acta Materialia. 157 (**2018**) 228–244. https://doi.org/10.1016/j.actamat.2018.07.009.

[62] Y. Motemani, M. Nili-Ahmadabadi, M.J. Tan, M. Bornapour, S. Rayagan, Effect of cooling rate on the phase transformation behavior and mechanical properties of Ni-rich NiTi shape memory alloy, Journal of Alloys and Compounds. 469 (**2009**) 164–168. https://doi.org/10.1016/j.jallcom.2008.01.153.

[63] Y.Q. Zhang, S.Y. Jiang, Y.N. Zhao, M. Tang, Influence of cooling rate on phase transformation and microstructure of Ti-50.9%Ni shape memory alloy, Transactions of Nonferrous Metals Society of China (English Edition). 22 (**2012**) 2685–2690. https://doi.org/10.1016/S1003-6326(11)61518-5.

[64] M.S. Velipaşaoğlu, M.S. VELİPAŞAOĞLU, The Determination of The Functional Fatigue Life of High Temperature Shape Memory Alloys After Cold Rolling Process, MSc Thesis, Graduate School of Science and Engineering of Hacettepe University, Ankara, (**2020**).

[65] K.C. Atli, I. Karaman, R.D. Noebe, A. Garg, Y.I. Chumlyakov, I. V. Kireeva, Improvement in the shape memory response of Ti50.5Ni 24.5Pd25 high-temperature shape memory alloy with scandium microalloying, Metallurgical and Materials Transactions A: Physical Metallurgy and Materials Science. 41 (**2010**) 2485–2497. https://doi.org/10.1007/s11661-010-0245-z.

[66] K.C. Atli, I. Karaman, R.D. Noebe, Influence of tantalum additions on the microstructure and shape memory response of Ti50.5Ni24.5Pd25 high-

temperature shape memory alloy, Materials Science and Engineering A. 613 (**2014**) 250–258. https://doi.org/10.1016/j.msea.2014.06.104.

[67] O. Benafan, R.D. Noebe, S.A. Padula, R. Vaidyanathan, Microstructural response during isothermal and isobaric loading of a precipitation-strengthened Ni-29.7Ti-20Hf high-temperature shape memory alloy, Metallurgical and Materials Transactions A: Physical Metallurgy and Materials Science. 43 (**2012**) 4539–4552. https://doi.org/10.1007/s11661-012-1297-z.

[68] H.H. Saygili, THE DEVELOPMENT OF A FATIGUE TEST MACHINE TO INVESTIGATE THE FUNCTIONAL FATIGUE LIFE OF HIGH TEMPERATURE SHAPE MEMORY ALLOYS AND THE DETERMINATION OF THE FUNCTIONAL FATIGUE LIFE OF THESE ALLOYS, MSc Thesis, Graduate School of Science and Engineering of Hacettepe University, Ankara, (**2018**)

[69] O. Akgul, H.O. Tugrul, B. Kockar, Effect of the cooling rate on the thermal and thermomechanical behavior of NiTiHf high-temperature shape memory alloy, Journal of Materials Research. 35 (**2020**) 1572–1581. https://doi.org/10.1557/jmr.2020.139.

[70] W. Abuzaid, H. Sehitoglu, Functional fatigue of Ni50.3Ti25Hf24.7 – Heterogeneities and evolution of local transformation strains, Materials Science and Engineering A. 696 (**2017**) 482–492. https://doi.org/10.1016/j.msea.2017.04.097.

[71] H.H. Saygili, H.O. Tugrul, B. Kockar, Effect of Aging Heat Treatment on the High Cycle Fatigue Life of Ni50.3Ti29.7Hf20 High-Temperature Shape Memory Alloy, Shape Memory and Superelasticity. 5 (**2019**) 32–41. https://doi.org/10.1007/s40830-018-00202-5.

[72] P. Wollants, J.R. Roos, L. Delaey, Thermally- and stress-induced thermoelastic martensitic transformations in the reference frame of equilibrium thermodynamics,

Progress in Materials Science. 37 (**1993**) 227–288. https://doi.org/10.1016/0079-6425(93)90005-6.

[73] P. Gabbott, A Practical Introduction to Differential Scanning Calorimetry, Principles and Applications of Thermal Analysis. (**2008**) 1–50. https://doi.org/10.1002/9780470697702.ch1.

[74] S. Qiu, V.B. Krishnan, S.A. Padula, R.D. Noebe, D.W. Brown, B. Clausen, R. Vaidyanathan, Measurement of the lattice plane strain and phase fraction evolution during heating and cooling in shape memory NiTi, Applied Physics Letters. 95 (**2009**) 1–4. https://doi.org/10.1063/1.3245308.

7. APPENDIX

APPENDIX 1 – Microscope images of Ni50Ti25Hf25 at. % SMA during functional fatigue

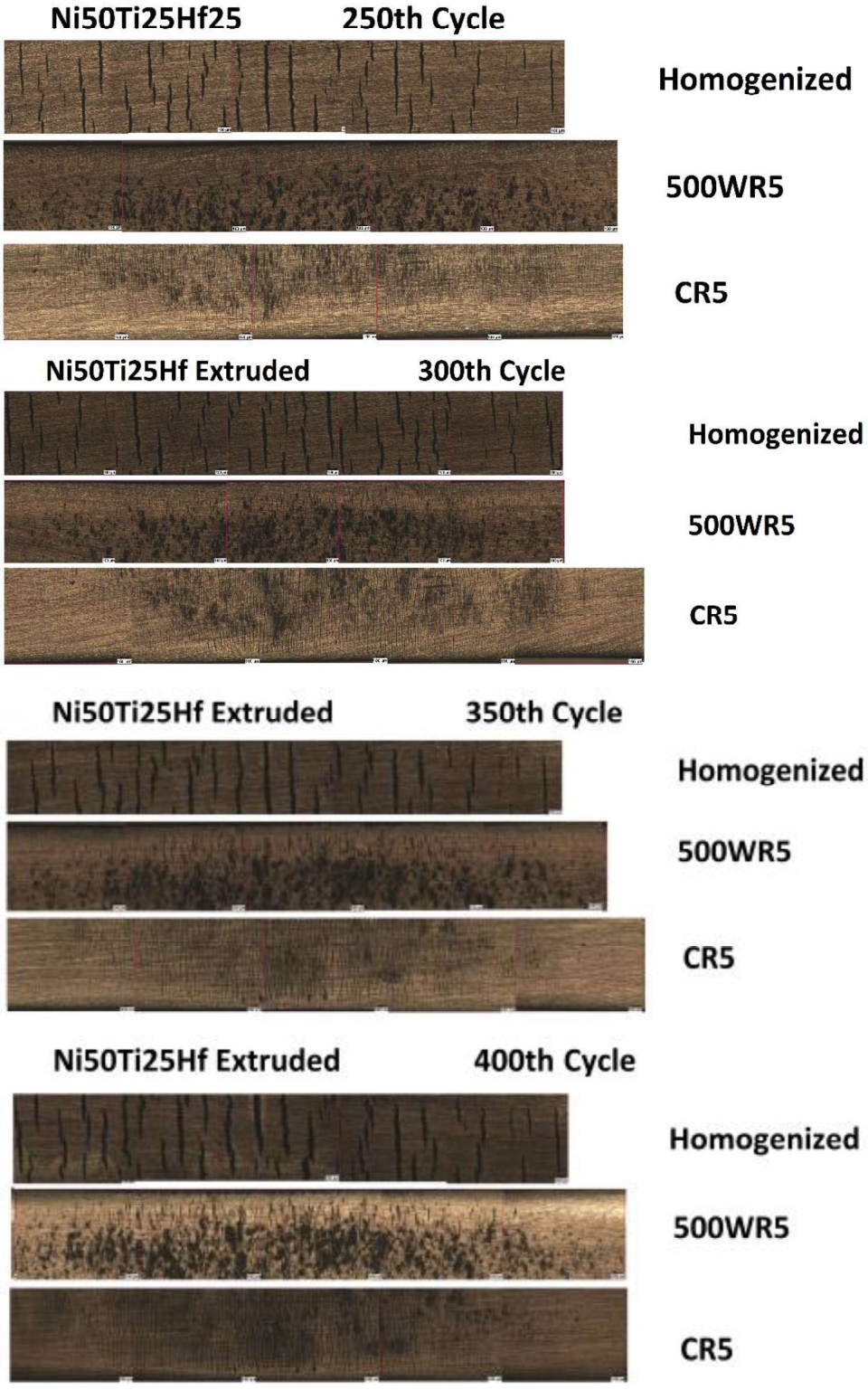

Ni50Ti25Hf Extruded 450th Cycle

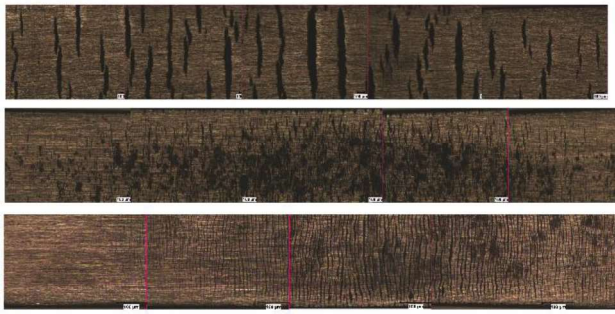

Homogenized

500WR5

CR5

Ni50Ti25Hf Extruded 500th Cycle

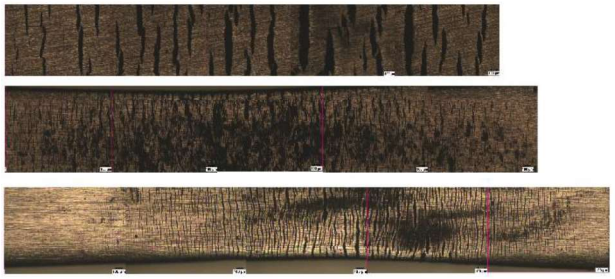

Homogenized

500WR5 490th Cycle*

CR5

Ni50Ti25Hf Extruded 550th Cycle

Homogenized

APPENDIX 4 – Publications

O. Akgul, H.O. Tugrul, B. Kockar, Effect of the cooling rate on the thermal and thermomechanical behavior of NiTiHf high-temperature shape memory alloy, Journal of Materials Research. 35 (2020) 1572–1581. https://doi.org/10.1557/jmr.2020.139.